Brigham Young University
BYU ScholarsArchive

All Theses and Dissertations

2011-02-16

Thermodynamic, Sulfide, Redox Potential, and pH Effects on Syngas Fermentation

Peng Hu
Brigham Young University - Provo

Follow this and additional works at: https://scholarsarchive.byu.edu/etd

 Part of the Chemical Engineering Commons

BYU ScholarsArchive Citation

Hu, Peng, "Thermodynamic, Sulfide, Redox Potential, and pH Effects on Syngas Fermentation" (2011). *All Theses and Dissertations*. 2919.
https://scholarsarchive.byu.edu/etd/2919

This Dissertation is brought to you for free and open access by BYU ScholarsArchive. It has been accepted for inclusion in All Theses and Dissertations by an authorized administrator of BYU ScholarsArchive. For more information, please contact scholarsarchive@byu.edu, ellen_amatangelo@byu.edu.

Thermodynamic, Sulfide, Redox Potential, and pH Effects on Syngas Fermentation

Peng Hu

A dissertation submitted to the faculty of
Brigham Young University
in partial fulfillment of the requirements for the degree of

Doctor of Philosophy

Randy S. Lewis, Chair
Thomas A. Knotts IV
William R. McCleary
Larry L. Baxter
David O. Lignell

Department of Chemical Engineering

Brigham Young University

April 2011

Copyright © 2011 Peng Hu

All Rights Reserved

ABSTRACT

Thermodynamic, Sulfide, Redox Potential, and pH Effects
on Syngas Fermentation

Peng Hu
Department of Chemical Engineering
Doctor of Philosophy

Recently, work in ethanol production is exploring the fermentation of syngas (primarily CO, CO_2, and H_2) following gasification of cellulosic biomass. The syngas fermentation by clostridium microbes utilizes the Wood-Ljungdahl metabolic pathway. Along this pathway, the intermediate Acetyl-CoA typically diverges to produce ethanol, acetic acid, and/or cell mass.

To develop strategies for process optimization, a thermodynamic analysis was conducted that provided a detailed understanding of the favorability of the reactions. Thermodynamic analysis provided identification of potentially limiting steps. Once these limiting reactions were identified, further thermodynamic analysis provided additional insights into the ways in which reaction conditions could be adjusted to improve product yield as well as minimize the effect of such bottlenecks. In this way, strategies to enhance product formation were effectively formed. A thermodynamic analysis regarding electron utilization suggested that it would be unlikely that H_2 is utilized in favor of CO for electron production when both species are present. Therefore, CO conversion efficiency to products will be sacrificed during syngas fermentation since some of the CO will make electrons at the expense of product and cell mass formation. Furthermore, the analysis showed the thermodynamic difference of ethanol production, acetate production, and acetate to ethanol conversion, at varying reaction conditions, such as at different pH and redox potential levels. These differences were then incorporated into a strategy to optimize production of desired product, improve bioreactor design, and decrease the amount of by-product formed.

Based on the thermodynamics analysis, experiments with varying experimental conditions were performed. The results showed that sulfide concentration in the media changed. In order to assess the effects of experimental conditions on syngas fermentation and decrease the experimental variability, experiments with controlled sulfide, redox potential, and pH were designed and the results indicated that these factors play key roles on cell growth, product formation and product distribution. Furthermore, experimental conditions had different effects on fermentation during different phases. For example, cell growth is much better at pH=5.8 than pH=4.5. However, the ethanol production rate at pH=4.5 is better than pH=5.8. A strategy involving controlling the pH and redox potential at different phases was effectively applied to improve ethanol production. This work provided significant insights on how varying experimental conditions can affect the syngas fermentation process.

Keywords: ethanol, syngas, fermentation, Wood-Ljungdahl metabolic pathway, thermodynamics, redox potential, pH

ACKNOWLEDGMENTS

I am grateful for all I have received throughout these years during my PhD studies at Brigham Young University. It would be impossible to finish my dissertation without the support of numerous people.

I want to first thank my advisor Dr. Randy Lewis for the invaluable help he has given me. He has always encouraged me and has enlightened me through his innovative thought and wide knowledge. I thank Dr. Thomas Knotts, Dr. William McCleary, Dr. Larry Baxter, and Dr. David Lignell for their continuous help these years. As committee members of my dissertation, they helped me a lot with conducting research, preparing proposal, and writing my dissertation.

Many thanks go to five undergraduate students in our lab with whom I worked to perform the research: Spencer Bowen, Dila Banjade, Hannah Davis, Lee Jacobsen, and James Horton. They have contributed a lot of time and ideas to this project. I want thank other graduate students in the Lewis lab who have shared their wisdom in my PhD studies these years. Also, I want thank Serena Jacobson and Linda Bosley, who are secretaries in Chemical Engineering Department, for their patient help.

Finally, I am grateful to my family. Special thanks I give to my wife, Yong. Without her I would be a very different person today, and it would have been certainly much harder to finish a PhD. I am also grateful to my parents, Hu Guodong and Xiao Yuhua, whose love and support have always strengthened me in my life.

TABLE OF CONTENTS

LIST OF TABLES

LIST OF FIGURES

1. Introduction

1.1 Ethanol as an alternative fuel

Energy demands have generally increased since the 1970's. It is projected that the worldwide reserves of fossil oil will be completely depleted in the near future (Geller 2001; Bilgen 2004). In addition, although fluctuating with time, the trend of crude oil prices has increased (Figure 1-1). The average crude oil price has changed from $24 per barrel in January 1991 to $76 per barrel in October 2010, and peaked at $149 on June 30 2008 (Energy Information Administration, 2010). The issues of oil depletion and price have induced an increasing interest in alternative fuels such as ethanol. Ethanol is currently used as a combined fuel with gasoline (from 5-85%), derived primarily from corn.

In the United States, large-scale fuel ethanol production has emerged as an initial biofuel and has experienced a rapid increase in production during the last several decades. The historic production of ethanol for fuels in the United States since 1985 is shown in Figure 1-2. The annual fuel ethanol production in the U.S. has increased from 610 million gallons in 1985 to 10.6 billion gallons in 2010, a 17-fold increase. A total of 187 ethanol refineries were operating in 26 states in January 2010which is a 10% increase from 2009 and a 274% increase from 2000. In addition, another 15 ethanol refineries are currently under construction. (RFA, 2010)

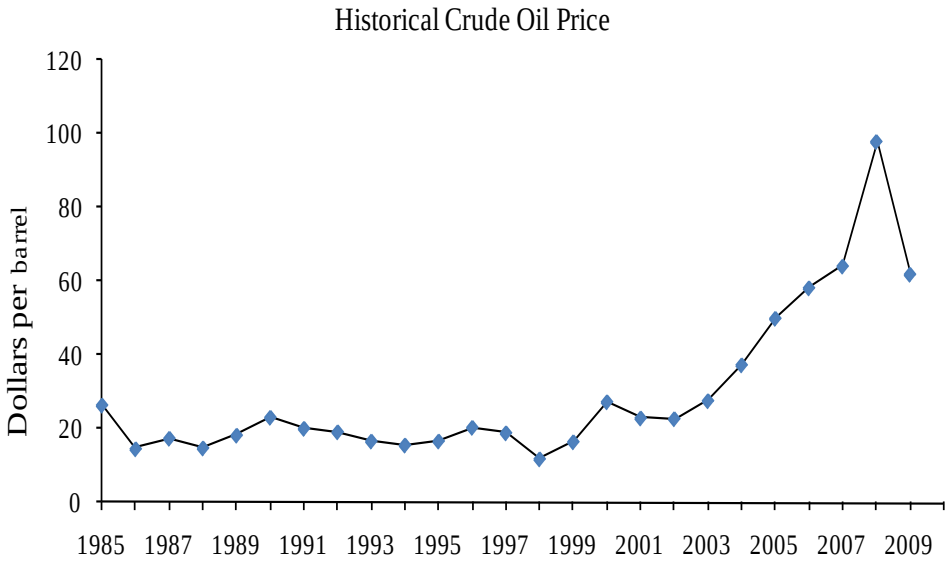

Figure 1-1.Historic average of world crude oil prices (Energy Information Administration, 2010)

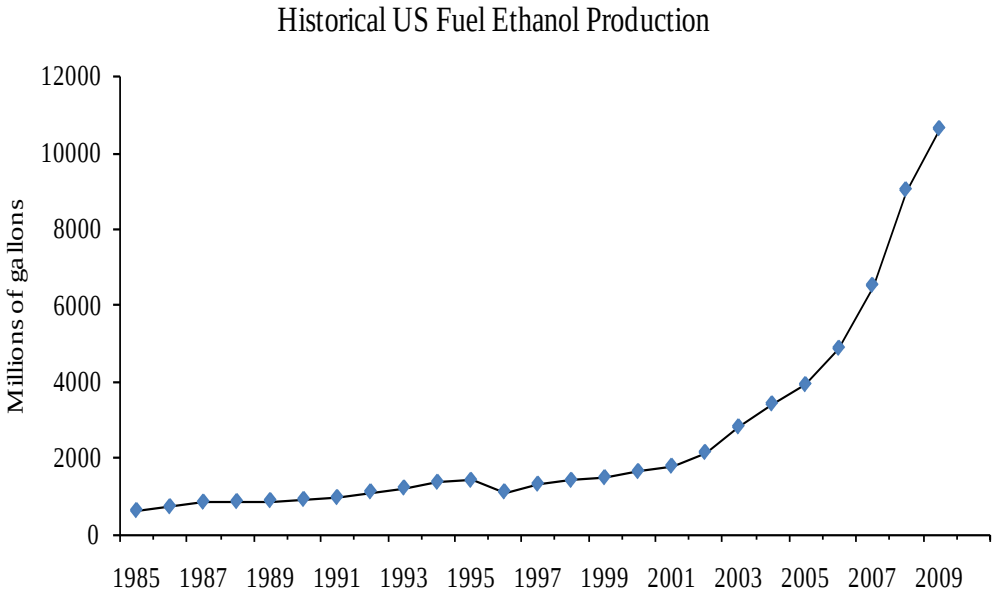

Figure 1-2.Historic fuel ethanol production in the United States (RFA, 2010 a)

1.2 Advantages and disadvantages of fuel ethanol

There are several benefits to using ethanol as an alternative fuel including environmental, economic, and social benefits. In the United States, nearly 70% of the total greenhouse gas (CO_2, CH_4, and NO_x) emissions are from the transportation and electricity generation industries. Combustion of fossil fuels releases CO_2 which had been sequestered from the atmosphere millions of years ago back into the atmosphere. This increases the amount of the CO_2 in the atmosphere. By contrast, CO_2 released during fuel ethanol utilization can potentially be recycled during the production of additional biomass. Thus, net greenhouse gas emissions would be lower when utilizing renewable resources as compared to fossil fuel.

Ethanol is also known to enhance engine efficiency as well as to reduce other environmental emissions. Ethanol and other solvents containing element oxygen produce less carbon monoxide (CO), nitrogen oxides (NO_x), and smog agents (e.g. ozone) than ordinary gasoline (He, 2003; Hsieh, 2002). In addition, ethanol can be produced from agricultural feedstocks and can be produced domestically. The domestic production of ethanol has the potential to improve the country's trade deficit by decreasing the dependence on imported oil and may also increase employment opportunities in rural areas. Furthermore, the reduction of the dependence on imported oil improves national security.

Although there are numerous positive impacts associated with fuel-ethanol, several drawbacks about fuel ethanol still exist. For example, the energy content of ethanol is less than that of gasoline. The HHV (higher heating value) of ethanol is 89 MJ/gallon, whereas the HHV of gasoline is about 132 MJ/gallon (DOE, 2005). Depending upon location, ethanol can be more expensive than gasoline. A report released from RFA compares the retail prices of fuel ethanol and gasoline in Chicago, IL, between 8/6/2010 and 10/22/2010 (RFA, 2010 b). The report shows

that retail gasoline price was averaged $2.75/Gallon during that period, while the retail fuel ethanol price was averaged $2.03/Gallon. Based on the price and energy content, the ethanol price for unit energy (2.28 cents/MJ) is actually higher than gasoline price (2.08 cents/MJ). This indicates that using ethanol may be more expensive in the end even if the price of ethanol per Gallon in the gas station is less expensive than gasoline.

The environmental benefits of ethanol from biomass are also questioned (DOE, 2010). Although most studies show that ethanol from corn (the current primary ethanol source) has a slightly positive net fossil energy value, which means the energy in the consumed fossil fuel is less than the energy in the produced ethanol (Hill 2006), other studies still show that corn ethanol has a negative net fossil energy (more input energy than output energy) (Pimentel 2001; Patzek 2005). The debate on the energy efficiency of ethanol production from corn increases concerns on whether ethanol production from corn/starch is worthwhile.

From a waste standpoint, an average of 13 liters of wastewater is produced for every liter of ethanol generated from corn (Pimentel 2001) which increases the environmental impacts. Currently, almost all ethanol production uses food crop. If a huge reduction of crop production occurs, for example due to bad weather, people will be not only short of food, but also short of fuel. This will greatly impact the food market and also result in in-secure fuel conditions (Srinivasan 2009; Yang 2009).

Besides from the corn/starch platform, fuel ethanol production can be also from other methods, for example from cellulose platform. But no one is currently perfect and a lot of issues need to be figured out. With regards to ethanol from cellulose via enzymatic saccharification, it does not directly impact food market, but the low carbon conversion from biomass to fuel ethanol may limit the commercialization of ethanol production with this technology. For

instance, lignin, which accounts for about 30% of the carbon of biomass, cannot be effectively used via the enzymatic hydrolysis method (Dayton 2003). With a comparison, via syngas fermentation method for ethanol production, lignin can be used to produce CO and CO_2. But CO potentially cannot be solely used for product formation because some CO needs to be used to produce electrons which are required for the ethanol process.

As is evident, there are several unanswered questions with regards to the efficacy of ethanol production and its impact towards the attainment of sustainable alternative fuels. Although corn ethanol appears to not be a viable option, cellulosic-generated ethanol is still a promising technology but several questions need to be addressed. This work will address key issues associated with fermentation parameters on cell growth and product formation.

1.3 Production of fuel ethanol

Currently ethanol production occurs through two primary platforms: a starch/sugar-based platform and a cellulosic platform (Lynd 1996). Figure 1-3 shows a general overview of these two processes. Feedstocks may include sugar-based crops such as beets and cane, starch-based crops such as corn, barley, wheat, and potatoes, and lignocellulosic-based materials such as wood, corn stover, and grasses.

In the starch/sugar-based platform, starch-based crops (corn, sugar cane, etc.) are used for ethanol production via fermentation. Corn is currently the most popular crop used in the starch/sugar method. (Joel 2007). Wet milling and dry milling are the two main processes used to form the sugars needed for fermentation. The wet milling process involves liquid extraction and yields secondary products of corn gluten feed, corn gluten meal and corn oil. The dry milling

process is generally smaller and simpler and gives distiller grains that can be used for animal feed besides the ethanol product (Wang 2007).

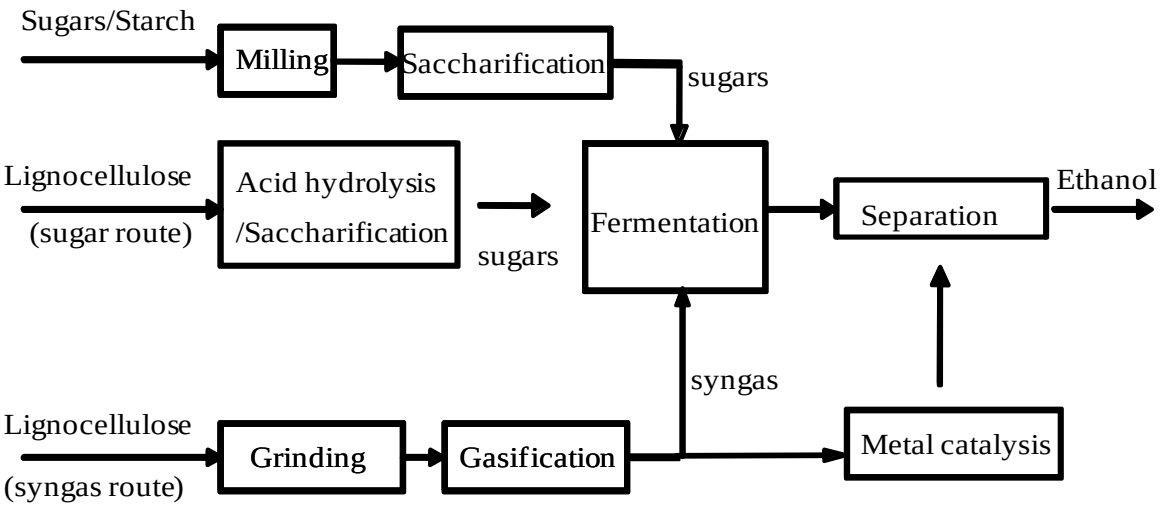

Figure 1-3. Ethanol production process (Modified from Lewis 2010)

The cellulosic platforms include: syngas fermentation, syngas conversion via Fisher-Tropsch synthesis, and cellulosic fermentation. Synthesis gas or syngas is a gas mixture primarily consisting of carbon monoxide (CO), carbon dioxide (CO_2), and hydrogen (H_2) on a dry basis. Syngas can be produced from various sources, such as natural gas, coal, petroleum coke and cellulosic biomass (Dayton 2003). During the syngas fermentation processes, cellulose is gasified to syngas and then fermented to ethanol using bacteria. For Fisher-Tropsch synthesis, syngas is converted to ethanol and other hydrocarbons via metal catalysts. As for cellulosic fermentation, cellulose is converted to simple sugars using enzymes and then converted to ethanol via fermentation.

Fermentation of sugars. For this process, three main steps are involved in ethanol production: biomass pretreatment, cellulose saccharification, and fermentation. In order for

saccharification to occur, pretreatment of the lignocellulosic material is applied due to the crystalline structure of the lignocellulosic material. Pretreatment processes to expose the cellulosic and hemi-cellulosic components to enzymes include acid, ammonia, steam, and alkaline chemicals (Shleser 1994; Weil 2002; Kadar 2004). The cellulose and hemi-cellulose are then treated with enzymes called cellulases and xylanases to break down the cellulose and hemi-cellulose fractions into fermentable six- and five- carbon sugars, respectively. The sugars are then fermented to ethanol using organisms such as genetically-engineered *Escherichia coli* (Ingram 1997), *Saccharomyces cerevisiae* (Ho 2000) and *Zymomonas mobilis* (Picataggio 1997). In some cases, the saccharification and fermentation occur simultaneously (Kadar 2004). Disadvantages of this process include the high cost of enzymes, the formation of waste streams (including lignin), and the need for economic subsidies, although major efforts are being extended to reduce or eliminate these disadvantages (Weil 2002; Wyman, 2003; Novozymes, 2004).

Metal-catalytic conversion of syngas. Catalytic conversion of syngas using metal catalysts, such as Fe, Co, Ru and Ni, is currently the primary industrial method to produce fuels from syngas. During the conversion, CO and H_2 are converted into fuels, including ethanol and other hydrocarbons, resulting from a series of metal-catalytic reactions. The most important conversion methods are Fischer-Tropsch Synthesis (FTS) involving the production of liquid hydrocarbons from CO and H_2 mixtures over a transition metal catalyst. Several plants based on FTS have been commercialized, for example Sasol in South Africa (Dry 2002). With regards to FTS conversion technologies using biomass-generated syngas, there are still some barriers. The severe reaction conditions with high temperature and pressure limit the applications and require high energy inputs. In addition, the heat removal duty resulting from the strong exothermic

reactions during the process is still a serious challenge. Also, the selectivity of catalytic conversion is low and some catalysts are very sensitive to biomass-generated syngas contaminants and are easily poisoned (Subramani 2008).

Fermentation of syngas. An alternative route to metal-catalytic conversion of syngas is fermentation of syngas to fuels. Several microbial catalysts (bacteria) are capable of consuming syngas and producing useful end-products, including alcohols and acids. Although there are still some challenges with this method, including biomass availability, process efficiency, and sustainability of bio-refinery facilities, the bio-catalytic method is a promising technology. This method circumvents problems such as high pressure, high temperature, and catalyst poisoning for metal-catalytic ethanol production (Ragauskas 2006). However, there are still many areas to address with regards to sustainability of a commercial process including bioreactor design, syngas impurity effects on the process, utilization efficiency of the syngas, and ethanol productivity. In general, ethanol production from syngas fermentation has great potential but many issues still need to be addressed. The focus of this work is related to the syngas fermentation process.

Although there are several different methods for ethanol production, no one is commercially perfect. One problem with corn fermentation is that the production process has a low energy output/input ratio compared to cellulosic processes. For example, the ratio of energy output to fossil energy input (in planting corn, fertilizer, transportation, etc.) in the corn fermentation processes is estimated to be at best 1.3:1 and at worst 0.9:1 (Hill 2006, Pimentel 2001; Patzek 2005). As a comparison, although the reported values vary for cellulosic processes, the realistic estimate of the ratio of energy output to fossil energy input is about 10:1, suggesting a strong potential for a viable biomass to ethanol process (Kim 2005; Wang 2005; Wang 2007).

Besides a higher energy output/input ratio, ethanol production from cellulosic processes appears to be a more economical route than the starch/sugar process because of the abundant availability of cellulosic material and the renewable nature of cellulose (Lynd 1996). A wide variety of raw materials can be utilized as a feedstock such as prairie grasses, wood chips, solid municipal wastes, paper wastes and agricultural residues (Lynd 1996). From a U.S. Department of Energy report, 550 million acres of land could be potentially used for energy crops, which could produce 10.8 million barrels/day of fuel ethanol (DOE, 2005). In comparison, the crude oil imported by US is 12.0 million barrels/day in 2007 (DOE, 2010). (Although the theoretical fuel ethanol production seems to be close to the amount of imported crude oil, it is unlikely that fuel ethanol will solely eliminate the dependency on imported oil due to potential limitations associated with biomass growth, transportation, and production. A more realistic route to replace imported oil will likely be associated with multiple forms of various alternative fuels.)

In cellulosic platforms for ethanol production, cellulosic gasification has advantages over cellulosic fermentation in that gasification is also well-suited to raw materials such as softwoods that are normally difficult to handle (Dayton 2003). A second main advantage is that gasification can break cellulosic, hemicellulosic and lignin bonds that are difficult to break using fermentative or enzymatic reactions. Thus, cellulosic gasification to syngas seems to provide a greater carbon conversion potential to ethanol as compared to the cellulosic fermentation process (McKendry 2002). A general introduction of this route would be helpful to understand this emerging ethanol production method.

1.4 Metabolic pathway of syngas fermentation

Several organisms can convert syngas to ethanol and acetic acid, including *Clostridium ljungdahlii, Clostridium autoethanogenum, and Clostridium. carboxidivorans* (Abrini 1994., Vega 1990). Recently, *Clostridium* strains P7 (Liou 2005) and P11 (Kundiyana 2010) have also been shown to produce ethanol and acetic acid from syngas. These microbes are novel solvent-producing anaerobic microbial catalysts that were isolated from the sediment of an agricultural settling lagoon. *Clostridium* P7 forms acetate, ethanol, butyrate, and butanol as end-products. The optimum pH range for this strain is 4.5-7.0 and the optimum temperature range is 37-40 ºC (Liou 2005). The bacterium used in this project is *Clostridium* strain P11.

Syngas fermentation in the above *Clostridium* follows the acetyl-CoA (Wood-Ljungdahl) pathway, which is shown in Figure 1-4 (Wood 1986; Ljungdahl 1986). In the acetyl-CoA metabolic pathway, CO and/or CO_2, as carbon sources, are converted into the two-carbon acetyl-CoA intermediate through two different branches. In the methyl branch, one CO_2 molecule is converted to a methyl moiety. During the conversion, six electrons and one ATP are utilized. In the carbonyl branch, two electrons are utilized to reduce one CO_2 molecule to CO via the carbon monoxide dehydrogenase (CODH) enzyme. CO is then incorporated with the methyl moiety to form acetyl-CoA via the acetyl-CoA synthase enzyme. CO can also be used to form acetyl-CoA directly, rather than being produced from CO_2 reduction. Once acetyl-CoA is produced, it can be used for producing cell mass, ethanol, and/or acetic acid.

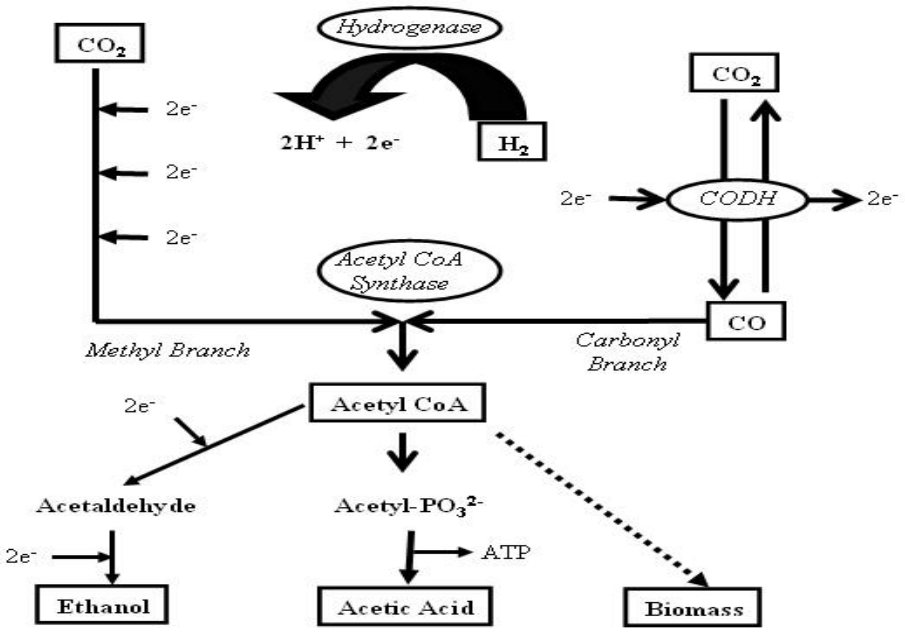

Figure 1-4.Part of the Acetyl-CoA (Wood-Ljungdahl) pathway (Hurst 2010)

1.5 Stoichiometry of ethanol and acetate production

As noted above, the conversion from syngas to product is electron intensive. Electrons required for the metabolic process are donated by reduced electron carriers that obtain electrons from either H_2 via the hydrogenase enzyme and/or from CO via the CODH enzyme. Although there are many electron carriers, common two-electron carrier pairs found in biological systems include NAD^+/NADH, $NADP^+$/NADPH, and ferredoxin (Ragsdale, 2008). For example, if NAD^+/NADH is the electron carrier pair, the electron production reactions from H_2 and CO are:

$$H_2 + NAD^+ \leftrightarrow H^+ + NADH \quad (1.1)$$

$$CO + H_2O + NAD^+ \leftrightarrow CO_2 + H^+ + NADH \quad (1.2)$$

Recall that $NADH/NAD^+$ is only one pair of possible electron carriers. If other electron carrier pairs are involved in the reaction, such as ferredoxin or $NADPH/NADP^+$, the oxidized and reduced forms of the carrier pairs could replace the respective electron carrier pairs in reactions 1.1 and 1.2.

For the carbon utilization associated with product formation of ethanol and acetic acid, both CO and CO_2 can be used as carbon sources. The general reaction for ethanol production from both CO and CO_2 (ignoring details such as ATP utilization) is:

$$CO + CO_2 + 5\ NADH + 5\ H^+ \leftrightarrow C_2H_6O + 5\ NAD^+ + 2\ H_2O \quad (1.3)$$

With only CO_2 as the carbon source, the reaction is:

$$2\ CO_2 + 6\ NADH + 6\ H^+ \leftrightarrow C_2H_6O + 6\ NAD^+ + 3\ H_2O \quad (1.4)$$

With only CO as the carbon source, the reaction is:

$$2\ CO + 4\ NADH + 4\ H^+ \leftrightarrow C_2H_6O + 4\ NAD^+ + H_2O \quad (1.5)$$

During syngas fermentation (reactions 1.3 through 1.5), reducing equivalents (e.g. NADH molecules containing two electrons) are required to reduce CO and/or CO_2 to ethanol. The required electrons come from H_2 (reaction 1.1) and/or CO (reaction 1.2). However, for syngas fermentation, the most efficient process for converting available carbon (both CO and

CO_2) to carbon-containing products would involve utilization of H_2first rather than CO to obtain needed electrons.

If all electrons come from H_2 (reaction 1.1), the following overall reactions associated with reactions 1.3 to 1.5 become:

$$CO + CO_2 + 5\ H_2 \leftrightarrow C_2H_6O + 2\ H_2O \quad (1.6)$$

$$2\ CO_2 + 6\ H_2 \leftrightarrow C_2H_6O + 3\ H_2O \quad (1.7)$$

$$2\ CO + 4\ H_2 \leftrightarrow C_2H_6O + H_2O \quad (1.8)$$

In these three reactions, the conversion efficiency from the carbon source (CO and CO_2) to ethanol is 100%. However, the feasibility of such a conversion would depend upon fermentation conditions such as the gas composition, efficiency of enzymes, and the thermodynamically-preferred pathways.

If CO is used as an electron source when H_2 is present, the oxidized product in the form of CO_2 may potentially become a lost carbon source for product formation. Thus, the carbon conversion efficiency of CO to product formation would be reduced. The most inefficient process for converting available carbon (both CO and CO_2) to carbon-containing products would involve utilization of CO rather than H_2 to obtain needed electrons. If all electrons come from CO (reaction 1.2), reactions 1.3 to 1.5 all result in the same net overall reaction:

$$6\ CO + 3\ H_2O \leftrightarrow C_2H_6O + 4\ CO_2 \quad (1.9)$$

In this case, the conversion efficiency from carbon source (CO) to ethanol is only 33%. Thus, based on the two scenarios of either H_2 as the sole electron source or CO as the sole electron source, the carbon-conversion efficiency can range from 33% to 100%. It is clear that the best scenario for ethanol production is when H_2 can be the sole source.

For acetate production, the three reactions when CO/CO_2, only CO_2, or only CO is present as the carbon source are, respectively:

$$CO + CO_2 + 3\ NADH + 3\ H^+ \leftrightarrow C_2H_4O_2 + 3\ NAD^+ + H_2O \quad (1.10)$$

$$2\ CO_2 + 4\ NADH + 4\ H^+ \leftrightarrow C_2H_4O_2 + 4\ NAD^+ + 2\ H_2O \quad (1.11)$$

$$2\ CO + 2\ NADH + 2\ H^+ \leftrightarrow C_2H_4O_2 + 2\ NAD^+ \quad (1.12)$$

Again, the most efficient process for converting available carbon (both CO and CO_2) to acetate would involve utilization of H_2 rather than CO to obtain needed electrons. If all electrons are from H_2 (reaction 1.1), the overall stoichiometry for acetate production becomes:

$$CO + CO_2 + 3\ H_2 \leftrightarrow C_2H_4O_2 + H_2O \quad (1.13)$$

$$2\ CO_2 + 4\ H_2 \leftrightarrow C_2H_4O_2 + 2\ H_2O \quad (1.14)$$

$$2\ CO + 2\ H_2 \leftrightarrow C_2H_4O_2 \quad (1.15)$$

In these three overall reactions, the conversion efficiency from the carbon source (CO and CO_2) to acetate is 100%. Similarly, when all electrons come from CO, the overall stoichiometry for the most inefficient process for syngas fermentation is:

$$4\ CO + 2\ H_2O \leftrightarrow C_2H_4O_2 + 2CO_2 \quad (1.16)$$

In this case, the conversion efficiency of carbon is reduced to 50%.

1.6 Concerns regarding ethanol production from syngas

For ethanol production via syngas fermentation, several issues must be addressed to assess the commercial viability of the process. These issues include carbon utilization efficiency, cell growth, ethanol production, product distribution, gas mass transfer rates, effects of syngas impurities, energy output vs. input, and product recovery. This work will focus on the issues of carbon utilization efficiency and possible methods to increase cell growth and ethanol production.

The highest carbon utilization efficiency would be achieved if all electrons came from H_2. In practice, although it is very unlikely that there would be sufficient H_2 in syngas to provide all electrons, the question arises as to whether H_2 can be utilized in favor of CO for electron production (when both species are present) the highest possible efficiency of CO conversion to products. As can be seen from reactions 1.1 and 1.2, several important experimental parameters, such as pH, NADH/NAD^+ (related to redox potential), and gas partial pressures could affect the reactions contributing to electron production that can affect carbon conversion efficiency. Thus, it is important to assess the effects of these factors on syngas fermentation.

Besides the carbon conversion efficiency, the carbon utilization reactions (1.3 through 1.5 for ethanol production, and 1.10 through 1.12 for acetate production) show that NADH/NAD^+ and H^+ are always involved. Because H^+ and NADH are reactants and NAD^+ is a product of the mentioned reactions, an obvious hypothesis is that higher H^+ concentrations (i.e. lower pH) and

higher NADH/NAD^+ ratios favor cell growth and product formation during syngas fermentation. However, it is not clear how these factors quantitatively change cell growth as well as the relative production between ethanol and acetate. Thus, a quantitative assessment of these factors on cell growth and product formation is additionally beneficial for understanding the process of syngas fermentation.

Experimentally, the concentration of H^+ is directly related to the pH of the system so that H^+ effects can be assessed easily. For the NADH/NAD^+ ratio, it is difficult to monitor directly. However, as reducing equivalents, ratios of NADH/NAD^+ or other electron carrier pairs are strongly affected by the redox potential (E) of the system (Lee 2008). Thus, this work will quantitatively explore key fermentation parameters (pH, redox potential, ionic strength, and gas partial pressures) associated with electron production, the metabolic pathways (related to conversion efficiency), and the resulting cell growth and product formation of ethanol and acetic acid during syngas fermentation.

1.7 Research objectives

Objective #1: Thermodynamic modeling of electron production

As noted above, the dual functionality of CO as both a carbon source and an electron source has major implications since CO utilization for electron production comes at the expense of using the carbon of CO for product formation. The aim of this objective was to explore the relative thermodynamic favorability of electron production from H_2 and CO. A thermodynamic model was developed to assess the effects of pH, ionic strength, gas partial pressure, and electron carriers on whether H_2 or CO is the preferred source of electron production during typical syngas fermentation conditions.

Objective #2: Thermodynamic modeling of metabolic pathway

Since the reactions noted above for ethanol and acetic acid production actually involve several metabolic pathway steps, the redox potential, pH and gas partial pressures can greatly affect key steps in the pathway. The aim of this objective was to assess the thermodynamics of metabolic pathway steps to determine potential limiting steps during syngas fermentation. The analysis would enable recommendations of design strategies (pH, redox potential, gas partial pressure) regarding bioreactor design and fermentation optimization. To achieve this objective, a thermodynamic model of the acetyl-CoA metabolic pathway based on transformed thermodynamics was developed and a detailed hypothetical analysis of varying pH, electron carrier ratio, and gas partial pressure was conducted to address potential bottleneck issues.

Objective #3: Assessing the fate of cysteine-sulfide in bioreactors

Since reducing equivalents (for example $NADH/NAD^{+}$) are strongly affected by the redox potential of the system and can thus affect the product formation, the analysis of the fate of cysteine-sulfide in bioreactors was studied. Cysteine-sulfide is widely used as a reducing agent for changing the redox potential of fermentation systems. Preliminary studies showed that sulfide does not remain at initial concentrations in bioreactors such that the redox potential can change during fermentation if redox is not controlled. The aim of this objective was to determine why and how the sulfide concentration changes and the associated effect on the redox potential. The rate of sulfide loss was measured and models regarding sulfide loss in batch and continuous reactors were proposed. The assessment of the fate of sulfide enables the ability to experimentally design bioreactors which are able to maintain desired sulfide concentrations in order to assess sulfide effects on growth and product formation during syngas fermentation.

Objective #4: Modulating sulfide to enhance fermentation

The aim of this objective was to explore how cysteine and sulfide under both controlled and non-controlled conditions can affect syngas fermentation. Based on the model developed in the previous objective, studies in which the cysteine and sulfide levels were maintained at a given concentration were performed to assess the effects of cysteine and sulfide on growth and product formation.

Objective #5: Enhancing syngas fermentation via adjusting redox potential (E) and pH

Besides the addition of external reducing agents (cysteine-sulfide, cysteine, or sulfide), redox potential is an intrinsic factor associated with the reducing equivalents (for example $NADH/NAD^+$), which are involved in the reactions along the metabolic pathways of syngas fermentation. Also, pH is another important factor which is associated with the concentration of H^+ during syngas fermentation. The aim of this objective was to explore how the syngas fermentation can be optimized by adjusting redox potential and pH. The purpose for the pH control is that the redox potential is likely associated with the pH. These two factors have to be assessed together. Experiments with controlled redox levels and pH were performed to assess whether control of the external redox potential (as compared to intrinsic control by cells) can be used to optimize the fermentation process. In addition, since the optimum experimental conditions may vary for cell growth and product formation, experiments with adjusting redox potential and pH during the fermentation were conducted. Experimental results were connected with the thermodynamic analysis from Objectives #1 and #2 to help understand the fermentation process that could lead to optimized design conditions.

2. Literature review

The purpose of the work presented in this dissertation is to assess key fermentation aspects that could lead to a more efficient syngas fermentation process. A more efficient process would result in increased cell growth and ethanol production, as well as a decrease in the variability of the syngas fermentation process. The following literature review and preliminary studies outlines the current state of syngas fermentation and identifies areas for research with regards to syngas fermentation.

2.1 Reactions involved in acetyl-CoA pathway

An introduction of the metabolic pathway for syngas fermentation was briefly outlined in Chapter 1. In this section, the reactions involved in the acetyl-CoA pathway are more extensively reviewed. This is beneficial for further discussion regarding electron sources and metabolic pathway modeling. The Acetyl-CoA (or Wood-Ljungdahl) metabolic pathway for ethanol or acetic acid production (excluding cell growth) consists of 13 enzymatic steps composing a methyl and a carbonyl branch (Ljungdahl 1986) as shown in Figure 2-1. During fermentation, acetyl-CoA (CH_3COO-COOA) is formed as an intermediate of the metabolic pathway. Once formed, acetyl-CoA can then be used in a variety of ways: building block for cell material, acetate, or liquid fuels such as ethanol and butanol. The two predominant paths discussed in this

project are the formation of acetate (also known as acetogenesis) and the formation of ethanol (also known as solventogenesis). In the pathway, two electron production reactions (from either H_2 or CO) are critical for product formation.

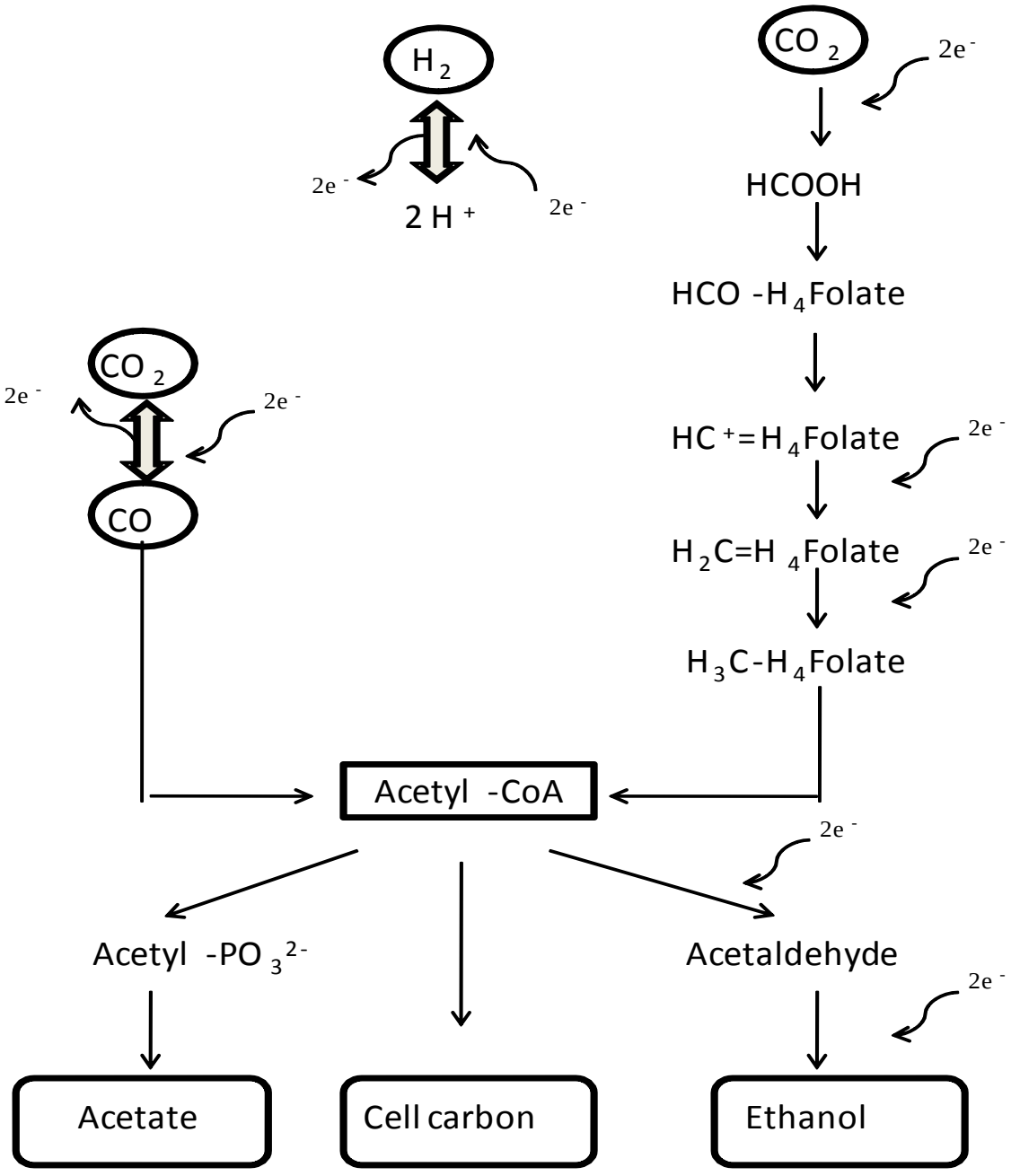

Figure 2-1.Simplified Acetyl-CoA metabolic pathway

2.1.1 Electron production

The entire metabolic pathway (Figure 2-1) is in essence a series of reducing reactions which reduce CO and CO_2 to ethanol and acetate. Electrons required for the metabolic process are donated by reduced electron carriers that obtain electrons from either H_2 via the hydrogenase enzyme and/or from CO via the CODH enzyme as shown:

$$H_2 \leftrightarrow 2\ H^+ + 2\ e^- \quad (2.1)$$

$$CO + H_2O \leftrightarrow CO_2 + 2\ H^+ + 2\ e^- \quad (2.2)$$

Common two-electron carrier pairs found in biological systems include NAD^+/NADH, $NADP^+$/NADPH, and ferredoxin (Ljungdahl 1986). The electron carriers for every step depend on the bacterium and the fermentation condition (Ragsdale 2008). Currently, the electron carriers for *Clostridium P11* have not been identified. For most of the work addressed in this study, the reducing equivalents utilized in reactions along the metabolic pathway are expressed as $NADH/NAD^+$ since this electron carrier pair is very common in physiological systems. In some cases, ferredoxin as an electron carrier is also addressed. One notable aspect of using $NADH/NAD^+$ is that the concentration data are readily available in published literature (Girbal 1995; Guedon 2000; Desvaux 2001).The details of these two reactions regarding the electron production and the possible carbon utilization efficacy will be discussed in Chapter 3.

2.1.2 Methyl branch

In the methyl branch of the metabolic pathway, one molecule of CO_2 is converted to formate, which binds with H_4folate and is eventually reduced to a methyl moiety through the following reactions (Ljungdahl 1986):

$$CO_2 + NADH + H^+ \leftrightarrow HCOOH + NAD^+ \quad (2.3)$$

$$HCOOH + ATP + H_4Folate \leftrightarrow HCO\text{-}H_4Folate + ADP + P_i \quad (2.4)$$

$$HCO\text{-}H_4Folate + H^+ \leftrightarrow CH^+\text{=}H_4Folate + H_2O \quad (2.5)$$

$$CH^+\text{=}H_4Folate + NADH \leftrightarrow CH_2\text{=}H_4Folate + NAD^+ \quad (2.6)$$

$$CH_2\text{=}H_4Folate + NADH + H^+ \leftrightarrow CH_3\text{-}H_4Folate + NAD^+ \quad (2.7)$$

Step 2.3 is the reduction of CO_2 to formate (HCOOH) by the enzyme formate dehydrogenase (FDH) with the help of reducing equivalents. Steps 2.4 through 2.7 involve the cofactor tetrahydrofolate (H_4Folate). In step 2.4, formate is bound to H_4Folate to form a formyl group (HCO-H_4Folate) at the expense of one ATP. Finally, steps 2.5 through 2.7 are a series of reducing reactions to reduce the bound formyl to a bound methyl group (CH_3-H_4Folate).

Notably, though the methyl branch starts with the reduction of CO_2, if CO is available, CO can be oxidized to CO_2 in step 2.2 from which a portion of the CO_2 (but not all) can then be used as a carbon source. Obtaining reducing equivalents from CO would reduce the conversion efficiency of CO to product.

2.1.3 Carbonyl branch and acetyl-CoA synthesis

In the carbonyl branch, CO is incorporated with the methyl moiety (CH_3-H_4Folate) which is produced from the methyl branch to form acetyl-CoA via the acetyl-CoA synthase enzyme (ACS).

$$CH_3\text{-}H_4\text{Folate} + CO + CoA \leftrightarrow \text{Acetyl-CoA} + H_4\text{Folate} \quad (2.8)$$

During this step, H_4Folate in the methyl moiety is released and is then recycled in the methyl branch. Of course, when CO_2 is present, CO_2 may be reduced to CO via CODH and CO is in turn involved in reaction 2.8. The conversion from CO_2 to CO is just the reverse reaction of 2.2:

$$CO_2 + 2\ H^+ + 2\ e^- \rightarrow CO + H_2O \quad (2.2\ a)$$

2.1.4 Fate of Acetyl-CoA

Acetyl-CoA is an important metabolic intermediate. It is the source for cellular carbon as well as cellular energy. The pathway of acetyl-CoA for cell growth is often associated with the production of acetate. However, other products, such as ethanol, butanol, and butyrate, may also be formed (Ljungdahl 1986). To produce acetate, acetyl-CoA releases CoA via the enzyme phospho-transacetylase in step 2.9.

$$\text{Acetyl-CoA} + P_i \leftrightarrow \text{Acetyl-}P_i + CoA \quad (2.9)$$

Then, the resulting acetyl phosphate is reacted with ADP to produce acetate ($C_2H_4O_2$) and generate ATP in step 2.10.

$$\text{Acetyl-}P_i + ADP \leftrightarrow C_2H_4O_2 + ATP \quad (2.10)$$

This branch of the pathway is usually favored by the bacterium during its exponential growth phase as it provides the bacterium with energy in the form of ATP. It is often known as the acetogenic phase of metabolism, which also results in a decrease in pH of the medium due to acid production (Rao 1987). It is important to note that one ATP is consumed in step 2.4 and one ATP is produced in step 2.10. Thus, the net ATP for acetate production is zero. Since ATP is required for growth, ATP must additionally be produced from outside of the Woods-Ljungdahl pathway. Two chemiosmotic mechanisms have been proposed, either a proton gradient is generated to synthesize proton-dependent ATP production or a sodium gradient is generated to synthesize sodium-dependent ATP. The proton-gradient mechanism has been shown to involve an electron transport system and has often been associated with the presence of enzymes which generate electrons (Drake 2004). Thus, electron production from H_2 and CO (reactions 2.1 and 2.2) can contribute to ATP production. It should also be noted that electrons utilized in the production of ATP are not consumed and can therefore still be utilized in the metabolic pathway to produce alcohols or acids.

Besides forming cell mass and acetate via acetyl-CoA, ethanol is also produced through reactions 2.11 and 2.12.

$$\text{Acetyl-CoA} + NADH + H^+ \leftrightarrow C_2H_4O + CoA + NAD^+ \quad (2.11)$$

$$C_2H_4O + NADH + H^+ \leftrightarrow C_2H_6O + NAD^+ \quad (2.12)$$

Acetyl-CoA is reduced to acetaldehyde in step 2.11 via acetaldehyde dehydrogenase followed by the reduction of acetaldehyde to ethanol in step 2.12 via alcohol dehydrogenase. The reactions for acetate and ethanol from the same intermediate acetyl-CoA suggest a possible strategy for product selectivity. Production of acetate from acetyl-CoA generates ATP, which is associated with cell growth. However, production of ethanol consumes reducing equivalents (for example NADH), which is strongly associated with the redox potential of the system. Besides two-carbon products (acetate, ethanol), four-carbon products, such as butyric acid and butanol, are also able to be formed by joining two molecules of acetyl-CoA although the production is often more difficult. In Chapter 3, reactions regarding the electron production will be discussed for addressing the efficacy of carbon utilization. In Chapter 4, discussion regarding the reactions involved in the metabolic pathway will be addressed for outlining the strategies on the cell growth and product formation enhancement.

2.2 Current studies on syngas fermentation

Syngas fermentation for ethanol production based on the acetyl-CoA metabolic pathway is an emerging area and the research on the process is far from being thoroughly understood. So far, results from published literature show that temperature, pH, reducing agents, redox potential, gas partial pressure, gas compositions, and media components have significant effects on cell growth and ethanol production (Abrini 1994; Hurst 2010). Optimization of these parameters is critical for assessing the potential sustainability of ethanol from syngas.

Studies have shown that bacteria utilizing the acetyl-CoA metabolic pathway usually show a “biphasic batch fermentation pattern” (Girbal 1995).The bacteria produce acids such as acetate during their exponential growth phase (acetogenesis) and then switch to ethanol production when the bacteria enter the stationary phase (solventogenesis). Several factors have been found to affect this switch from acetogenesis to solventogenesis, such as pH, ATP demand, availability of nutrients, availability of reducing equivalents, and enzyme activities (Meyer 1986).

During the last several years, a greater understanding regarding cell growth has been made. For instance, one study regarding syngas fermentation using *Clostridium P7* shows that a higher CO partial pressure results in faster cell growth and higher ethanol production (Hurst 2010). Another study on syngas fermentation using *Clostridium P11* assessed the feasibility of incorporating cotton seed extract (CSE) as a media component, showing that CSE can replace all the vitamin and mineral media components in the normal media, which has potential to greatly reduce the cost of media preparation (Kundiyana 2010). Nevertheless, all the reported values show that cells grow much slower than typical bacteria, which have growth rates of ~1 hr^{-1} (Blanch and Clark, 1997). Bioreactor design and process optimization need to be done to increase growth rates.

Another potential issue which may limit the application of syngas fermentation is the relatively low conversion from carbon source to product. Yields for the conversion of CO to ethanol, as calculated from laboratory-scale experiments, are shown in Table 2-1. In general, most studies showed yields of 15-25%. According to the stoichiometry analysis of Equation 1.9 where CO alone is used as the carbon and electron source, the molar theoretical yield is 17%. If H_2 was also present and used as the sole electron source, the maximum yield would increase to

100% (see reaction 1.6). Although all studies did include H_2, the studies in which yields approached 17% suggest that the cells preferred growth on CO alone (i.e. CO was used as both an electron source and a carbon source). For the study where the yield was 25%, H_2 must have been used (at least partially) for the electron source. Although a general conclusion can be derived indirectly from the yields, the reason for the CO preference over H_2 is still unclear. In Chapter 3, a thermodynamic analysis regarding CO and H_2 preference as electron source will be discussed.

Table 2-1.Yield of ethanol from CO (Lewis 2010)

Microorganism	Yield (mol ethanol/mol CO)	Reference
C. ljungdahlii	0.008	Vega 1989
C. ljungdahlii	0.25	Younesi 2005
C. carboxidivorans	0.15	Rajagopalan 2002
C. carboxidivorans	0.16	Liou 2005

From preliminary studies, *Clostridium* P11 was observed to follow the biphasic batch fermentation pattern in both batch and continuous reactors. In addition, ethanol production in continuous reactors was more than double that in batch reactors as shown in Figure 2-2. (Note that a part of the experimental data in Figure 2-2 is from Frankman 2009). Except for the ethanol production in Continuous Run #6, results from other runs are very consistent with each other. When cells reached the stationary phase (Days 6 to 10), the average cell mass in both batch and continuous bioreactors were at the same level, ranging from 0.30 to 0.32 g/l. However, the rates

of ethanol production were different as noted by the higher ethanol concentrations obtained with the continuous reactors. The rates during non-growth phase in continuous and batch bioreactors, on a per mass basis, were observed as 3.2 and 1.5 g day^{-1} g^{-1}_{cell}, respectively.

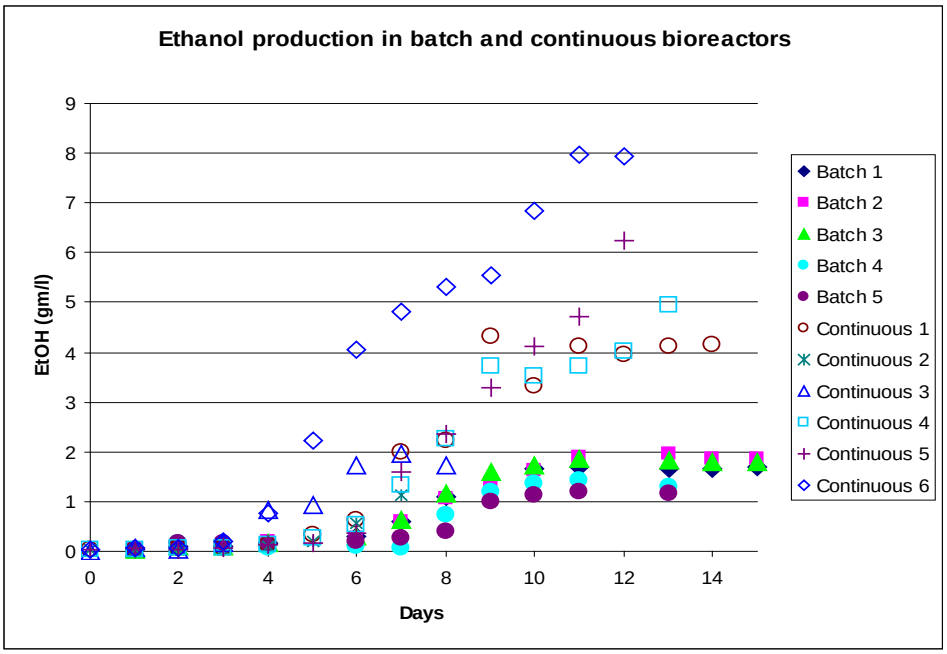

Figure 2-2.Ethanol production in batch-gas and continuous-gas bioreactors

Furthermore, as observed in Figure 2-3, a conversion from acetic acid to ethanol was observed in the continuous reactors after the acetic acid concentration reached a maximum, but the conversion was not observed in the batch reactors. Research on syngas fermentation via *Clostridium* P11 is still in the beginning phase. From the preliminary studies, it is clear that the cell concentration is low (<0.32 g/l), ethanol concentration is low (<9 g/l), and the ethanol production rate is also not fast (~3.2 g day^{-1} g $^{-1}$cell). More interestingly, although Continuous Run #6 started with the same conditions of the other runs, the ethanol production was much

higher than with the other runs. The differences may be from the random errors from run to run, or from the variations caused by the physiological processes of bacteria. Such variability results in the difficulty of analyzing the experimental results and may lead to confounded conclusions. It is of interest to conduct experiments with controlled conditions to diminish the variance as well as to increase both cell growth and ethanol production.

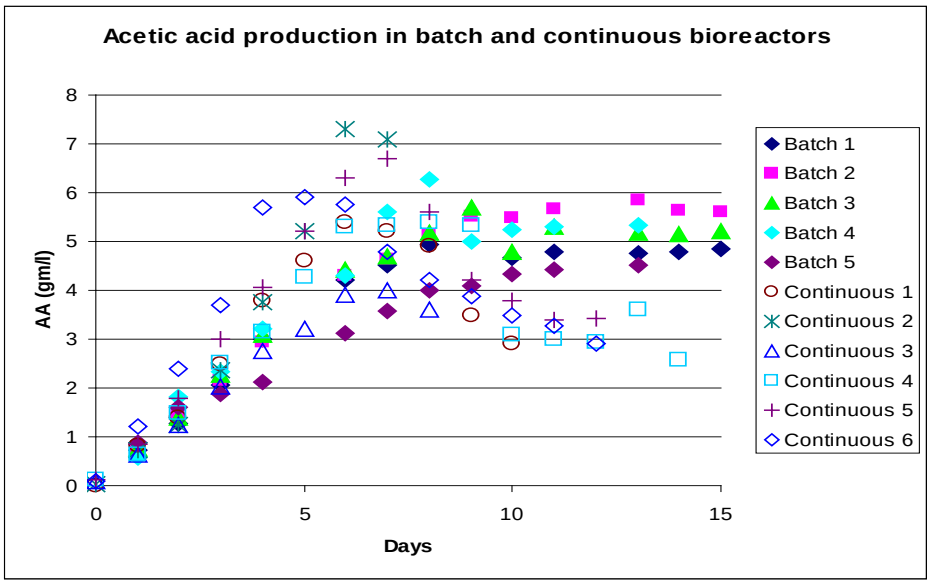

Figure 2-3.Acetate production in batch-gas and continuous-gas bioreactors

Based on the above findings and literature review, syngas fermentation is a promising technology but the research is still in the very beginning phase. As is evident from the review, several key issues, such as cell growth, ethanol production, gas utilization efficiency, mass transfer, product distribution, gas impurities, and product recovery, still need to be addressed to assess the efficiency of syngas fermentation. In this work, both thermodynamic modeling (Chapter 3, 4) and laboratory experiments (Chapter 5, 6, 7) were conducted to help provide more

clarity to syngas fermentation issues, specifically with regard to assessing effects of gas partial pressure, reducing agents (i.e. redox potential), and pH on issues of carbon utilization efficiency, cell growth, and product formation.

2.3 Transformed thermodynamics

Syngas fermentation is a complicated process with numerous reactions involved. A thermodynamic analysis can be utilized to compare the relative favorability of reactions involved in the acetyl-CoA metabolic pathway, which is beneficial to address the issues such as whether CO or H_2 is more favorable for electron production, or what key bottlenecks are associated with ethanol production. The criterion for spontaneous change, or "driving force", of a reaction is provided by the Gibbs free energy change of the reaction. A negative Gibbs free energy of the reaction means that the reaction will proceed forward. A positive Gibbs free energy of the reaction means that the reaction will go in the reverse direction. If the Gibbs free energy is zero, equilibrium is obtained. The more negative the Gibbs energy change of reaction, the higher the "driving force" for the reaction, which translates into higher favorability for the reaction in question. However, conditions common in biological systems i.e., changing pH, ionic strength, etc., impact traditional thermodynamics to such an extent as to render traditional thermodynamic analysis of biological systems impractical and invalid. Also, species in biological systems often have multiple forms. For example, ATP has forms of ATP^{4-}, $HATP^{3-}$, H_2ATP^{2-}, etc. Thus, a reaction involving ATP may be actually a series of simultaneous reactions with multiple forms. This issue increases the complication of traditional thermodynamic analysis.

A method was developed recently, designated as transformed thermodynamics, for deriving transformed Gibbs free energies (which included the Debye-Hückel theory). This method enables effective thermodynamic analysis in biological systems which include multiple forms of species involved in reactions. Substitution of classical Gibbs free energies with these transformed Gibbs free energies will therefore accommodate accurate thermodynamic analysis of biological systems in aqueous solution (Alberty 2000; 2001). Another advantage is that the pH and ionic strength are embedded in the transformed thermodynamic properties. Therefore, once the transformed Gibbs free energy of formation for each species is tabulated, calculating the Gibbs free energy of reaction with varying pH and ionic strength is simple. It should be noted that transformed values at various pH, temperature, and ionic strengths have not been reported. The work reported in Chapters 3 and 4 extends the transformed thermodynamic analysis over a broader range. A thermodynamic model was developed in Chapter 3 to assess whether H_2 or CO is the preferred source of electron production during typical syngas fermentations. In Chapter 4, the acetyl-CoA metabolic pathway was modeled and a hypothetical analysis of varying experimental conditions was conducted to address potential bottleneck issues of the metabolic pathway.

2.4 Reducing agents used in anaerobic fermentation

Reducing equivalents, which are related to electron production, gas utilization efficiency, and reducing reactions involved in the metabolic pathway, are very critical in syngas fermentation. During the fermentation process, the environment should be anaerobic with a negative redox potential since the metabolic process is highly reductive. The redox potential is

defined as the affinity of a chemical solution for electrons compared with hydrogen. It describes all chemical reactions in which atoms have their oxidation number changed. In the media surrounding the cells, oxidation reactions happen at a more positive redox potential and reduction reactions happen at a more negative redox potential—the latter being critical for ethanol production.

Many studies have focused on reducing agents used to adjust the redox potential such as sodium sulfide, cysteine, titanium (III)-citrate, potassium ferricyanide, and methyl viologen (Bryant 1961; Rao 1987; Jee 1987; Sridhar 2001). Cysteine-sulfide is one of the widely used reducing agents for anaerobic fermentation. It can scavenge residual O_2, lower the redox potential, or possibly act as a sulfide source for cell growth or enzyme reactions. However, cysteine-sulfide (or sulfide alone) studies have shown some contradictory results during fermentation. Some work has showed that sodium sulfide has positive effects on anaerobic fermentation. Bryant's studies using *Ruminal bacteria* showed that cells could not grow without reducing agents, and low levels of Na_2S alone or in combination with cysteine resulted in higher cell growth than cysteine alone (Bryant 1961). From Shah's studies using *Clostridium thermoaceticum*, the substitution of Na_2S for cysteine resulted in a greater acetic acid yield (Shah, 1997).

On the other hand, others presented opposite results that showed sodium sulfide had no effects on cell growth or was worse than other reducing agents. From Jones' research using *Rumen bacteria*, cells could grow in the environment without any reducing agent (Jones 1980). In Gaddy's patent using *Clostridium ljungdahlii*, no sulfide was involved in the optimized media recipe (Gaddy 1997). Another study showed that the substitution of titanium citrate for sodium sulfide greatly improved the growth of *Methanolthermus-fervidus* and increased the production

of methanol (Pepper 1993). Sim's results showed that sodium sulfide had no effect on the growth of *Clostridium aceticum* (Sim and Kamaruddin 2008). Furthermore, the optimal sulfide concentrations used in fermentations varied greatly, ranging from 0.05 g/L to 35 g/L (Bryant 1961; Rao 1987; Jee 1987; Shah 1997; Sridhar 2001; Kaden 2002; Balusu 2005).

A variety of reducing agents may be used to adjust the redox potential of the media and the effects of these reducing agents are strongly dependent upon the bacterium and system. Therefore, to develop a viable commercial process for syngas fermentation to ethanol, it is important to understand the effects of reducing agents, such as sulfide, on cell growth and ethanol production. The assessment and applications of reducing agents on syngas fermentation optimization are discussed in Chapters 5 to 6. In Chapter 5, the fate of sulfide in a continuous-gas and batch-gas bioreactor are assessed and modeled. In addition, the associated effect on the redox potential was assessed. The model enables experiments to be designed for bioreactor studies to maintain desired sulfide concentrations. Maintaining constant sulfide levels provides a more efficient assessment of sulfide effects on growth and product formation during syngas fermentation, which is discussed in Chapter 6.

2.5 Redox potential and pH effects on fermentation

In addition to research focusing on reducing agents during anaerobic fermentation, several studies focusing on the redox potential have also been reported. Studies have shown that the redox potential is correlated with cell growth and product formation (Kim 1988). In Kim's study using *Clostridium acetobutylicum*, it was shown that the maximum productivity of butanol and butyric acid were both found at a redox potential of -250 mV. The specific production was

also affected by the redox potential. Additional studies have shown that the redox potential affects cell's growth and the switch between acetogenesis and solventogenesis (Rao 1987; Kwong 1992; Jee 1987). An excess availability of reducing equivalents has been found to initiate solventogenesis (Girbal 1995; Meyer 1986). Artificial electron carriers like methyl viologen, benzyl viologen and neutral red are known to alter the electron flow by forming NADH, which in turn promotes alcohol production (Girbal 1995; Klasson 1992). Girbal et al. (1995) demonstrated that adding 1mM neutral red to an acetogenic culture caused a deviation in the electron flow towards NADH production. This pool of NADH generated might be responsible for the change in the metabolism of the bacteria towards solventogenesis. Girbal et al. reported a 3-fold increase in ethanol production on the addition of 1mM neutral red to *C. acetobutylicum* cultures (Girbal 1995). Other research showed that the NAD_{red}/NAD_{ox} concentration ratio is strongly correlated with the redox potential of the system (Lee 2008). Thus, the redox potential change in the bioreactor may affect the NAD_{red}/NAD_{ox} ratio, and further influence the cell growth and product formation.

Additional studies have shown that the redox potential affects the product distribution. In Sridhar's study (Sridhar 2001) using *Clostridium thermosuccinogenes*, the fraction of acetate, formate, lactate and ethanol was compared at different redox potentials. It showed that the fraction of product was affected by the redox potential of the system, and the effects were different for different products. For instance, lactate production was not significantly influenced by redox potential. However, a more negative redox potential was good for acetate and formate production, but bad for ethanol production.

Recent studies observed that *Clostridium* P11 bacteria grow at approximately -200 mV and the transition from acetogenesis to solventogenesis occurs with a drop of ~50 mV in the

redox level (Frankman 2009). However, additional experiments are required to assess that if maintaining the redox level at -200 mV can induce cells to grow to higher optical densities before leveling off; and if dropping the redox level by -50 mV earlier on in the experiment can induce ethanol production at an earlier time. Therefore, it is valuable to assess the effects of redox potential on the fermentation from syngas to acetic acid and ethanol by adjusting the redox levels of the media. Moreover, the optimal redox levels for cell growth and ethanol production need to be determined experimentally.

With regards to pH effects, one study showed the addition of acetate and butyrate to batch cultures was found to shorten the acetogenic phase and induce solventogenesis (Gottschal 1981). It was proposed by Gottschal that this was due to the dissipation of the pH gradient (Δ pH) by acetate and butyrate as the intracellular pH could achieve the same low value as the culture medium. The conclusion from Gottschal's work is that "though a low pH does not itself provoke solventogenesis, it does seem to be a prerequisite". Another study using *C. acetobutylicum* showed that the solventogenesis phase was induced in a lower pH range which resulted from the accumulation of acetate production (Long 1984). Although several studies regarding pH effects exist, the reason (e.g. pH, redox potential, etc.) why the switch from acetate production to ethanol production happens is still un-clear. Moreover, the levels of redox potential and pH associated with optimal cell growth and/or product formation vary significantly among bacteria and substrates. More importantly, redox potential and pH may interactively affect the fermentation. Research needs to be done in distinguishing these two factors. In Chapter 7, an optimization for syngas fermentation based on the thermodynamic models developed in Chapter 3, 4 and based on the experimental tools developed in Chapter 5, 6 were conducted by controlling pH and redox potential.

2.6 Conclusions

Based on the above literature review, syngas fermentation for ethanol production is still in the early stages of development. Several key issues that are addressed in this work include the following:

- Assessment of whether H_2 or CO is the preferred source of electron production during typical syngas fermentation conditions.
- Thermodynamic analysis of the metabolic pathway to assess the potential bottleneck steps on syngas fermentation, resulting in design strategy suggestions regarding bioreactor design and fermentation optimization.
- Assessment of the fate of reducing agents (cysteine-sulfide) and the associated redox potential associated with syngas fermentation.
- Assessment of the effects of sulfide in a controlled environment to explore how sulfide affects cell growth and product formation during syngas fermentation.
- Development of controlled redox potential experimental conditions, along with pH control, to assess not only the effect on cell growth and ethanol production, but also to reduce the variability of the fermentation parameters to better analyze experimental results.

3. Thermodynamic analysis of electron production

3.1 Introduction

Syngas fermentation typically follows the acetyl-CoA (or Wood-Ljungdahl) pathway in which CO and/or CO_2, as carbon sources, are converted into the two-carbon acetyl-CoA intermediate through two different branches (Ljungdahl 1986). In the methyl branch, one CO_2 molecule is converted to a methyl moiety. During the conversion, six electrons are utilized. In the carbonyl branch, two electrons are utilized to reduce one CO_2 molecule to CO via the carbon monoxide dehydrogenase (CODH) enzyme. CO is then incorporated with the methyl moiety to form acetyl-CoA via the acetyl-CoA synthase enzyme. CO can also be used to form acetyl-CoA directly, rather than being produced from CO_2 reduction. Alcohols, acids, and cell mass are all in turn produced from the acetyl-CoA intermediate.

From literature, syngas fermentation typically occurs at a pH range from 4.5 to 7, and the initial ionic strength of media is calculated to be less than 0.1 M based on published media compositions (Datar 2004; Munasinghe 2010; Rajagopalan 2002). However, it is important to note that the reported values are based on the extracellular conditions which are not necessarily the values at the site of the reaction located at some point within the bacteria. For a proper thermodynamic analysis related to pH, it is important to address pH effects associated with the pH at the site of the reaction.

Several publications have addressed the difference between the internal pH and external pH. Generally, there is a pH gradient across the cell membrane. Studies have shown that a change in the external pH can result in a change in the internal pH. For example, it was shown that the internal pH of *Methanobacterium thermoautotrophicum* decreased from 6.7 to 5.7 when the media pH decreased from 6.7 to 5.5 (Jarrell 1980). Another study with *Clostridium acetobutylicum* showed that internal pH changes from 6.6 to 5.5 when the media pH changed from 6.5 to 4.4 (Girbal 1995). Similar findings were also observed in Valli's research, in which the internal pH changed from 7 to 5 when media pH changed from 7 to 2 (Valli 2005). Similarly, in Skidmore's research using *Clostridium* P11, the internal pH was found to decrease from 6 to 5 when the media pH decreased from 6 to 4.5 in one study. However, in another study, the internal pH remained relatively constant at around 5.5 when the media pH changed from 6 to 4.5 (Skidmore 2010). Moreover, some research has shown that the pH changes depend upon the different metabolism phases of the cells. Research with *Clostridium thermoaceticum* showed that when media pH changed from 7 to 3.5, the internal pH changed from 7 to 4 if cells were in the growth phase. However, the internal pH changed from 7 to 5.4 if cells were in the stationary phase (Baronofsky 1984). From the studies mentioned above, it is clear that a change in the external pH can affect the internal pH, although the internal pH has some resistance to the external pH change. Thus, if the external pH decreases, the internal pH tends to decrease as well, but the decrease is smaller than that of the external pH (Ljungdahl 1986). In most reports, the internal pH for viable cells ranged from pH 5 to pH 7, depending on the bacteria and fermentation conditions.

Another issue regarding parameters affecting syngas fermentation is the location of the enzyme where the reaction occurs. For instance, if the enzyme is membrane-bound, the pH near

the enzyme would likely be at a pH somewhere between the external and internal values. If the enzyme is in the cytosol, the pH would be more closely aligned with the internal pH. According to one study, electron production enzymes associated with syngas fermentation (e.g. hydrogenase and CODH) are believed to be membrane-bound, indicating the reactions happen at a pH condition likely between the internal and external pH (Drake 2004; Ragsdale 2008). Another study observed that only half of the CODH/ACS is membrane-bound, but another half is soluble in the cytosol (Rohde 2002). For the FDH enzyme, one study showed that there are three different types of FDH enzymes: one is membrane-bound and two are soluble (Jormakka 2003). For other syngas fermentation reactions not directly using a gas substrate, the reactions are believed to happen in the cytosol (Drake 2004). Basically, the enzyme properties of membrane-bound or soluble in cytosol are complicated and may depend upon microbes. It's difficult to say where the reactions occur without detailed analysis. In general, it appears that electron production reactions occur with membrane-bound enzymes, but other reactions are with cytosol-soluble enzymes.

In this work, it is wise to assess the effects of pH based on internal pH, but with a broader range due to the wide range of internal pH values observed in studies noted above. Because syngas fermentation usually happens in media where the pH ranges from 4.5 to 7 (Datar 2004; Munasinghe 2010), it is reasonable to assume the internal pH is a little more neutral. In this work (including subsequent chapters), the discussion will mainly focus on a pH ranging from 5-7 and an ionic strength ranging from 0.05 to 0.25 M. Therefore, this broad range of conditions when performing the thermodynamic analysis will include a typical subset of reaction conditions within bacteria that can occur at pH levels somewhere between external and internal pH

conditions. An advantage of exploring a pH range is that quantitative trends from the analysis can help provide insights regarding the effects of changes in the reaction conditions.

As noted above, the production of the acetyl-CoA intermediate is electron intensive. Electrons required for the metabolic process are donated by reduced electron carriers that obtain electrons from either H_2 via the hydrogenase enzyme and/or from CO via the CODH enzyme. Although there are many electron carriers, common two-electron carrier pairs found in biological systems include NAD^+/NADH, $NADP^+$/NADPH, and ferredoxin (Ragsdale 2008). For syngas fermentation, the most efficient process for converting available carbon (both CO and CO_2) to carbon-containing products would involve utilization of H_2 rather than CO to obtain needed electrons. Although it's very unlikely that there would be sufficient H_2 in syngas to provide all electrons, the question arises as to whether H_2 can be utilized in favor of CO for electron production (when both species are present) to provide the highest efficiency of CO conversion to products. If CO is used as an electron source when H_2 is present, the oxidized product in the form of CO_2 may potentially become a lost carbon source for product formation. Thus, the carbon conversion efficiency of CO to product formation would be reduced.

3.2 Research objective

The dual functionality of CO as both a carbon source and an electron source has major implications since CO utilization for electron production comes at the expense of using the carbon of CO for product formation. The objective of this research is to address the competitive question of electron production between CO and H_2during typical syngas fermentation conditions.

To achieve this objective, a thermodynamic analysis of electron production from H_2 or CO was modeled for the NAD^+/NADH electron carrier pair according to:

$$H_2 + NAD^+ \leftrightarrow H^+ + NADH \quad (3.1)$$

$$CO + H_2O + NAD^+ \leftrightarrow CO_2 + H^+ + NADH \quad (3.2)$$

The thermodynamic analysis involved comparing the change in the Gibbs free energy of reaction for each of the above reactions in association with pH, ionic strength, and gas partial pressures of CO, H_2, and CO_2. Although the analysis could be performed using classical Gibbs free energies, the analysis was performed using transformed Gibbs free energies since there are many advantages of using transformed thermodynamics when analyzing biological systems. For instance, once the transformed Gibbs free energy of formation for each species is tabulated, calculating the Gibbs free energy of reactions with varying pH and ionic strength is simple; furthermore, use of transformed thermodynamics also enables incorporation of multiple forms of biological species (e.g. ATP^{4-}, $HATP^{3-}$, and H_2ATP^{2-}) in the analysis of other reactions along the metabolic pathway (Alberty 2001).

3.3 Calculation of transformed thermodynamics

The transformed Gibbs free energy of reaction at temperature T ($\Delta_rG'_T$) provides the criterion as to whether a reaction will go forward or reverse at the given biological conditions and also gives some indication as to the "driving force" of the reaction. A more negative $\Delta_rG'_T$ indicates a higher "driving force" in the forward direction since increasing reactant

concentrations relative to product concentrations lead to a more negative $\Delta_r G'_T$. As defined (Alberty 2001), $\Delta_r G'_T$ is:

$$\Delta_r G'_T = \Delta_r G'^0_T + RTlnQ \tag{3.3}$$

Where $\Delta_r G_T'^0$ is the standard transformed Gibbs free energy of reaction at temperature T and Q is

$$Q = \frac{(a_A)^a (a_B)^b \ldots (a_C)^c}{(a_X)^x (a_Y)^y \ldots (a_Z)^z} \tag{3.4}$$

Note that the numerator denotes the activity (a) of products A, B, C, etc. and the denominator denotes the activity of reactants X, Y, Z, etc. The powers shown in Equation 3.4 are the stoichiometric coefficients of the products and the reactants associated with the reaction.

Utilization of equation 3.3 based on transformed thermodynamics requires the exclusion of H atoms and charge balances when describing biochemical reactions (Alberty 1996). Accordingly, reactions 3.1 and 3.2 become:

$$H_{2\,(aq)} + NAD_{ox} \leftrightarrow NAD_{red} \tag{3.5}$$

$$CO_{(aq)} + NAD_{ox} + H_2O \leftrightarrow CO_{2(aq)} + NAD_{red} \tag{3.6}$$

Note that NAD^+ is represented as NAD_{ox} (oxidized form) and NADH is represented as NAD_{red} (reduced form). Recall that NAD_{red}/NAD_{ox} is only one pair of possible electron carriers. If other electron carrier pairs, such as ferredoxin (Ragsdale 2008), are involved in the reaction, the

oxidized and reduced forms of the carrier pairs could replace the NAD_{ox} and NAD_{red} terms in reactions 3.5 and 3.6.

For the reactions shown above, equation 3.3 for each reaction is:

$$\Delta_5 G'_T = \Delta_5 G'^0_T + RTln\frac{[NAD_{red}]}{[H_2][NAD_{ox}]} \quad (3.7)$$

$$\Delta_6 G'_T = \Delta_6 G'^0_T + RTln\frac{[NAD_{red}][CO_2]}{[CO][NAD_{ox}]} \quad (3.8)$$

Here, the activity of all dilute species is defined as the aqueous concentration divided by a reference concentration of 1 M. Additionally, all gases (H_2, CO, CO_2) are represented as dissolved species in water. For reactions with water as a reactant or product in aqueous solution, the activity of water is unity. $\Delta_r G_T'^0$ values are derived from standard Gibbs free energies of formation ($\Delta_f G^0_{i,298.15K}$) defined at 298.15 K and ionic strength (I) of zero and standard enthalpies of formation ($\Delta_f H^0_i$) that are assumed independent of temperature (Alberty 2001). Table 3-1 shows the standard values for the species involved in the reactions noted above along with values for the NADP and ferredoxin electron carrier.

To obtain $\Delta_r G_T'^0$ at 310 K for syngas fermentation reactions (see equations 3.7 and 3.8), $\Delta_f G^0_{i,298.15K}$ (at I=0 M) is first adjusted to 310 K according to

$$\Delta_f G^0_{i,310K} = \left(\frac{310\ K}{298.15\ K}\right)\Delta_f G^0_{i,298.15K} + \left(1 - \frac{310\ K}{298.15\ K}\right)\Delta_f H^0_i \quad (3.9)$$

Table 3-1.Standard Gibbs free energy of formation ($\Delta_f G^0$) and standard enthalpy of formation ($\Delta_f H^0$) at T=298.15 K and I=0 M. $N_{H,i}$ is the number of hydrogen atoms in a species, and z_i is the charge number

Species	$\Delta_f G^0$ (kJ mol^{-1})	$\Delta_f H^0$ (kJ mol^{-1})	Molecular Formula	$N_{H,i}$	z_i	Reference
H_2 (aq)	17.6	-4.2	H_2	2	0	Alberty 2003
CO (aq)	-119.9	-120.96	CO	0	0	Alberty 2003
CO_2 (aq)	-386	-413.8	CO_2	0	0	Sandler 2006
NAD_{ox}	0	0	$C_{21}H_{26}N_7O_{14}P_2^-$	26	-1	Alberty 2003
NAD_{red}	22.65	-31.94	$C_{21}H_{27}N_7O_{14}P_2^{2-}$	27	-2	Alberty 2003
H_2O	-237.17	-285.83	H_2O	2	0	Alberty 2003
$NADP_{ox}$	-835.18	0	$C_{21}H_{25}N_7O_{17}P_3^{3-}$	25	-3	Alberty 2003
$NADP_{red}$	-809.19	-29.18	$C_{21}H_{26}N_7O_{17}P_3^{4-}$	26	-4	Alberty 2003
$Ferredoxin_{ox}$	0	N/A	N/A	0	1	Alberty 2003
$Ferredoxin_{red}$	38.07	N/A	N/A	0	0	Alberty 2003

Afterwards, $\Delta_f G^0_{i,310K}$ is then transformed for pH and ionic strength due to the Debye-Hückel theory, which yields the standard transformed Gibbs free energy of formation at 310 K ($\Delta_f G'^0_{i,310K}$) according to

$$\Delta_f G'^0_{i,310K}(pH, I) = \Delta_f G^0_{i,310K} - N_{H,i} RT ln 10^{-pH} - RT\alpha\left(z_i^2 - N_{H,i}\right) I^{1/2}/(1 + BI^{1/2}) \quad (3.10)$$

Where α is the Debye-Hückel constant (1.17582 kg$^{1/2}$ mol$^{-1/2}$), RTα = 9.20483 x 10^{-3}T – 1.28467 x 10^{-5} T^2 + 4.95199 x 10^{-8}T^3, B= 1.6 kg$^{1/2}$ mol$^{-1/2}$, $N_{H,i}$ is the number of hydrogen atoms in a species, and z_i is the charge number (Alberty 2001, Goldberg 1991).

Using Equation 3.10, Table 3-2 shows the calculated values of $\Delta_f G'^0_{i,310K}$ for various species as a function of pH and ionic strength. Note that since $N_{H,i}$ and z_i are zero for CO and CO_2, $\Delta_f G'^0_{i,310K}$ for these species does not change with pH and ionic strength. Once $\Delta_f G'^0_{i,310K}$ is calculated, $\Delta_r G_T{}'^0$ values used in Equations 3.7 and 3.8 are found according to

$$\Delta_r G'^0_T = \sum v_i \Delta_f G'^0_{i,T} \quad (3.11)$$

Where v is the stoichiometric coefficient for the species (negative for reactant and positive for product). As seen in the above transformed analysis, the pH and ionic strength dependence are now associated with the $\Delta_r G'^0_T$ term rather than the Q term as is the case for classical Gibbs free energy analysis.

Equation 3.10 is derived based on Debye-Hückel theory with using the extended Debye-Hückel law to express the activity coefficient (γ_i):

$$ln\,\gamma_i = \frac{\alpha \cdot z_i^2 \cdot I^{1/2}}{1 + B \cdot a \cdot I^{1/2}} \quad (3.12)$$

The extended Debye-Hückel law (equation 3.12) provides high accuracy when the ionic strength (I) is less than 0.1 M. However, for solutions of greater ionic strengths, other equations, such as the Davies equation or the Pitzer equation, could be applied to provide more accurate results at higher ionic strength. For instance, the Davies equation provides high accuracy (error < 5%) for solutions with ionic strength up to 0.5 M (Ball 2003). In Alberty's work, the transformed Gibbs free energy of formation for species with ionic strength up to 0.25 M was calculated and this range of ionic strength was utilized for this study (Alberty 2001). The concern arises as to whether Alberty's method provides acceptable accuracy for a biological system at typical conditions.

Table 3-2.Standard transformed Gibbs free energy of formation ($\Delta_f G_{310K}^{'0}$) in kJ mol^{-1} as a function of pH and ionic strength (I)

Species	I/M	pH 5	pH 6	pH 7
H_2 (aq)	0	77.85	89.73	101.60
	0.05	78.87	90.75	102.62
	0.1	79.15	91.03	102.90
	0.25	79.57	91.45	103.32
CO (aq)	any	-119.86	-119.86	-119.86
CO_2 (aq)	any	-384.90	-384.90	-384.90
NADox	0	771.86	926.24	1080.61
	0.05	784.61	938.99	1093.36
	0.1	788.12	942.49	1096.86
	0.25	793.37	947.74	1102.11
NADred	0	826.40	986.71	1147.02
	0.05	838.13	998.44	1158.75
	0.1	841.35	1001.66	1161.97
	0.25	846.18	1006.49	1166.80
H_2O	0	-175.86	-163.98	-152.11
	0.05	-174.84	-162.96	-151.09
	0.1	-174.56	-162.68	-150.81
	0.25	-174.14	-162.26	-150.39
$NADP_{ox}$	0	-126.62	21.83	170.25
	0.05	-118.46	29.98	178.41
	0.1	-116.24	32.22	180.66
	0.25	-112.86	35.58	184.01
$NADP_{red}$	0	-68.72	85.65	240.03
	0.05	-63.62	90.75	245.12
	0.1	-62.22	92.15	246.53
	0.25	-60.12	94.25	248.63
$Ferredoxin_{ox}$	0	0	0	0
	0.05	-0.51	-0.51	-0.51
	0.1	-0.65	-0.65	-0.65
	0.25	-0.81	-0.81	-0.81
$Ferredoxin_{red}$	0	39.58	39.58	39.58
	0.05	38.58	38.58	38.58
	0.1	39.58	39.58	39.58
	0.25	39.58	39.58	39.58

The activity coefficient (γ_i) due to the Davies equation is:

$$ln\,\gamma_i = \alpha \cdot z_i^2 \cdot \left(\frac{I^{1/2}}{1+I^{1/2}} - 0.3 \cdot I\right) \quad (3.13)$$

Table 3-3 compares the calculated $\Delta_f G'^0_{310\,K}$ at pH 6 of 23 species involved in the acetyl-CoA pathway by using equation 3.12 or equation 3.13 for evaluating $\Delta_f G'^0_{310\,K}$. Since a higher ionic strength increases the thermodynamic inaccuracy associated with the extended Debye-Hückel law, the comparison was carried out at a high ionic strength of 0.5 M, which is the upper limit of the Davies equation. It should be noted that this high ionic strength is not very probable for a typical fermentation process. Table 3-3 shows that for most species, the errors between using the extended Debye-Hückel law versus the Davies equation for most species (18 of 23) at I=0.5 M are less than 1%. Only one species (acetaldehyde) shows a high error of 8.5%. For the work in this chapter, acetaldehyde is not utilized. Acetaldehyde is utilized in Chapter 4 at I<0.1M, and for this case, the error between the two methods is negligible. Therefore, for all thermodynamic analysis, the extended Debye-Hückel law is utilized.

3.4 Standard transformed Gibbs free energy of reactions

Figure 3-1 shows the values of $\Delta_{3.5}G'^0_T$ and $\Delta_{3.6}G'^0_T$ for reactions 3.5 and 3.6, respectively, as a function of pH and ionic strength. Note that $\Delta_{3.5}G'^0_T > \Delta_{3.6}G'^0_T$ at all pH and ionic strength and that electron production from both H_2 and CO is favorable at standard conditions since the values are always negative. The more negative value for the CO reaction suggests that producing electrons from CO is more favorable than producing electrons from H_2.

Table 3-3.The comparison of Standard transformed Gibbs free energy of formation ($\Delta_f G_{310\,K}^{'0}$)in kJ mol^{-1} between Alberty's method and using Davies equation at pH 6 and ionic strength (I) of 0.5 M

	Alberty	Davies	% err
H_2 (aq)	91.78	91.36	-0.46
CO (aq)	-119.86	-119.86	0
CO_2 (total)	-548.61	-548.82	0.04
NAD_{ox}	951.92	946.69	-0.55
NAD_{red}	1010.34	1005.52	-0.48
ATP	-2313.14	-2313.49	0.02
ADP	-1448.94	-1450.39	0.10
P_i	-1059.08	-1059.11	0.003
Formate	-312.37	-312.37	0
H_4Folate	842.99	838.18	-0.57
HCO-H_4Folate	711.41	706.6	-0.68
CH-H_4Folate	835.75	831.36	-0.53
CH_2-H_4Folate	890.3	885.49	-0.54
CH_3-H_4Folate	906.3	901.07	-0.58
CoA	-11.23	-11.43	1.75
AcetylCoA	-78.56	-79.19	0.80
Acetyl-P	-1122.71	-1123.34	0.06
Acetaldehyde	10.55	9.72	-8.54
Acetate	-255.76	-256.18	0.16
Ethanol	42.56	41.31	-3.03
H_2O	-161.93	-162.35	0.26
$NADP_{ox}$	-258.62	-264.64	2.27
$NADP_{red}$	-212.82	-216.58	1.74

It is interesting to note that ionic strength has very little impact on$\Delta_r G_T^{'0}$ for both reactions, with a slight increase when ionic strength approaches to 0 M. On the other hand, the pH has a large effect on $\Delta_r G'^0_T$ for both reactions with a decreasing effect as pH increases. This can have significant implications in syngas fermentation depending upon the reactor pH. A higher pH favors more electron production at standard conditions. However, assessing $\Delta_r G_T^{'}$ rather than $\Delta_r G_T^{'0}$, as shown below, provides greater insights into the real thermodynamics.

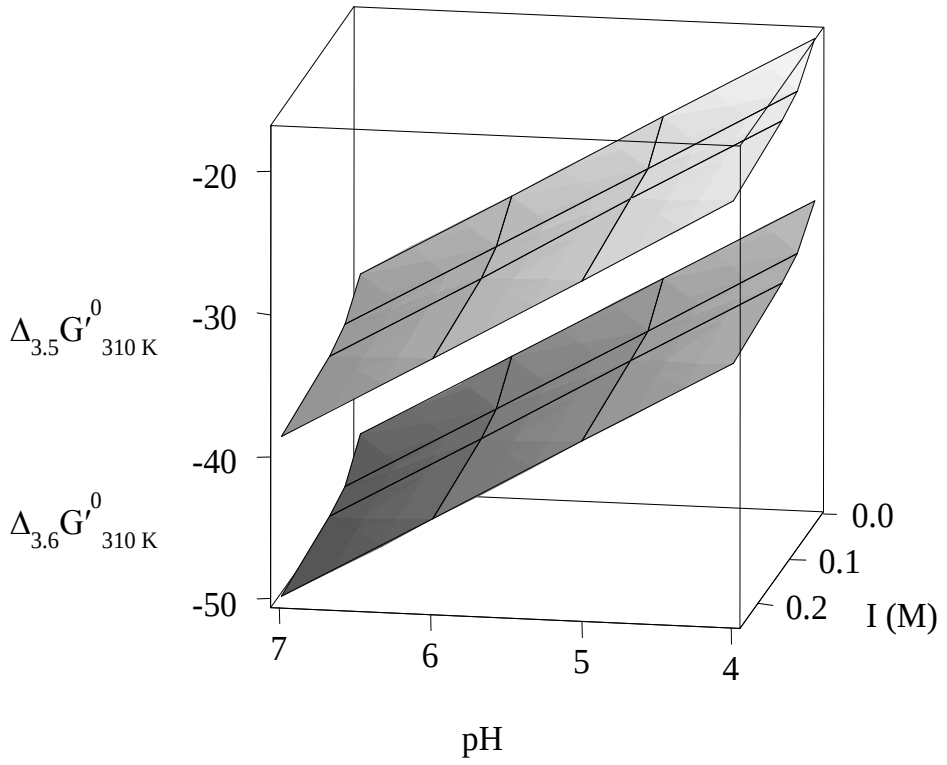

Figure 3-1.Standard transformed Gibbs free energy of reaction ($\Delta_r G'^{0}_{310\ K}$)in kJ mol^{-1} as a function of pH and ionic strength (I) for reaction 3.5 (electron production from H_2) and reaction 3.6 (electron production from CO)

3.5 Transformed Gibbs free energy of reactions

To better determine the thermodynamically-preferred source of electron production utilized in the metabolic pathway $\Delta_r G'_T$ was assessed at various reactant and product concentrations that could occur during syngas fermentation. Since the value of $\Delta_r G'^{0}_T$ becomes more positive with decreasing pH and decreasing ionic strength (leading to a more unfavorable thermodynamic state) and a typical internal pH for syngas fermentation occurs in the range of 5 to 7, $\Delta_r G'_T$ was evaluated as a function of Q (see equation 3.3) when $\Delta_r G'^{0}_T$ was fixed at pH 5 and I=0 M. Since $\Delta_r G'^{0}_T$ is the only term affected by pH and I (which is an advantage for using

transformed thermodynamics), the analysis would give a "worse-case" scenario of the thermodynamics under the various reactant and product concentrations. As for evaluating Q, the NAD_{red}/NAD_{ox} concentration ratio, the dissolved CO/CO_2 concentration ratio, and the dissolved H_2 concentration were varied according to typical values that would be observed during syngas fermentation.

During biomass gasification, a review of literature showed typical initial syngas compositions (mole %) ranging from 14 – 48% CO, 9 – 20% CO_2, and 5 – 32% H_2 (Munasinghe 2010). Using Henry's Law with $C_i = H_i P_i$ at a syngas total pressure of 1 atm, the equivalent dissolved concentration range is 0.17 – 0.58 mM CO, 4.3 – 9.6 mM CO_2, and 0.05 – 0.30 mM H_2. Here, for each species *i*, C_i is the dissolved gas concentration, H_i is the Henry's Law constant and P_i is the gas partial pressure. Henry's Law constants at 310 K are H_{CO} = 1.2 mM/atm, H_{CO2} = 48 mM/atm, and H_{H2} = 0.83 mM/atm (Lide 1995). Based on this information, the dissolved H_2 concentration could vary between 0 and 0.3 mM since H_2 is consumed during fermentation. As for the dissolved CO/CO_2 concentration ratio, this ratio was varied between 0 (when CO runs out) and 0.13 (based on the highest expected ratio from initial composition data). Finally, a NAD_{red}/NAD_{ox} concentration ratio of 0.1 to 3 was utilized which is consistent with most reported experimental measurements ranging from 0.1 to 2.1 (Girbal 1995; Guedon 2000; Desvaux 2001).

Based on the ranges noted above, Figures 3-2a and 3-2b show values of $\Delta_r G'_T$ for the two reactions at pH 5 and I=0 M. Both figures show similar trends with an increasing $\Delta_{3.5} G'_T$ and $\Delta_{3.6} G'_T$ when NAD_{red}/NAD_{ox} increases. This is expected according to equations 3.7 and 3.8. However, it should be noted that in all cases the thermodynamics are more favorable for electron production from CO (reaction 3.6) rather than from H_2 (reaction 3.5). In fact, for the range of H_2

concentrations and NAD_{red}/NAD_{ox} ratios shown, $\Delta_{3.5}G'_T$ is positive under a large portion of the conditions as shown in Figure 3-3. Under such conditions, electron production from H_2 would not occur and electrons would only be produced via CO. Even as CO is diminishing during fermentation (i.e. the CO/CO_2 ratio is approaching zero), the thermodynamics are favorable for electron production from CO at the expense of using carbon from CO to form valuable products. To look at this issue at the other pH extreme, $\Delta_r G'_T$ was evaluated as a function of Q (see equation 3.3) when $\Delta_r G'^0_T$ was fixed at pH 7 and I=0 (Figure 3-4). Comparing $\Delta_r G'^0_T$ between pH 5 and 7, Figures 3-4a and 3-4b have the same shape as Figures 3-2a and 3-2b but the values for both reactions are all ~12 kJ/mol lower. Because pH only affects the values of $\Delta_r G'^0_T$ and the values of $\Delta_r G'^0_T$ at pH 7 for both reactions are ~12kJ/mol more negative than at pH 5 (Fig 3-1), a change from pH 5 to pH 7 makes both reactions more thermodynamically favorable. However, adjustment of pH does not change the relative difference between $\Delta_{3.5}G'_T$ and $\Delta_{3.6}G'_T$ such that electron production from CO is still more favorable than from H_2. In other words, a change of pH does not change the relative favorability between generating electrons from CO in comparison to electrons from H_2.

Notably, although electron production from CO is still more favorable than electron production from H_2 at these conditions, the positive $\Delta_r G'^0_T$ for the H_2 reaction is no longer present at pH 7. This indicates that H_2 can also be potentially used as an electron source at these conditions. Thus, the conversion efficiency from CO to product can potentially increase with increasing pH since some electrons could be produced from H_2 at the higher pH.

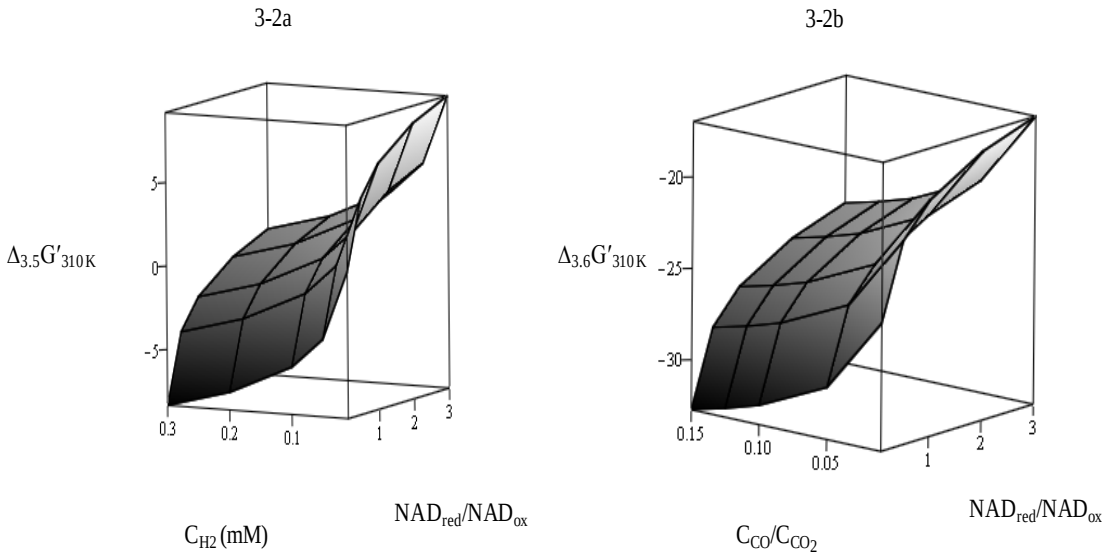

Figure 3-2.Transformed Gibbs free energy of reaction ($\Delta_r G'_{310\,K}$) in kJ mol^{-1} at pH 5 and ionic strength of 0 M for (3.2a) electron production from H_2 via reaction 3.5 as a function of the NAD_{red}/NAD_{ox} ratio and the dissolved H_2 concentration and for (3.2b) electron production from CO via reaction 3.6 as a function of the NAD_{red}/NAD_{ox} ratio and the dissolved CO/CO_2 ratio

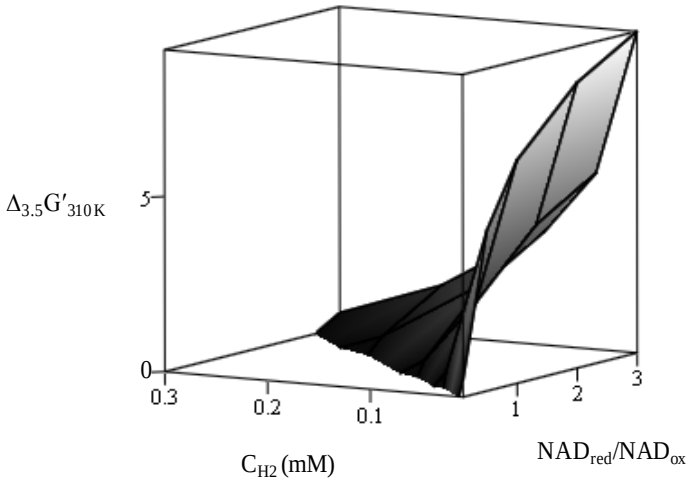

Figure 3-3.Positive values of the transformed Gibbs free energy of reaction ($\Delta_r G'_{310\,K}$) in kJ mol^{-1} at pH 5 and ionic strength of 0 M for electron production from H_2 via reaction 3.5 as a function of the NAD_{red}/NAD_{ox} ratio and the dissolved H_2 concentration

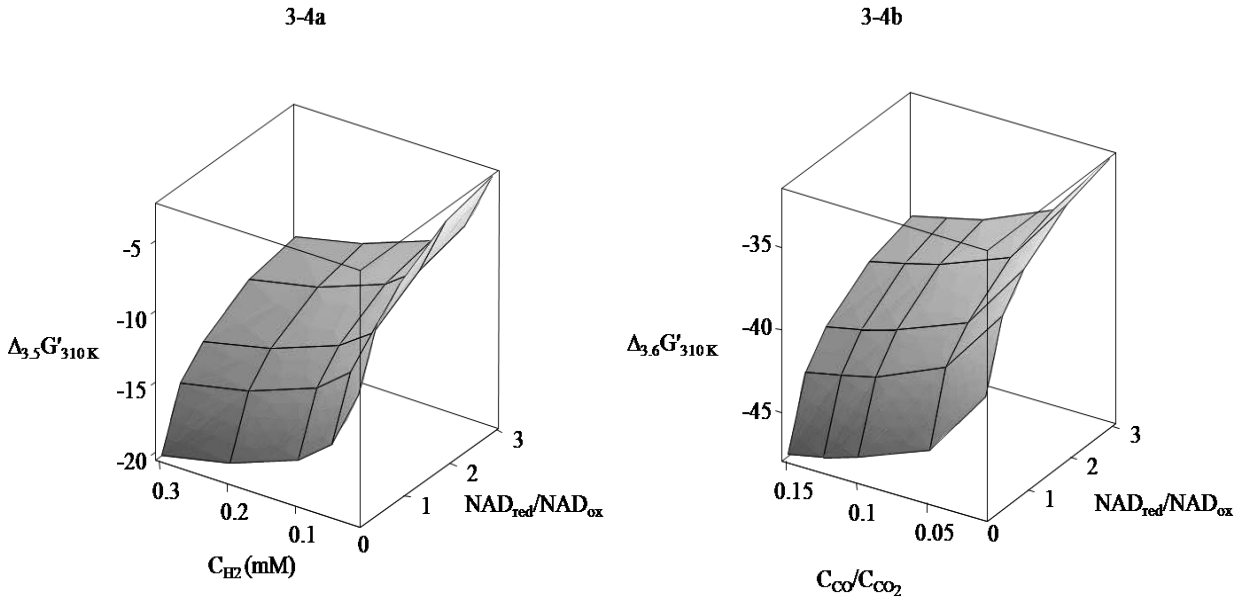

Figure 3-4.Transformed Gibbs free energy of reaction ($\Delta_r G'_{310\,K}$) in kJ mol^{-1} at pH 7 and ionic strength of 0M for (3-4a) electron production from H_2 via reaction 3.5 as a function of the NAD_{red}/NAD_{ox} ratio and the dissolved H_2 concentration and for (3-4b) electron production from CO via reaction 3.6 as a function of the NAD_{red}/NAD_{ox} ratio and the dissolved CO/CO_2 ratio

3.6 Transformed Gibbs free energy of reactions if using other electron carriers

Recall that $NADH/NAD^+$ is only one pair of the electron carriers. Other common electron carriers include ferredoxin, $NADPH/NADP^+$ and so on. It is valuable to assess the effects of the electron carriers on the relative favorability of these two electron production reactions. If ferredoxin is acting as electron carrier, reactions 3.5 and 3.6 become:

$$H_{2\,(aq)} + Fd_{ox} \leftrightarrow Fd_{red} \quad (3.14)$$

$$CO_{(aq)} + Fd_{ox} + H_2O \leftrightarrow CO_{2(aq)} + Fd_{red} \quad (3.15)$$

Where Fd_{ox} indicates the oxidized form of ferredoxin and Fd_{red} indicates the reduced form of ferredoxin.

Figures 3-5a and 3-5b show $\Delta_r G'_T$ for the reactions when ferredoxin is used as the electron carrier rather than NAD_{red}/NAD_{ox}. For the ferredoxin calculation of $\Delta_f G_i^0$ at 310 K (equation 3.9), $\Delta_f H_i^0$ of ferredoxin is unavailable in literature. Since $\Delta_f H_i^0$ typically accounts for less than a 5% correction for $\Delta_f G_i^0$ calculated for other species in Table 3-1, it was assumed that the $\Delta_f H_i^0$ term was negligible for temperature corrections of ferredoxin. Trends similar to those noted for NAD_{red}/NAD_{ox} are observed, with the major difference being that the $\Delta_r G'$ values calculated using ferredoxin are more negative than those calculated using NAD_{red}/NAD_{ox}. Thus, thermodynamically, ferredoxin is a more favorable electron carrier under similar biological conditions. As seen, electron production from CO is still more favorable than electron production from H_2 and this conclusion appears to be independent of the electron carrier.

Recall that there still exist some other naturally available electron carriers. Although the electron production from CO is always more favorable than the electron production from H_2 if both reactions use the same electron carrier, it is possible that different electron carriers can be used for different electron-producing species. For instance, it is possible that the CO reaction via the CODH enzyme prefers to use $NADH/NAD^+$, but the H_2 reaction via hydrogenase prefers to use $NADPH/NADP^+$. For these scenarios, the relative favorability could still be compared using the above thermodynamic model, but the specific electron carriers for different enzymatic reactions should be experimentally determined to provide the inputs for the model.

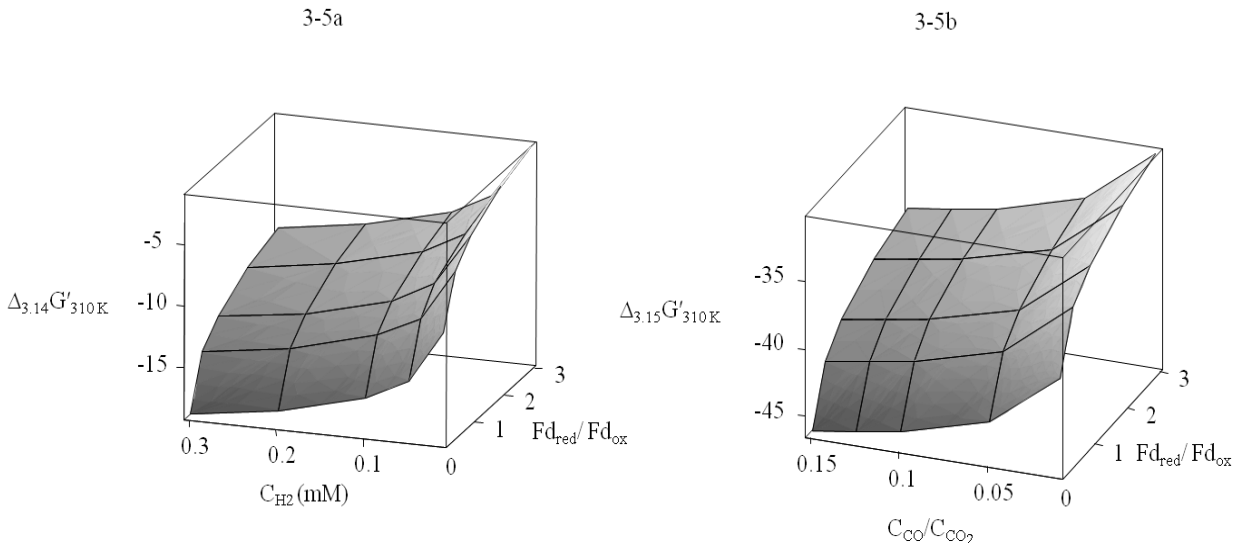

Figure 3-5.Transformed Gibbs free energy of reaction ($\Delta_r G'_{310\,K}$) in kJ mol^{-1} at pH 5, and ionic strength of 0 M for (3-5a) electron production from H_2 via reaction 3.14 with ferredoxin (Fd) as the electron carrier as a function of the Fd_{red}/Fd_{ox} ratio and the dissolved H_2 concentration and for (3-5b) electron production from CO via reaction 3.15 with Fd as the electron carrier as a function of the Fd_{red}/Fd_{ox} ratio and the dissolved CO/CO_2 ratio

3.7 Discussion

As observed in Figure 3-1, an increasing pH results in a decreasing $\Delta_r G_T'^0$ (and thus $\Delta_r G_T'$) for both electron-producing reactions. As noted above, $\Delta_r G_T'$ is below zero for both reactions at pH 7 but at pH 5 the electron production from H_2 is thermodynamically unfavorable under most conditions. Increasing the ionic strength shows the same trend, but the effect is not as strong as that of increasing pH. With regards to the original question of whether H_2 can be utilized in favor of CO for electron production (when both species are present) to provide the highest efficiency of CO conversion to products, the above analysis shows that at any given pH and I, the $\Delta_r G_T'$ of electrons from CO is always more negative than $\Delta_r G_T'$ of electrons from H_2 when both species are present. Thus, electron production via CO is more thermodynamically

favorable than from H_2. Unfortunately, electron production via CO directly competes with the production of acetyl-CoA which is required for cell growth and product formation. This competition would reduce the efficiency of CO carbon conversion to cell mass and products.

If reaction conditions could be adjusted in such a way that electron production from H_2 became the favored source, there could be more cell growth and product formation due to the increased efficiency of CO carbon conversion. Since adjusting pH and ionic strength does not help, one possibility is adjusting the partial pressure of the gases. In order to compare the relative thermodynamics of reactions 3.5 and 3.6, the difference of $\Delta_{3.5}G'_T$ and $\Delta_{3.6}G'_T$ is

$$\Delta_{3.5}G'_T - \Delta_{3.6}G'_T = \Delta_{3.5}G'^0_T - \Delta_{3.6}G'^0_T + RTln\frac{[H_2]}{\left(\frac{[CO]}{[CO_2]}\right)} \quad (3.16)$$

If Equation 3.16 is positive, electron production from CO is more thermodynamically favorable compared to electron production from H_2. If negative, electron production from H_2 is favored. The value of Equation 3.16 can be explored for different values of C_{CO}/C_{CO2} and C_{H2}. Note that this difference is independent of the electron acceptor. Comparing figures 3-2a and 3-2b, $\Delta_{3.6}G'_T$ is always more negative than $\Delta_{3.5}G'_T$ at any given combination of C_{CO}/C_{CO2} and C_{H2}, leading to a positive value for Equation 3.16. Although not clearly shown, when H_2 is present, the C_{CO}/C_{CO2} ratio would have to approach zero (or in practice, C_{CO}=0) before the values of Equation 3.16 become negative. Thus, in practice, thermodynamics suggests that H_2 cannot be utilized in favor of CO for electron production when both species are present.

Although electron production from CO is more favorable, it would be beneficial to have some electrons produced from H_2 to help the CO carbon conversion efficiency. In studies involving syngas fermentation using bacterium P7, both CO and H_2 were utilized throughout the

growth phase (Datar 2004). This confirms that electrons can be produced simultaneously from H_2 and CO. On the other hand, some studies have shown that H_2 has only been utilized after CO has been depleted or H_2 has not been utilized at all (Younesi 2005). In this latter study using *Clostridium ljungdahlii*, CO, H_2 and CO_2 utilization were compared for total reactor pressures ranging from 0.8 to 1.8 atm. For all runs, CO consumption began after about 10 hours, with most of the CO being consumed by 60 hours. CO_2 was also produced primarily during this period, which indicates that CO was utilized as an electron source via CO to CO_2 conversion. Over the same period of time, H_2 consumption was nearly zero for all different pressures, indicating that CO is clearly favored as the major electron source. Furthermore, once CO was depleted, H_2consumption (and CO_2 consumption as the carbon source) began in only the reactors with high total pressures $\geq$ 1.6 atm. On the other hand, the reactors with lower total pressures $\leq$ 1.4 atm did not consume H_2, even after the CO was depleted in some runs. Additional studies of syngas fermentation by *Butyribacterium methylotrophicum* further addresses CO and H_2 utilization (Heiskanen 2007). When the CO content is high, no H_2 is consumed; however, H_2 (and CO_2) is consumed as CO levels approach zero.

Several possibilities could explain these results. One possibility for the difference in H_2 consumption when CO is not present could be the thermodynamics in which lower partial pressures of H_2 and/or lower pH results in a positive $\Delta_{3.5}G'_T$. Thus, experimental conditions can have a great impact on H_2 utilization. A second possibility is that hydrogenase is inhibited by CO in a concentration dependent manner (Hurst 2005). As for the experiments in which CO and H_2 are utilized simultaneously, the CO inhibition of hydrogenase could potentially be low and the reactor conditions could be thermodynamically favorable for electron production from both CO and H_2. Obviously, more detailed experimental analysis would need to be conducted to confirm

these hypotheses. However, it is clear that reactor conditions can greatly affect the carbon conversion efficiency of CO. In all cases, CO conversion efficiency is sacrificed since electron production comes from CO at the expense of making product.

In Chapter 1, one critical issue regarding syngas fermentation was carbon utilization efficiency. It was shown that electrons generated from H_2 would lead to the best carbon conversion efficiency. Ideally, there may be an optimal syngas composition to achieve the maximum carbon utilization. However, from the above analysis, CO is always more thermodynamically favored than H_2 as an electron source and H_2 may not be utilized at some reactor conditions. Thus, it doesn't appear feasible to adjust the fermentation conditions (pH, ionic strength, or gas composition) in order to increase the electron production from H_2 relative to that from CO.

Although the thermodynamic analysis has shown that electron production from CO is more favorable than from H_2, the relative rates of electron production should also be considered to understand the preferred source of electron production. For instance, a more negative transformed Gibbs free energy of reaction does not correlate with faster reaction rates. Thus, if the forward rate of electron production from CO was found to be much less than the forward rate from H_2, it is possible that H_2 could be the preferred source of electron production. Although reported rate constants for both electron production from CO (CO oxidation) and H_2 (H_2 uptake) vary, few studies actually compared the two. In the study using *C. thermoaceticum*, it was shown that for the same cell mass CO oxidation occurred at 57,500 μmol/min compared to H_2 uptake occurring at 0.91 μmol/min (Menon 1996). Although it is possible that enzyme concentrations can vary during a fermentation process which can affect the relative rates, it is clear from this study that CO oxidation is much faster than H_2 uptake for this bacteria. This finding concurs with

the thermodynamic analysis that CO will be the preferred electron source, thereby decreasing the conversion efficiency of CO to products and cell mass.

3.8 Conclusions

This thermodynamic analysis led to several findings regarding syngas fermentation.

- $\Delta_r G_T^{'}$ for electron production from CO is negative (thermodynamically favorable) for typical reaction conditions.
- $\Delta_r G_T^{'}$ for electron production from H_2 can vary between thermodynamically favorable and unfavorable depending upon the reaction conditions.
- Electron production from CO is always more thermodynamically favorable compared to electron production from H_2 and this is independent of pH, ionic strength, gas partial pressure, and electron carrier pairs.
- It doesn't appear feasible to adjust the reaction conditions (pH, ionic strength, or gas composition) in order to increase the electron production from H_2 relative to that from CO.

Thus, this study suggests that it would be unlikely that H_2 is utilized in favor of CO for electron production when both species are present. Therefore, CO conversion efficiency will be sacrificed during syngas fermentation since some of the CO will make electrons at the expense of product and cell mass formation.

4. Thermodynamic analysis of reactions involved in the metabolic pathway

4.1 Introduction

Syngas fermentation generally follows the acetyl-CoA (or Wood-Ljungdahl) metabolic pathway, which consists of a methyl and a carbonyl branch (Ljungdahl 1986). In the methyl branch of the metabolic pathway, one molecule of CO_2 is converted to formate, which binds with H_4folate and is eventually reduced to a methyl moiety, while in the carbonyl branch one molecule of CO_2 is reduced to a molecule of CO. The CO molecule (which can also be used directly without reduction from CO_2) is then incorporated with the methyl moiety to form acetyl-CoA, which is an intermediate for cell growth, acetate formation, and ethanol production. Acetyl-CoA is thus the intermediate carbon source for all product formation and cell growth. In this work, two predominant paths discussed are the formation of acetate (also known as acetogenesis) and the formation of ethanol (also known as solventogenesis).

Syngas fermentation is generally a process of reducing gaseous carbon sources (CO, CO_2) to two-carbon products (ethanol, acetate). The electron production for providing reducing equivalents was already discussed in Chapter 3. In this chapter, the focus is on the entire acetyl-CoA metabolic pathway.

4.2 Research objective

While it is good to know the reactions that occur to facilitate product formation, that knowledge alone is limited in application. In order to develop strategies to enhance product formation, a deeper understanding of the metabolic pathway is necessary. From the reactions of ethanol (1.3 through 1.5) and acetate (1.10 through 1.12) production, an obvious hypothesis is that higher H^+ concentrations (lower pH) and higher NADH/NAD^+ ratios (more negative E) are better for product formation during syngas fermentation because H^+ and NADH are reactants and NAD^+ is a product. However, although qualitative trends from adjusting E and pH can be estimated from the metabolic pathway, it would be beneficial to quantify the trends to address potential impacts of changing reaction conditions. In this study, a thermodynamic model of reactions involved in the acetyl-CoA metabolic pathway with varying experimental conditions (pH, ionic strength, NADH/NAD^+ ratios, and gas partial pressures) is developed and the strategies to enhance product formation are developed based on the model.

4.3 Method

The Gibbs free energy of reaction provides the criterion for spontaneous change and equilibrium. In this chapter, similar to Chapter 3, transformed thermodynamics derived by Alberty were used for modeling and analysis (Alberty 2001).

An obvious advantage for transformed thermodynamics over traditional thermodynamics is the convenience for dealing with species when multiple forms of the species exist in solution. For instance, ATP has several forms (e.g. ATP^{4-}, $HATP^{3-}$, and H_2ATP^{2-}) which co-exist in

solution and the amount of these forms depends upon the pH and ionic strength of the solution. Since species such as ATP are very common in biological systems, traditional thermodynamics is not easy to use. Use of transformed thermodynamics can avoid this problem of multiple forms of species and enables incorporation of multiple forms of biological species in the analysis of reactions along the metabolic pathway (Alberty 2001). As stated in Chapter 3, the transformed Gibbs free energy of formation for each species needs to be calculated from the standard Gibbs free energy of formation first. Table 4-1 shows standard formation properties for the species involved in the metabolic pathway.

A different issue between Chapter 3 and this chapter is that species discussed in Chapter 3 have only one active form (CO, H_2, etc) in the solution, but this chapter needs to deal with species with multiple forms in the solution. For species with only one form existing in a biological system (such as CO or H_2), $\Delta_f G'^0_{i,310K}$ for each species is derived directly from equation 3.10. However, for species with multiple forms (such as ATP), the transformed Gibbs free energy of formation of species with multiple (iso) forms ($\Delta_f G'^0_{iso,310K}$) must be derived by

$$\Delta_f G'^0_{iso,310K} = -RT \sum_{i=1}^{N_{iso}} \exp\left[-\Delta_f G'^0_{i,310K}/RT\right] \quad (4.1)$$

Where i represents different forms of the species, N_{iso} represents the total numbers of the forms, R is the gas constant, and T is the temperature. The values of $\Delta_f G'^0_{iso,310K}$ at varying pH levels and ionic strengths for all species in the metabolic pathway are calculated and shown in Table 4-2. For species in which only one form exists in biological systems, $\Delta_f G'^0_{i,310K}$ is the same as $\Delta_f G'^0_{iso,310K}$. Also recall that since $N_{H,i}$ and z_i are zero for some species (e.g. CO and CO_2),

$\Delta_f G'^0_{i,310K}$ for these species does not change with pH and ionic strength. The standard transformed Gibbs energy of reaction ($\Delta_r G'^0_T$) is found by the equation (Alberty, 2001):

$$\Delta_r G'^0_T = \sum v_i \Delta_f G'^0_{iso,310K} \tag{4.2}$$

The nomenclature regarding transformed thermodynamics remains the same as discussed in Chapter 3.

In the previous Chapter, the transformed Gibbs free energy of reaction $\Delta_r G'_T$ at actual experimental conditions has been defined to:

$$\Delta_r G'_T = \Delta_r G'^0_T + RTlnQ \tag{4.3}$$

where Q is

$$Q = \frac{(a_A)^a (a_B)^b \ldots (a_C)^c}{(a_X)^x (a_Y)^y \ldots (a_Z)^z} \tag{4.4}$$

The definitions of parameters in these two equations are the same as in the previous Chapters.

Table 4-1.Standard Gibbs free energy of formation ($\Delta_f G^0$) and standard enthalpy of formation ($\Delta_f H^0$) at T=298.15 K and I=0 M. $N_{H,i}$ is the number of hydrogen atoms in a species, and z_i is the charge number (Alberty 2003)

Species	$\Delta_f G^0$ (kJ mol^{-1})	$\Delta_f H^0$ (kJ mol^{-1})	$N_{H,i}$	Z_i
ATP^{4-}	-2768.1	-3619.21	12	-4
$HATP^{3-}$	-2811.48	-3612.91	13	-3
H_2ATP^{2-}	-2838.18	-3627.91	14	-2
ADP^{3-}	-1906.13	-2626.54	12	-3
$HADP^{2-}$	-1947.1	-2620.94	13	-2
H_2ADP^{-}	-1971.98	-2638.54	14	-1
HPO_3^{2-}	-1096.1	-1299	1	-2
$H_2PO_3^{-}$	-1137.3	-1302.6	2	-1
Formate	-351	-425.55	1	-1
H_4Folate	0	N/A	23	0
HCO-H_4Folate	-131.58	N/A	23	0
CH^+=H_4Folate	30.44	N/A	22	1
CH_2=H_4Folate	47.31	N/A	23	0
CH_3-H_4Folate	-9.99	N/A	25	0
CoA^{-1}	0	N/A	0	-1
HCoA	-47.83	N/A	1	0
Acetyl-CoA	-188.52	N/A	3	0
Acetyl-PO_3^{2-}	-1219.39	N/A	3	-2
Acetyl-HPO_3^{-}	-1268.08	N/A	4	-1
Acetyl-H_2PO_3	-1298.26	N/A	5	0
Acetaldehyde	-139	-212.23	4	0
CH_3COO^{-}	-369.31	-486.01	3	-1
CH_3COOH	-396.45	-485.76	4	0
CH_3CH_2OH	-181.64	-288.3	6	0

Table 4-2.Standard transformed Gibbs free energy of formation ($\Delta_f G_{310\,K}^{'0}$)in kJ mol^{-1} as a function of pH and ionic strength (I) at 310 K

Species	I/M	pH 5	pH 6	pH 7
ATP	0	-2394.12	-2316.26	-2239.46
	0.05	-2391.56	-2314.37	-2238.80
	0.1	-2390.94	-2313.93	-2238.89
	0.25	-2390.06	-2313.41	-2239.23
ADP	0	-1534.48	-1457.05	-1380.90
	0.05	-1529.70	-1452.76	-1377.91
	0.1	-1528.42	-1451.65	-1377.24
	0.25	-1526.53	-1450.09	-1376.33
Pi	0	-1071.29	-1059.56	-1048.80
	0.05	-1070.80	-1059.23	-1049.28
	0.1	-1070.67	-1059.17	-1049.48
	0.25	-1070.47	-1059.10	-1049.84
Formate	0	-318.31	-312.37	-306.44
	0.05	-318.31	-312.37	-306.44
	0.1	-318.31	-312.37	-306.44
	0.25	-318.31	-312.37	-306.44
H_4Folate	0	682.80	819.36	955.92
	0.05	694.53	831.09	967.65
	0.1	697.76	834.32	970.88
	0.25	702.58	839.15	975.71
HCO-H_4Folate	0	551.22	687.78	824.34
	0.05	566.18	702.74	839.30
	0.1	566.18	702.74	839.30
	0.25	571.00	707.57	844.13
CH^+=H_4Folate	0	683.56	814.18	944.80
	0.05	694.26	824.89	955.51
	0.1	697.21	827.83	958.46
	0.25	701.62	832.24	962.86
CH_2=H_4Folate	0	730.11	866.67	1003.23
	0.05	741.84	878.40	1014.96
	0.1	745.07	881.63	1018.19
	0.25	749.89	886.46	1023.02
CH_3-H_4Folate	0	732.19	880.62	1029.06
	0.05	744.94	893.37	1041.81
	0.1	748.44	896.88	1045.31
	0.25	753.69	902.12	1050.56

Table 4-2. Continued

Species	I/M	pH 5	pH 6	pH 7
CoA	0	-18.14	-12.23	-6.49
	0.05	-17.63	-11.73	-6.08
	0.1	-17.49	-11.60	-5.97
	0.25	-17.28	-11.39	-5.82
Acetyl-CoA	0	-99.46	-81.65	-63.83
	0.05	-97.93	-80.12	-62.30
	0.1	-97.51	-79.70	-61.88
	0.25	-96.88	-79.07	-61.25
Acetyl-P	0	-1151.38	-1125.89	-1102.02
	0.05	-1150.62	-1124.29	-1100.65
	0.1	-1148.80	-1123.85	-1100.31
	0.25	-1148.00	-1123.21	-1099.82
Acetaldehyde	0	-17.30	6.45	30.20
	0.05	-15.26	8.49	32.23
	0.1	-14.70	9.05	32.80
	0.25	-13.86	9.89	33.64
Acetate	0	-276.72	-257.88	-239.95
	0.05	-275.37	-256.82	-238.92
	0.1	-275.02	-256.53	-238.64
	0.25	-274.49	-256.10	-238.22
Ethanol	0	0.78	36.40	72.02
	0.05	3.83	39.46	75.08
	0.1	4.68	40.30	75.93
	0.25	5.94	41.56	77.18

4.4 Reactions along the acetyl-CoA metabolic pathway

In Chapter 2, the reactions involved in the acetyl-CoA metabolic pathway were reviewed. However, applying transformed thermodynamics to the metabolic pathway requires the exclusion of H atoms and charge balances when describing biochemical reactions (Alberty 1996). Thus, reactions (reactions 2.1 to 2.12) involved in the metabolic pathway are rewritten below (reactions 4.5 to 4.16).

Accordingly, reactions for electron production become:

$$H_{2\,(aq)} + NAD_{ox} \leftrightarrow NAD_{red} \quad (4.5)$$

$$CO_{(aq)} + NAD_{ox} + H_2O \leftrightarrow CO_{2(aq)} + NAD_{red} \quad (4.6)$$

For convenience, the reducing equivalents utilized in reactions along the metabolic pathway are all represented as NAD_{ox} and NAD_{red}.

The methyl branch converts one CO_2 molecule to a methyl moiety through the following reactions:

$$CO_2 + NAD_{red} \leftrightarrow HCOOH + NAD_{ox} \quad (4.7)$$

$$HCOOH + ATP + H_4Folate \leftrightarrow HCO\text{-}H_4Folate + ADP + P_i \quad (4.8)$$

$$HCO\text{-}H_4Folate \leftrightarrow CH{=}H_4Folate + H_2O \quad (4.9)$$

$$CH{=}H_4Folate + NAD_{red} \leftrightarrow CH_2{=}H_4Folate + NAD_{ox} \quad (4.10)$$

$$CH_2{=}H_4Folate + NAD_{red} \leftrightarrow CH_3\text{-}H_4Folate + NAD_{red} \quad (4.11)$$

The methyl moiety (CH_3-H_4Folate) is then incorporated with CO to form acetyl-CoA via the acetyl-CoA synthase enzyme:

$$CH_3\text{-}H_4Folate + CO + CoA \leftrightarrow Acetyl\text{-}CoA + H_4Folate \quad (4.12)$$

Acetic acid is then produced from acetyl-CoA through the reactions

$$\text{Acetyl-CoA} + P_i \leftrightarrow \text{Acetyl-}P_i + \text{CoA} \quad (4.13)$$

$$\text{Acetyl-}P_i + \text{ADP} \leftrightarrow \text{Acetic Acid} + \text{ATP} \quad (4.14)$$

Also, ethanol is produced from acetyl-CoA through

$$\text{Acetyl-CoA} + NAD_{red} \leftrightarrow C_2H_4O + \text{CoA} + NAD_{ox} \quad (4.15)$$

$$CH_3COH + NAD_{red} \leftrightarrow C_2H_6O + NAD_{ox} \quad (4.16)$$

These 12 reactions (reactions 4.5 through 4.16) along the metabolic pathway could be divided into 4 groups. The first group comprises reactions 4.5 and 4.6, which provide reducing equivalents (NAD_{red}/NAD_{ox}) for other reducing reactions. The second group includes reactions 4.7 to 4.12 which are for the acetyl-CoA synthesis. The third group includes reactions 4.13 and 4.14, which represent the conversion from acetyl-CoA to acetate. The fourth group includes reactions 4.15 and 4.16 which represent the conversion from acetyl-CoA to ethanol. Most importantly, reactions in Groups 3 and 4 directly affect the production of either acetate or ethanol, which determines the selectivity and the effectiveness of making fuel ethanol.

4.5 Results and Discussion

As suggested by Equation 3.10, the variance in the pH of a system affects the thermodynamic properties of species, which then affects the relative thermodynamic favorability of various reactions. This is critical to assess since the pH profile of a system may shift as the fermentation progresses. As reported in literature, acetate is a growth-associated product during

syngas fermentation (Girbal 1995). Such results infer that as the fermentation proceeds, the pH will drop due to the accumulation of acetic acid when the pH is not controlled. Thus, at the beginning of a run, the pH is higher than it is by the time that the growth phase is completed and cell mass is stabilized. Therefore, understanding the quantitative effect of pH on the thermodynamic favorability of each reaction in the metabolic process provides insight into the way the thermodynamics of a system are changing throughout the fermentation. Such insight leads to the development of strategies to increase ethanol production. For instance, as the effect of varying pH is assessed, protocols could be developed to promote greater ethanol formation following cell growth. Besides pH, ionic strength (I) also affects the standard transformed Gibbs energies of a system as shown in equation 3.10. As mentioned in Chapter 3, a range of pH from 5-7 and ionic strength from 0.05 to 0.25 M was utilized in the assessment below.

4.5.1 $\Delta_r G_T'^0$ at different pH and ionic strength (I)

Figure 4-1 shows $\Delta_r G'^0_T$ (standard reference) of reactions 4.5 through 4.16 at pH 5with varying ionic strength of I=0.05 M and I=0.25 M. The values of $\Delta_r G'^0_T$ are very similar at the two ionic strengths, indicating that ionic strength only slightly affects the thermodynamics of these reactions. Thus, the effect of ionic strength is not addressed in the rest of this study and an ionic strength of I ≤ 0.1 M is used in all calculations. The following discussions are related to only the roles of pH and other experimental conditions in biological systems.

Similarly, Figure 4-2 shows $\Delta_r G'^0_T$ of reactions 4.5 through 4.16 at pH 7 and pH 5, respectively, when both are at an ionic strength of 0.05 M. At pH 7, $\Delta_r G'^0_T$ of reactions 4.5 and

4.6 are quite negative, reaction 4.7 is positive, and reactions 4.8 through 4.12 are negative. $\Delta_r G'^0_T$ of reactions 4.13 and 4.14 are just slightly positive, while reaction 4.15 is quite positive and reaction 4.16 is negative. At pH 5, reactions 4.5 and 4.6 are moderately negative, reaction 4.7 is positive, and reactions 4.8 through 4.12 are negative (reactions 4.9 and 4.11 are especially negative). Reaction 4.13 is almost zero, while reaction 4.14 is rather positive. Reaction 4.15 is positive and reaction 4.16 is very negative.

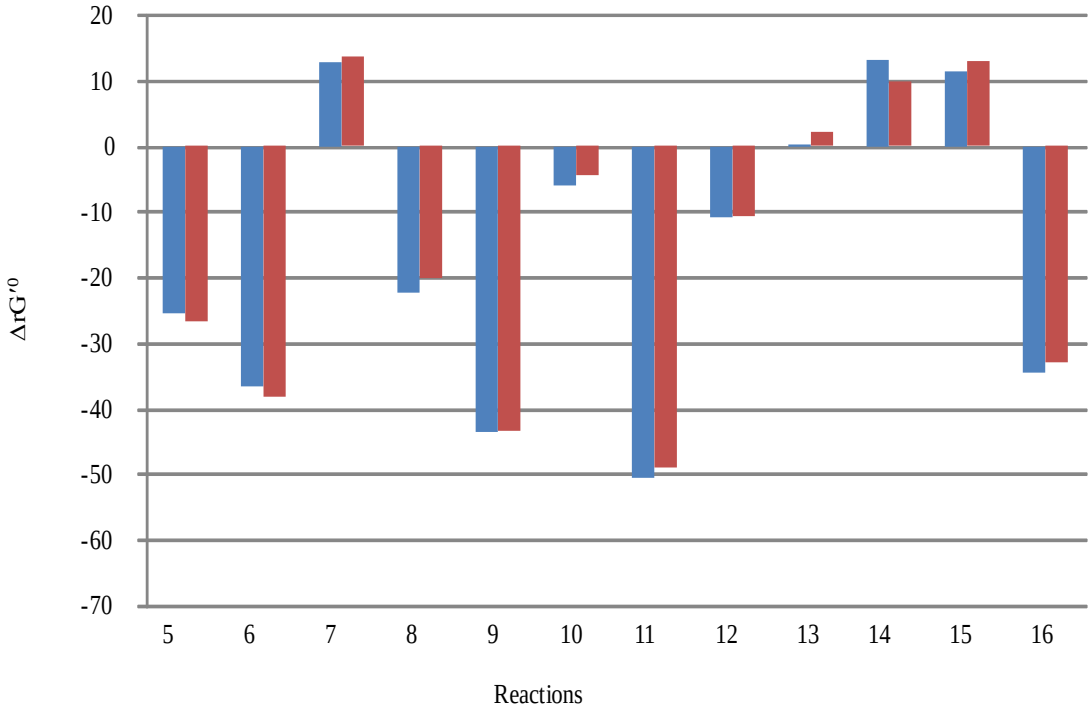

Figure 4-1.Standard transformed Gibbs free energy of reaction ($\Delta_r G'^0_{310K}$)in kJ mol^{-1} of the reactions involved in the acetyl-CoA metabolic pathway at pH 5 and varying ionic strengths (I) of I=0.05 M (Blue) and I=0.25 M (Red). For simplification, reaction 5 represents reaction 4.5, reaction 6 represents reaction 4.6, etc.

Reactions 4.5 and 4.6 deal with electron production and function essentially for providing electrons for the rest of the reactions of the metabolic pathway. From Figure 4-2, $\Delta_r G'^0_T$ for both electron production reactions are more negative at pH 7, which means that electron production is

more favorable at pH 7 than at pH 5under standard conditions. Since syngas fermentation requires extensive electrons, higher electron availability at higher pH may be beneficial for the electron limiting processes. The details regarding these two electron production reactions have been previously discussed in Chapter 3.

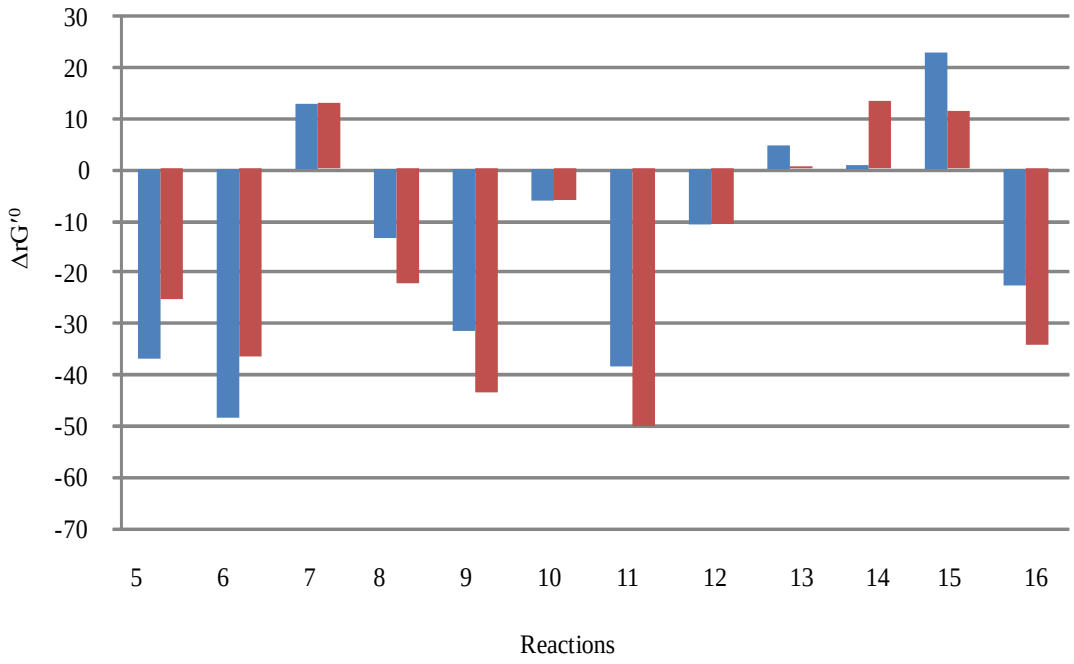

Figure 4-2.Standard transformed Gibbs free energy of reaction ($\Delta_r G'^{0}_{310K}$) in kJ mol^{-1} of the reactions involved in the acetyl-CoA metabolic pathway at I=0.05 M and varying pH of 7 (Blue) and pH 5(Red). For simplification, reaction 5 represents reaction 4.5; reaction 6 represents reaction 4.6, etc.

Reaction 4.7 is a starting step leading to the formation of Acetyl-CoA, and has a positive $\Delta_r G'^{0}_{T}$ value, which makes it thermodynamically unfavorable under standard reaction conditions. This step is a potential bottleneck to the process. However, cell growth and product formation occurring in experimental studies indicates that reaction 4.7 does in fact occur, which suggests that a more detailed analysis of the conditions necessary to make reaction 4.7 thermodynamically favorable is beneficial to fully understand the thermodynamics of product formation. On the

other hand, since reactions 4.8 through 4.12 compose the bulk of the metabolic pathway leading to the formation of Acetyl-CoA, which is a shared intermediate for both acetate and ethanol production, they have a more indirect effect on product selectivity. Moreover, reactions 4.8 through 4.12 all have negative $\Delta_r G'^0_T$ values, although the values are similar or more negative at pH 5than at pH 7, indicating that each reaction is thermodynamically favorable at standard conditions. A more detailed thermodynamic analysis of these reactions for assessing product formation at reactor conditions is not easy since the concentrations of intermediates are unavailable. The other key positive $\Delta_r G'^0_T$ values are notable during acetate production (reaction 4.14) and ethanol production (reaction 4.15) following the formation of Acetyl-CoA. Therefore, there are potential key thermodynamic bottlenecks during the formation of these two products. With these potential bottlenecks, there is the opportunity to identify key fermentation parameters (pH, ionic strength, redox control, etc.) that can be used to affect the relative rates of ethanol and acetate formation.

Accordingly, this study focuses on a more complete thermodynamic analysis of reactions with positive $\Delta_r G'^0_T$ values, which may thermodynamically limit the whole process, and reactions which directly affect the selectivity between ethanol and acetate. Thus, the remainder of the chapter focuses on an analysis of reactions 4.7, 4.13, 4.14, 4.15, and 4.16. Also recall that $\Delta_r G'^0_T$ is just dealing with the reactions at standard conditions when all reactants and products have concentrations of 1 M, which is not very likely in a real biological system. Thus, assessing$\Delta_r G'_T$, rather than $\Delta_r G'^0_T$ which is at standard conditions, provides greater insights into thermodynamic constraints.

4.5.2 Conversion from CO_2 to formate

The first point of interest with regard to Figure 4-2 is reaction 4.7, which is the conversion from CO_2 to formate. The values of $\Delta_{4.7}G_T^{\prime 0}$ at both pH 7 and pH 5are constant and positive at about 13.4 kJ/mol, which indicates that pH does not affect $\Delta_{4.7}G_T^{\prime 0}$ and this reaction is thermodynamically unfavorable at standard conditions. However, since several studies have demonstrated ethanol and acetic acid formation, reaction 4.7 clearly occurs despite the positive value of the standard Gibbs free energy of reaction. The experimental conditions where the Gibbs free energy of reaction shifts from positive to negative can be determined by using equation 4.3. This shift can only occur for certain values of Q for the reaction. Therefore, since CO_2 is a reactant and formate is the product, Figure 4-3 models the values of $\Delta_{4.7}G_T^{\prime}$ at varying formate concentrations (10^{-5} to 10^{-1} M) and NAD_{red}/NAD_{ox} ratios (0.1 to 3) when pH=6, I = 0.1 M and P_{CO2} = 0.3 atm. The model helps to determine the appropriate experimental conditions that make reaction 4.7 become thermodynamically favorable. The parameters (pH, I, and P_{CO2}) represent typical fermentation initial conditions as found in the majority of relevant literature (Girbal 1995; Payot 1998; Guedon 1999; Guedon 2000; Desvaux 2001) and the pH is similar to the typical internal pH conditions of syngas fermentation bacteria.

Figure 4-3 suggests that the most important factor affecting $\Delta_{4.7}G_T^{\prime}$ is the formate concentration. While the NAD_{red}/NAD_{ox} ratio does have some effect on the value of$\Delta_{4.7}G_T^{\prime}$, that effect appears to be minimal except as NAD_{red}/NAD_{ox} approaches zero, at which point$\Delta_{4.7}G_T^{\prime}$ increases. However, as the formate concentration approaches zero, $\Delta_{4.7}G_T^{\prime}$ decreases rapidly, ultimately resulting in negative values. In general, $\Delta_{4.7}G_T^{\prime}$ only goes negative when the formate concentration is 10^{-4} M or lower at a NAD_{red}/NAD_{ox} range between 0.5 and 3. Therefore, in

order for reaction 4.7 to become thermodynamically favorable, the formate concentration must be lower than 10^{-4} M. In fact, for the range of NAD_{red}/NAD_{ox} ratios shown, $\Delta_{4.7}G'_T$ is positive under most conditions as shown in Figure 4-4. Under such conditions, CO_2 cannot be converted into formate spontaneously. Since $\Delta_{4.7}G'_T$ only goes negative when the formate concentration is very low, it follows that very low formate concentrations should exist at the reaction site for CO_2 to formate conversion.

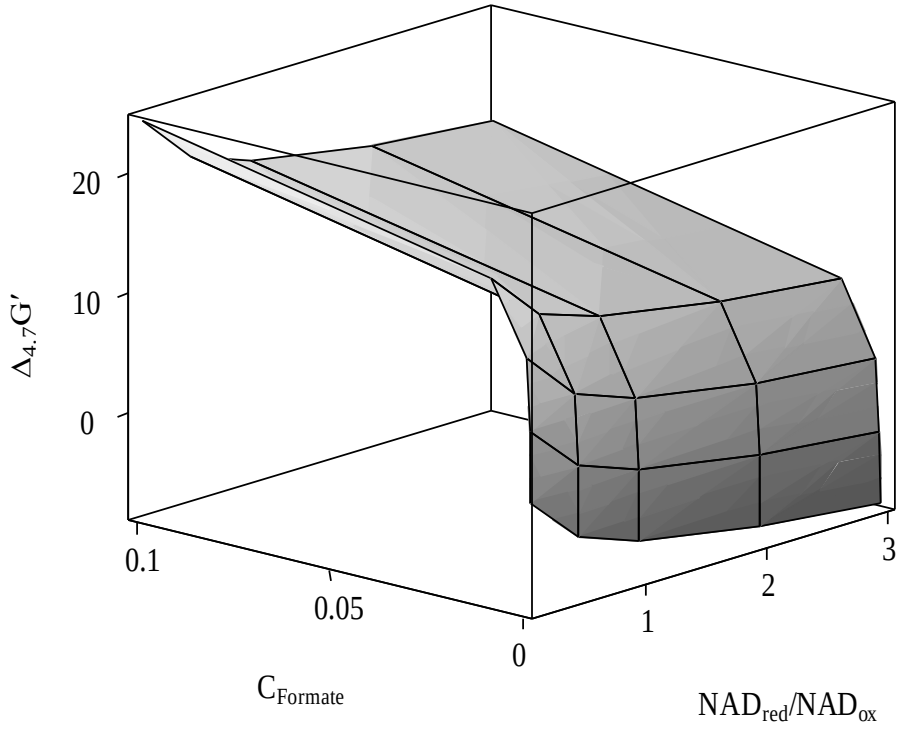

Figure 4-3.Transformed Gibbs free energy of reaction ($\Delta_{4.7}G'_{310\,K}$) in kJ mol^{-1} at ionic strength of 0.1 M and pH 6 for CO_2 to formate conversion (reaction 4.7) as a function of the NAD_{red}/NAD_{ox} ratio and the formate concentration when the CO_2 partial pressure in the headspace is 0.3 atm

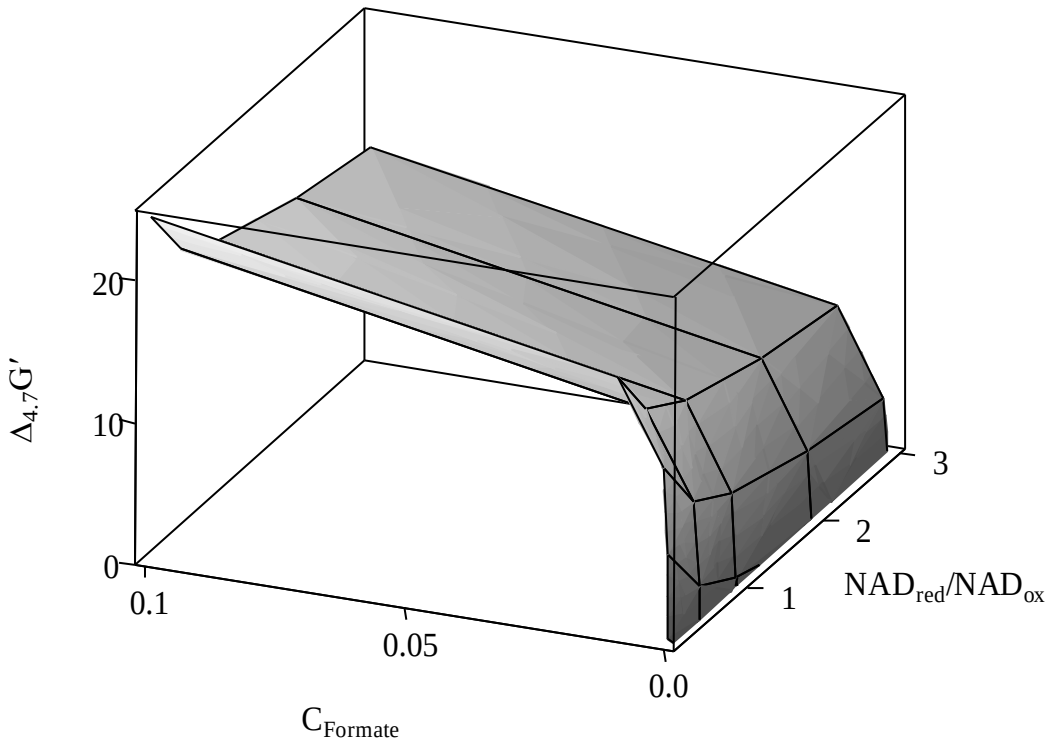

Figure 4-4.Positive values of the transformed Gibbs free energy of reaction ($\Delta_r G'_{310\,K}$) in kJ mol^{-1} at ionic strength of 0.1 M and pH 6 for CO_2 to formate conversion (reaction 4.7) as a function of the NAD_{red}/NAD_{ox} ratio and the formate concentration when the CO_2 partial pressure in the headspace is 0.3 atm

As a reactant, the concentration of CO_2 is another important issue which may affect the thermodynamic favorability of reaction 4.7. Obviously, decreasing CO_2 partial pressure will make the conversion from CO_2 to formate less favorable, which is not desirable. In this case, the formate concentration would need to be much lower than 10^{-4} M to keep the reaction progressing towards product. On the other hand, the effect of increasing the CO_2 partial pressure was studied. If the partial pressure of CO_2 is changed from 0.3 atm to a higher level, for example 0.7 atm, this trend remains consistent (Figure 4-5), though values of $\Delta_{4.7}G'_T$ decrease slightly at a similar formate concentration and NAD_{red}/NAD_{ox} ratio. This confirms that CO_2 to formate conversion can occur only at very low formate concentrations even when the partial pressure of CO_2 is at a very high level.

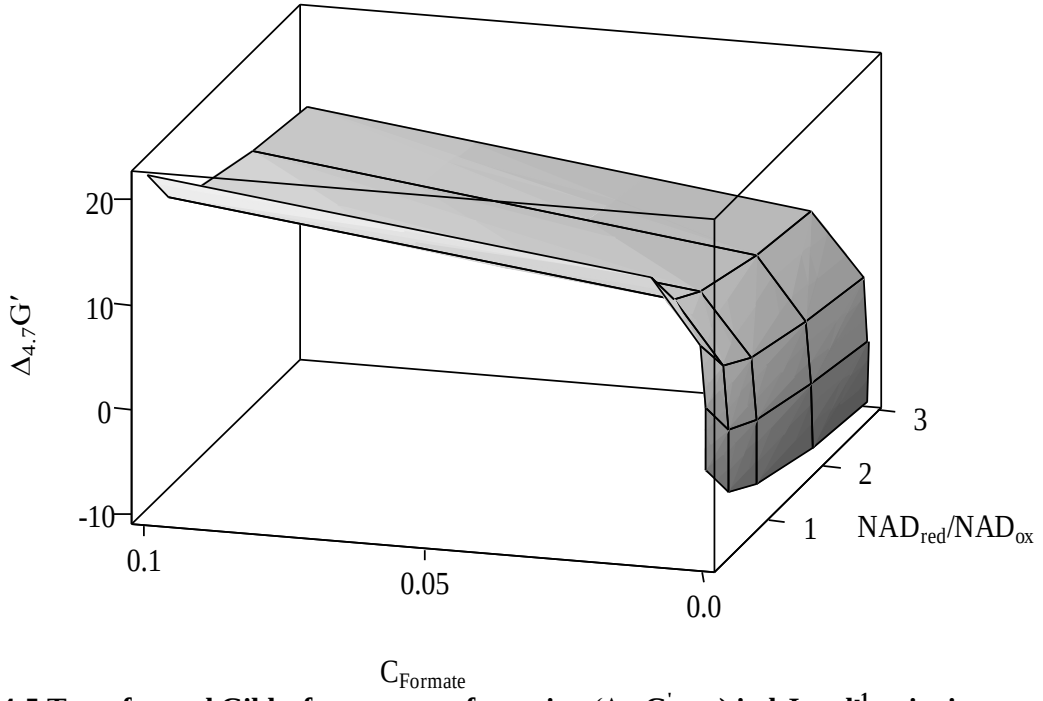

Figure 4-5.Transformed Gibbs free energy of reaction ($\Delta_{4.7}G'_{310\,K}$) in kJ mol^{-1} at ionic strength of 0.1 M and pH 6 for CO_2 to formate conversion (reaction 4.7) as a function of the NAD_{red}/NAD_{ox} ratio and the formate concentration when the CO_2 partial pressure in the headspace is 0.7 atm

Initially, it may seem that the way to overcome the thermodynamic bottleneck of reaction 4.7 would be to increase the formate dehydrogenase (FDH) enzyme activity of that reaction. However, the increase in FDH activity would still not necessarily yield the desired results unless thermodynamics are favorable. Therefore, the activity of FDH is not a likely bottleneck. Essentially, the forward kinetics of reaction 4.8 (formate removal), or even reactions beyond, must be extremely fast to allow reaction 4.7 to be thermodynamically favorable. Thus, the amount of 10-formyl-H_4Folate synthetase, the enzyme responsible for reaction 4.8, must be of sufficient activity to rapidly remove formate. In this sense, the activity of this enzyme may be a potential bottleneck to the formation of Acetyl-CoA. The same is true for other enzymes downstream of formate production. Since Acetyl-CoA is upstream of cell production, and cell

production has been very limited in all literature studies, it would be beneficial to further explore the potential bottlenecks between CO_2 utilization and Acetyl-CoA production.

4.5.3 Acetate formation

Unlike reaction 4.7, notable differences in $\Delta_r G'^0_T$ between the two pH levels occur for acetate formation (reactions 4.13 and 4.14) when the ionic strength is constant at I=0.05 M. At pH 7, reactions 4.13 and 4.14 are both positive ($\Delta_r G'^0_T$ = 4.9 kJ/mol and 0.8 kJ/mol, respectively) whereas at pH 5, reaction 4.13 is close to zero ($\Delta_r G'^0_T = 0.5$ kJ/mol) but reaction 4.14 is significantly more positive ($\Delta_r G'^0_T$ =13.4 kJ/mol) than it is at pH 7.

As with equation 4.3 above, the actual experimental conditions at which $\Delta_r G'_T$ shifts from positive to negative is determined by the value of Q. Table 4-3 shows the values of the equilibrium Q (denoted as Q_e) required for $\Delta_r G'_T = 0$ for the last two steps of acetate production.

Table 4-3.Q equilibrium values when the respective transformed Gibbs free energy of reactions for acetate production are equal zero

pH	5	6	7
$Q_{e,4.13}$ (acetyl-phosphate formation)	0.83	0.27	0.15
$Q_{e,\ 4.14}$(acetic acid formation)	0.0055	0.1	0.72

Since $\Delta_r G'_T$ needs to be less than zero to make a reaction proceed forward, and

$$0 = \Delta_r G'^0_T + RTlnQ_e \qquad (4.17)$$

Then, for the reaction to proceed in the forward direction

$$\Delta_r G_T^{'} = -RTlnQ_e + RTlnQ = RTln\left(\frac{Q}{Q_e}\right) < 0 \quad (4.18)$$

As shown in equation 4.18, any value of Q <Q_e listed in Table 4-3 will cause the corresponding reaction to have a negative $\Delta_r G_T^{'}$ value, meaning that the forward reaction will become thermodynamically favorable and acetate product will form.

With regards to reaction 4.14 for acetyl-CoA to acetate conversion,

$$Q_{4.14} = \frac{[Acetate]\cdot[ATP]}{[Acetyl{-}P_i]\cdot[ADP]} \quad (4.19)$$

For reaction 4.14 to be thermodynamically favorable to produce acetate, $Q_{4.14}$ must be less than Q_e listed in Table 4-3. Thus,

$$Z = \frac{[ATP]}{[Acetyl{-}P_i]\cdot[ADP]} < \frac{Q_e}{[Acetate]} \quad (4.20)$$

From previous experiments, acetate accumulation was observed in syngas fermentations around pH 5 to 6 with acetate concentrations ≥ 0.1 M. If the acetate concentration at the site of reaction within the bacteria is similar to the external concentration, Z would have to be <1 M^{-1} for acetate production at pH 6. Although the actual concentrations of ATP, ADP, and Acetyl-P_i are unavailable, it seems unlikely that the concentration of the Acetyl-P_i intermediate would be very high relative to the acetate concentration since intermediates in biological systems are usually small compared to products and Acetyl-P_i would build up at the expense of acetate formation. Therefore, the ATP/ADP ratio (not the ATP concentration) would have to be low to favor the

reaction in the forward direction. If the acetate concentration in the cell was lower than in solution, Z could be even larger from a thermodynamic standpoint, such that the forward reaction could thermodynamically occur with a larger ATP/ADP ratio.

An additional component to consider are the enzymes associated with reactions 4.13 and 4.14. Since thermodynamics are only a part of the answer, the kinetic aspect must also be addressed. For instance, if the phospho-transacetylase enzyme activity of reaction 4.13 is small compared to the acetate kinase enzyme activity of reaction 4.14, then the rate of 4.13 can be slow and the rate of 4.14 can be fast, thus favoring the formation of acetate over Acetyl-P_i. It should be noted that the activity is not just associated with the kinetic rates but also with the amount of enzyme. Thus, a large amount of acetate kinase relative to phosphor-transacetylase would be beneficial for acetate production.

In summary, acetate production is growth associated and the greatest formation rate will be at the higher pH. As the pH diminishes, acetate production and growth will essentially stop as demonstrated by the trend shown in Table 4-3. Therefore, pH is a critical controlling parameter to use for acetate production, although controlling the internal pH is very difficult. However, as noted in the beginning of Chapter 3, the external pH could have some effect on the internal pH such that external pH control could possibly be used to affect acetate production.

4.5.4 Ethanol formation

For ethanol production from acetyl-CoA, the relative favorability of reactions (4.15 and 4.16) is also strongly dependent upon pH. Reactions 4.15 and 4.16 exhibit trends that are very different from those of reactions 4.13 and 4.14. At pH 7, $\Delta_{4.15}G_T^{'}$ is quite positive (23.1 kJ/mol),

while $\Delta_{4.16}G_T^{'}$ is negative (-23.1 kJ/mol). However, at pH 5, $\Delta_{4.15}G_T^{'}$ is much less positive (11.5 kJ/mol), while $\Delta_{4.16}G_T^{'}$ is even more negative than before (-34.4 kJ/mol). Thus, the key thermodynamic bottleneck for ethanol production appears to be reaction 4.15.

Table 4-4 shows the values of the equilibrium Q (denoted as Q_e) required for $\Delta_r G_T^{'} = 0$ for the last two steps of ethanol production.

Table 4-4.Q equilibrium values when the respective transformed Gibbs free energy of reactions for ethanol production are equal zero

pH	5	6	7
$Q_{e,4.15}$ (acetaldehyde formation)	0.011	0.0012	0.00013
$Q_{e,4.16}$ (ethanol formation)	633322	62954	6283

With regards to reaction 4.15 for acetyl-CoA to ethanol conversion, $Q_{4.15}$ is required to be less than 0.00013 and 0.011 when pH is 7 and 5, respectively. Since reaction 4.15 is the conversion of acetyl-CoA to acetaldehyde, it is reasonable to conclude that the intermediate acetaldehyde cannot exist with a high concentration during syngas fermentation. However, it should also be noted that the Q_e value for reaction 4.16 is very large, irrespective of pH, though Q_e at pH 5has the largest value. This indicates that a small concentration of acetaldehyde is good enough to make ethanol. Thus, the continuous removal of acetaldehyde for ethanol formation promotes the whole process. Therefore, it appears that the amount of ethanol dehydrogenase enzyme or its activity is critical for rapid removal of acetaldehyde produced from reaction 4.15. Thus, a key issue for promoting ethanol formation will be the increasing rate of reaction 4.16, which is the conversion from acetaldehyde to ethanol. It is also noted that at lower pH, both reactions 4.15 and 4.16 have a larger Q_e than at higher pH, which indicates that there would be an increase in ethanol production with a decrease in pH.

In summary, the rapid removal of the product of reaction 4.15 is necessary make the whole process move forward. Due to the big Q_e value for reaction 4.16, this latter reaction should happen at all the typical pH conditions (pH 5-7) of syngas fermentation. However, the greater formation will be as the pH decreases because both reactions 4.15 and 4.16 have a larger Q_e at lower pH than at higher pH. As discussed with acetate production, controlling the internal pH is very difficult but the external pH could have some effect on the internal pH such that external pH control could possibly be used to enhance ethanol production.

4.5.5 Thermodynamics of the overall reactions

Besides pH and ionic strength, another factor which may affect the thermodynamics of the reactions along the metabolic pathway is the NAD_{red}/NAD_{ox} ratio. As reducing equivalents, NAD_{red} and NAD_{ox} are involved in a series of reactions, including reactions 4.5, 4.6, 4.7, 4.10, 4.11, 4.15, and 4.16. Reactions 4.5 and 4.6 are the electron production reactions, which provide the reducing equivalents. The other reactions are for the formation of Acetyl-CoA and the formation of ethanol from Acetyl-CoA. Note that acetic acid production does not need reducing equivalents from Acetyl-CoA, only for the formation of Acetyl-CoA. The thermodynamic effects of the NAD_{red}/NAD_{ox} ratio are more evident when looking at the overall reactions of ethanol and acetate formation. As noted in Chapter 1, it's obvious that more electrons (higher $NADH/NAD^+$) would benefit more product, but a quantitative understanding of reaction conditions on thermodynamics can help assess the effect of how a changing $NADH/NAD^+$ ratio can affect the product formation and distribution.

For ethanol production, the overall reaction is a combination of reactions 4.7-4.12 and 4.15- 4.16.

$$CO + CO_2 + 5\,NAD_{red} + ATP \leftrightarrow C_2H_5OH + 5\,NAD_{ox} + ADP + P_i + 2\,H_2O \quad (4.21)$$

For acetate production, the overall reaction is a combination of reactions 4.7-4.12 and 4.13- 4.14.

$$CO + CO_2 + 3\,NAD_{red} \leftrightarrow C_2H_4O_2 + 3\,NAD_{ox} + H_2O \quad (4.22)$$

Notably, 5 moles of reducing equivalents (NAD_{red}) are involved per mole of ethanol production, whereas 3 moles of reducing equivalents are involved per mole of acetate production. Thus, a small increase in the ratio of NAD_{red}/NAD_{ox} can greatly reduce the values of $\Delta_r G_T^{'}$ for these two reactions (making it more thermodynamically favorable) since the value of Q (see equation 4.4) is related to the NAD_{red}/NAD_{ox} ratio raised to the powers of 5 (for ethanol) and 3 (for acetate). For instance, for ethanol production (reaction 4.21), if all product and reactant concentrations are kept constant except for the NAD_{red}/NAD_{ox} ratio, the change of $\Delta_r G_T^{'}$ as a function of the change in NAD_{red}/NAD_{ox} ratio from condition A to condition B can be expressed as:

$$\Delta\Delta_{4.21}G_T^{'} = \Delta_{4.21}G_{T,B}^{'} - \Delta_{4.21}G_{T,A}^{'} = -RTln\left(\frac{(NAD_{red}/NAD_{ox})_B}{(NAD_{red}/NAD_{ox})_A}\right)^5 \quad (4.23)$$

Similarly, for acetate production (reaction 4.22), the change of $\Delta_r G_T^{'}$ as a function of the change in NAD_{red}/NAD_{ox} ratio from condition A to condition B can be expressed as:

$$\Delta\Delta_{4.22}G_T^{'} = \Delta_{4.22}G_{T,B}^{'} - \Delta_{4.22}G_{T,A}^{'} = -RTln\left(\frac{(NAD_{red}/NAD_{ox})_B}{(NAD_{red}/NAD_{ox})_A}\right)^3 \quad (4.24)$$

Figure 4-6 shows $\Delta\Delta_{4.21}G_T^{'}$ and $\Delta\Delta_{4.22}G_T^{'}$ for changes in the ratio of $(NAD_{red}/NAD_{ox})_B$ to $(NAD_{red}/NAD_{ox})_A$ from 0.1 to 4 where this ratio is denoted at $ratio_B/ratio_A$. As seen for both reactions, if the ratio decreases, the values of $\Delta\Delta_r G_T^{'}$ become more positive, which means that the values of $\Delta_r G_T^{'}$ increase and the reactions become more thermodynamically unfavorable. This is intuitive since the reaction needs reducing equivalents to proceed in the forward direction although quantitatively looking at effects can help understand the magnitude of thermodynamic changes when reaction conditions change. In contrast, if the ratio increases, the values of $\Delta_r G_T^{'}$ decreases. As is noticeable, the change in $\Delta_r G_T^{'}$caused by a small change in the NAD_{red}/NAD_{ox} ratio is significant. For example, if the ratio of NAD_{red}/NAD_{ox} changes from 1 to 3, $\Delta_{4.21}G_T^{'}$ for ethanol production decreases by 14 kJ/mol, and $\Delta_{4.22}G_T^{'}$ for acetate production decreases by 9 kJ/mol. Notably, although increasing the ratio of NAD_{red}/NAD_{ox} makes both $\Delta_{4.21}G_T^{'}$ and $\Delta_{4.22}G_T^{'}$ more negative, the decrease of $\Delta_{4.21}G_T^{'}$ is larger than the decrease for $\Delta_{4.22}G_T^{'}$. This indicates that increasing the ratio of NAD_{red}/NAD_{ox} increases more "driving force" for ethanol production than for acetate production, which is beneficial for product selectivity. In comparison with the pH effects, NAD_{red}/NAD_{ox} effects are more straightforward because NAD_{red} is the reactant and NAD_{ox} is the product in reactions involving NAD_{red}/NAD_{ox} as reducing equivalents. The higher the NAD_{red}/NAD_{ox} ratio, the better the reactions go forward.

As an electron carrier pair, the relative ratio of NAD_{red}/NAD_{ox} may be affected by many physiological parameters, although a key factor is likely the redox potential (Lee 2008). Usually, the more negative the redox potential, the higher the relative ratio of NAD_{red}/NAD_{ox}. Thus,

lowering the redox potential of the media may be used as a strategy to increase the ratio of NAD_{red}/NAD_{ox}, which then may lead to more ethanol production relative to acetate production.

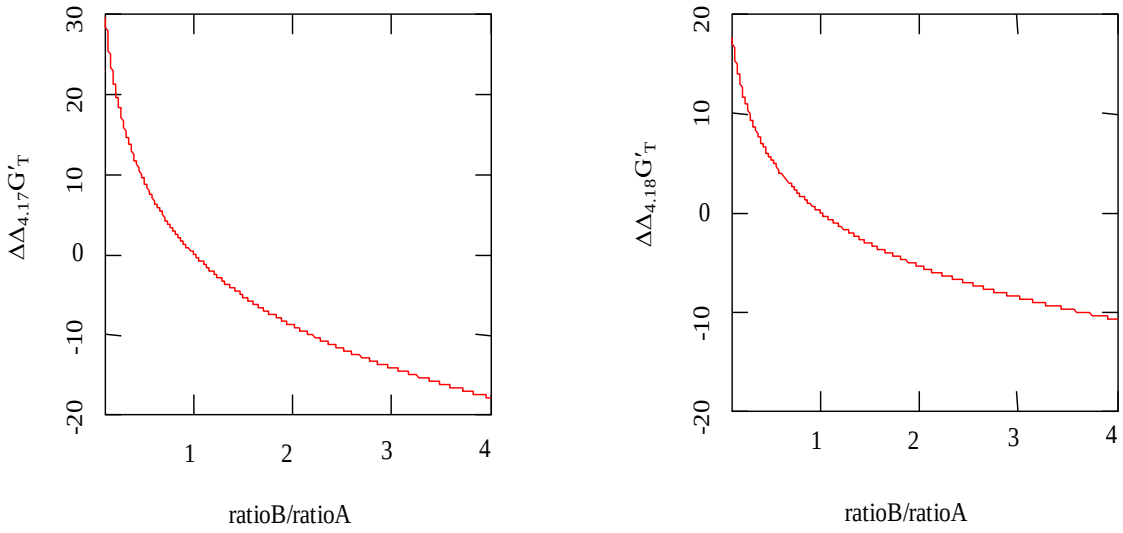

Figure 4-6.The change in the transformed Gibbs free energy of reaction from condition A to condition B for reaction 4.21($\Delta\Delta_{4.21}G'_T$) and 4.22 ($\Delta\Delta_{4.22}G'_T$) versus the change in the NAD_{red}/NAD_{ox} ratio

It is also beneficial to assess how varying the pH can affect the transformed Gibbs free energy of reaction (4.21, 4.22) for overall ethanol and acetate formation. Figure 4-7 shows the calculated values of $\Delta_{4.21}G_T'^0$ and $\Delta_{4.22}G_T'^0$. For both reactions, the standard Gibbs free energy is very negative, indicating that the both processes are thermodynamically favorable when looking at the overall reaction thermodynamics. $\Delta_r G_T'^0$ for both reactions decreases with the decrease of pH, though decreasing pH has greater effects on ethanol formation than on acetate formation. At pH=7, $\Delta_r G_T'^0$ for ethanol production is close to $\Delta_r G_T'^0$ for acetate production. However, at pH=5, $\Delta_r G_T'^0$ for ethanol production is much more negative than $\Delta_r G_T'^0$ for acetate production. Since ethanol and acetate are both converted from the intermediate acetyl-CoA, the different dependence of pH may result in the selectivity at varying pH values, with increased ethanol

formation being favorable as the pH is decreased. It should be noted the pH discussed here is the internal pH because the reactions happen within the cells. However, in Chapter 3, the literature review showed that the internal pH may be changed by adjusting the external pH. Thus, it is possible to adjust the media pH to change the product selectivity.

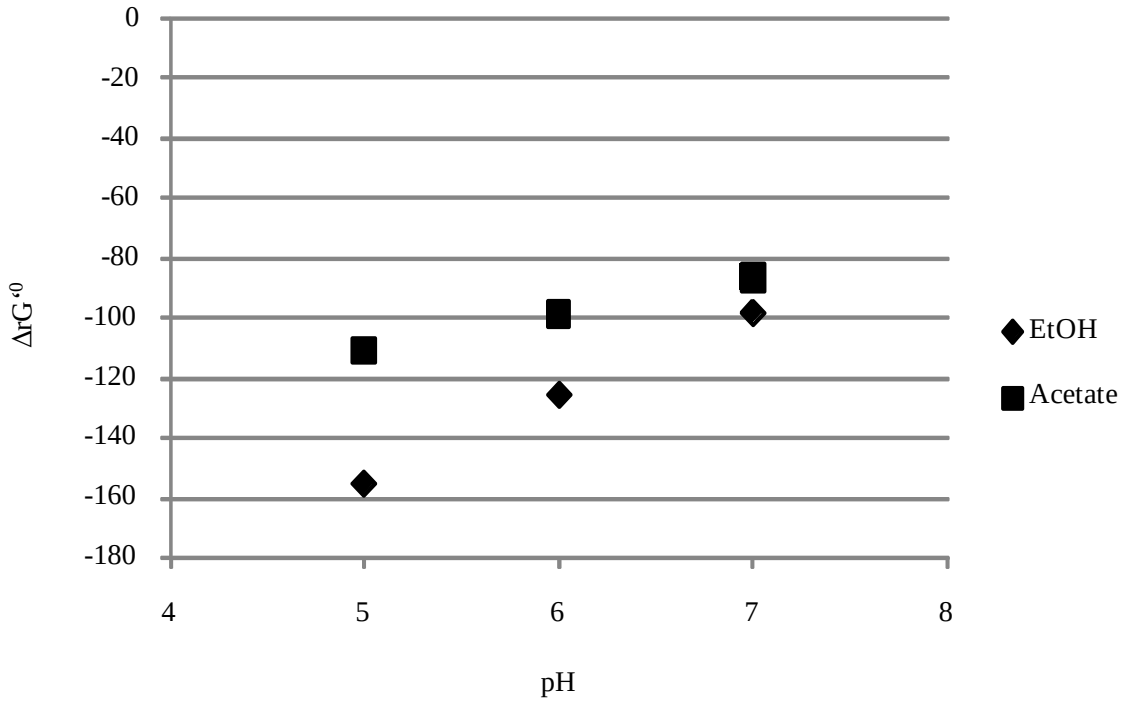

Figure 4-7.Standard transformed Gibbs free energy of reaction($\Delta_r G'^{0}_{310\,K}$)in kJ mol^{-1} of the combined reactions for ethanol (reaction 4.21) and acetate (reaction 4.22) production at varying pH when ionic strengths (I) of I=0.05 M

The thermodynamic favorability of a reaction is not only affected by the standard transformed Gibbs free energy, but also affected by the relative concentrations of reactants and products (previously denoted as Q). Figure 4-8 models $\Delta_r G'_{310\,K}$ for the acetate production reaction (4.22) with a varying NAD_{red}/NAD_{ox} ratio between 0.01 to 6 when the acetate concentration is 0.1 M and the partial pressures of CO and CO_2 are 0.4 atm and 0.3 atm, respectively. The values of acetate concentration, CO and CO_2 partial pressure are typical values

observed in preliminary experiments. It is not clear how close these values are to the reaction conditions within the cell. Nevertheless, it is obvious from Figure 4-8 that unless the NAD_{red}/NAD_{ox} is close to zero, the transformed Gibbs free energy for the combined reaction of acetate formation is always negative, resulting in high favorability. A similar plot for the combined reaction of ethanol formation may be also helpful to address the favorability of the reaction. However, the concentrations of ATP, ADP and phosphate are unavailable and the determination of such concentrations is beyond the scope of this work.

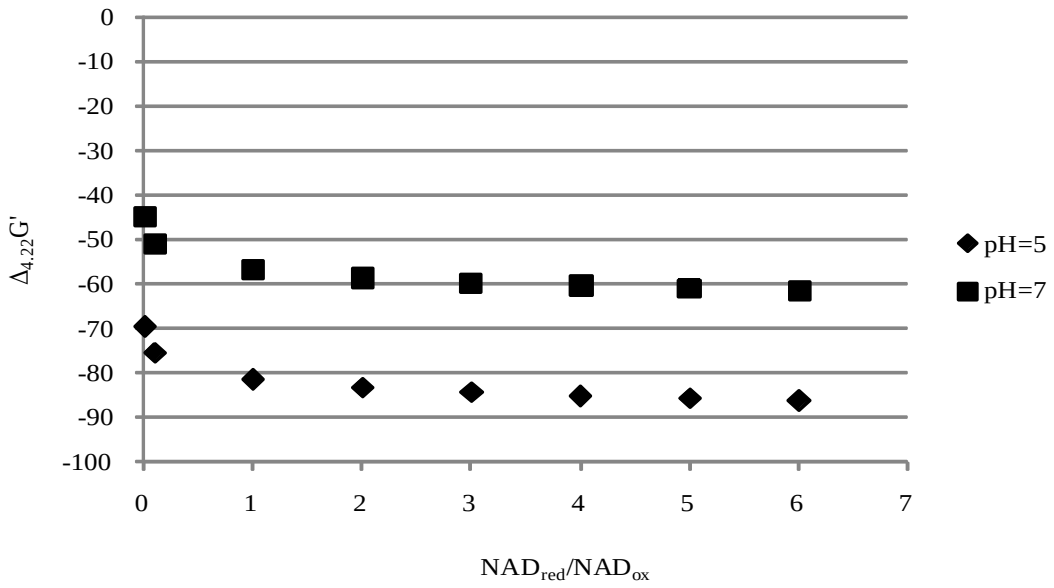

Figure 4-8.Transformed Gibbs free energy of acetate formation ($\Delta_{4.22}G'^{0}_{310\,K}$)in kJ mol^{-1}at varying NAD_{red}/NAD_{ox} ratios and pH 5and7, respectively, when ionic strengths (I) of I=0.05 M

From the above analysis for the overall reactions, the transformed Gibbs free energy of reaction is likely always negative. However, some specific steps, such as reaction 4.14 for acetate formation and reaction 4.15 for ethanol reaction, may thermodynamically limit the whole process. Thus, the optimization of key bottleneck steps would be beneficial for product formation and selectivity.

4.5.6 Conversion from acetate to ethanol

From earlier work, it was observed that the acetic acid concentration decreased after it reached a peak concentration for some, but not all, experiments (Frankman 2009). These observations occurred once cells reached a stationary phase. At the same time, the ethanol concentration increased. One possible explanation for the decrease in acetic acid (CH_3COOH) concentration is the conversion of acetic acid to ethanol (CH_3CH_2OH). However, it is unclear how reaction conditions may affect the thermodynamics of the conversion. It is also unclear as to why the conversion occurred in some instances but not in others. A greater understanding of the conversion process could lead to reactor designs in which acetate was first formed and then converted to ethanol.

One possible set of reactions leading to the conversion of ethanol (CH_3CH_2OH) from acetate (CH_3COOH) via the acetaldehyde intermediate (CH_3COH) are:

$$CH_3COOH + NAD_{red} \leftrightarrow CH_3COH + NAD_{ox} + H_2O \quad (4.25)$$

and

$$CH_3COH + NAD_{red} \leftrightarrow CH_3CH_2OH + NAD_{ox} \quad (4.26)$$

The transformed Gibbs free energy at standard conditions for these two reactions can be calculated using Table 4-2. While reaction 4.26 is thermodynamically favorable at standard conditions over the pH 5-7 range ($\Delta_r G_T^{'0}$ = -22.54 kJ/mol at pH 7 and -34.43 kJ/mol at pH 5), the standard transformed Gibbs free energy of reaction 4.25 is quite positive over the same pH range ($\Delta_r G_T^{'0}$ = 54.67 kJ/mol at pH 7 and 31.75 kJ/mol at pH 5), indicating that at standard conditions,

the conversion from acetic acid is not likely to occur. It appears that reaction 4.25 is the thermodynamic constraint for conversion. However, recall that $\Delta_r G_T' = \Delta_r G_T'^0 + RTlnQ$ and that for reaction 4.25, $Q = \frac{[CH_3COH]/[CH_3COOH]}{[NAD_{red}]/[NAD_{ox}]}$. Therefore, under certain reaction conditions, $\Delta_r G_T'$ for reaction 4.25 could go negative, thereby making the conversion of acetic acid into ethanol thermodynamically favorable. It should be pointed out again that the enzymes required for the conversion would be at pH conditions at their respective location within the cell.

Figure 4-9 plots $\Delta_{4.25} G_T'$ at both pH 7, 6, and 5 for varying values of Q with a logarithmic scale of the x-axis. At all pH levels, the $\Delta_{4.25} G_T'$ changes for different Q values follow similar trends, but $\Delta_{4.25} G_T'$ for the lower pH (pH = 5) is less positive throughout, indicating the reaction is more thermodynamically favorable with decreasing pH. Decreasing Q decreases $\Delta_{4.25} G_T'$ at all pH levels. At approximately Q < 10^{-5}, $\Delta_{4.25} G_T'$ goes negative for pH = 5, indicating that acetic acid to ethanol conversion can be thermodynamically favorable at that point. If the pH increases to 6, the required Q for the reaction to be thermodynamically favorable would be < 10^{-7}, which means it is much more difficult to happen at this condition. However, at pH 7, Q must be very close to zero (< 10^{-9} from calculation) for $\Delta_{7.2} G_T'$ to be negative. These results show that not only is lower pH better for acetic acid to ethanol conversion, but also, according to the definition of Q, the concentration of CH_3COH (the intermediate) must be very low in order for any such conversion to take place and/or the NAD_{red}/NAD_{ox} ratio must be high. As the pH increases, the concentration of CH_3COH (the intermediate) must be even lower and/or the NAD_{red}/NAD_{ox} ratio must be even higher for conversion to occur.

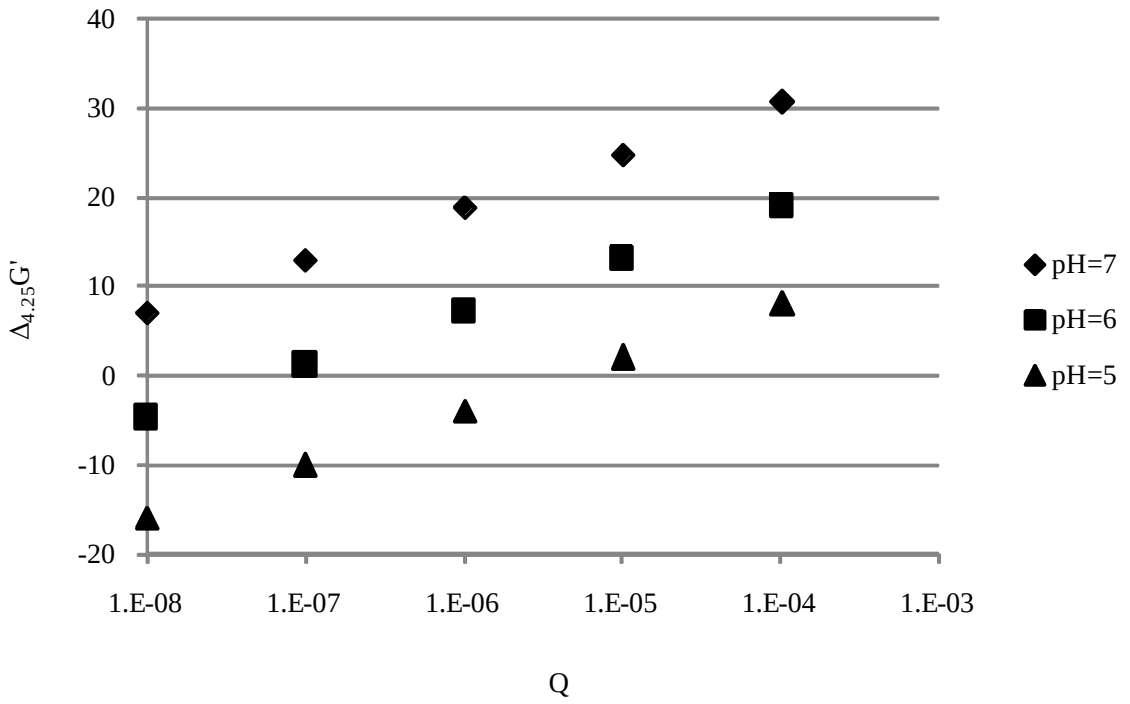

Figure 4-9.The transformed Gibbs free energy of reaction in kJ mol^{-1}for reaction 4.25 versus the change of Q at pH 7, pH 6, and pH 5

Thermodynamic analysis of the combined reaction for acetic acid conversion is also beneficial to assess the relative favorability of acetic acid conversion to ethanol. The net reaction when combining reactions 4.25 and 4.26 thus becomes

$$CH_3COOH + 2NAD_{red} \leftrightarrow CH_3CH_2OH + 2NAD_{ox} + H_2O \quad (4.27)$$

$\Delta_r G_T'^0$ of this reaction at pH = 7 is 32.13 kJ/mol, while $\Delta_r G_T'^0$ when pH = 5 is -2.68 kJ/mol. This again supports the above conclusions that lower pH is more favorable for acetic acid to ethanol conversion.

Figure 4-10 shows $\Delta_r G_T'$ of the combined reaction at pH7, 6 and 5 for varying Acetic Acid/Ethanol and NAD_{red}/NAD_{ox} ratios. At pH = 7, even runs with high AA/Ethanol and NAD_{red}/NAD_{ox} ratios cannot yield $\Delta_r G_T'$ values less than zero. In contrast, the $\Delta_r G_T'$ values at pH = 5 for most Acetic Acid/Ethanol ratios are negative. Only when the NAD_{red}/NAD_{ox} ratio goes to very low levels, the $\Delta_r G_T'$ values at pH = 5 become positive. Reasonably, the $\Delta_r G_T'$ values at pH = 6 are between the values of pH 7 and 5. But unless the NAD_{red}/NAD_{ox} ratio goes to very high, the $\Delta_r G_T'$ values are positive, indicating the reaction cannot happen. These results suggest that for the same conditions of Acetic Acid/Ethanol and NAD_{red}/NAD_{ox}, acetate to ethanol conversion will likely occur at pH 5 and high NAD_{red}/NAD_{ox} ratios, but not at pH 6 or 7. This further strengthens the conclusion that acetic acid to ethanol conversion cannot happen at higher pH, but lower pH and higher NAD_{red}/NAD_{ox} (more negative E) can induce the conversion.

The pH and E dependency of conversion from acetate to ethanol shows a potential method for increasing ethanol production. If the conversion from acetate to ethanol can be induced by adjusting the experimental pH and E, it would be possible to have both higher ethanol concentrations and higher product selectivity. Again, it should be noted the reactor pH is not the same as the internal pH. Although there is a correlation between external pH and internal pH, it is difficult to quantitatively adjust the internal pH because the internal pH has resistance to the external pH change. It is not possible to say what external pH would induce the acetate to ethanol conversion. Thus, the control of redox potential (E) of the media may be a more straightforward method to induce the conversion.

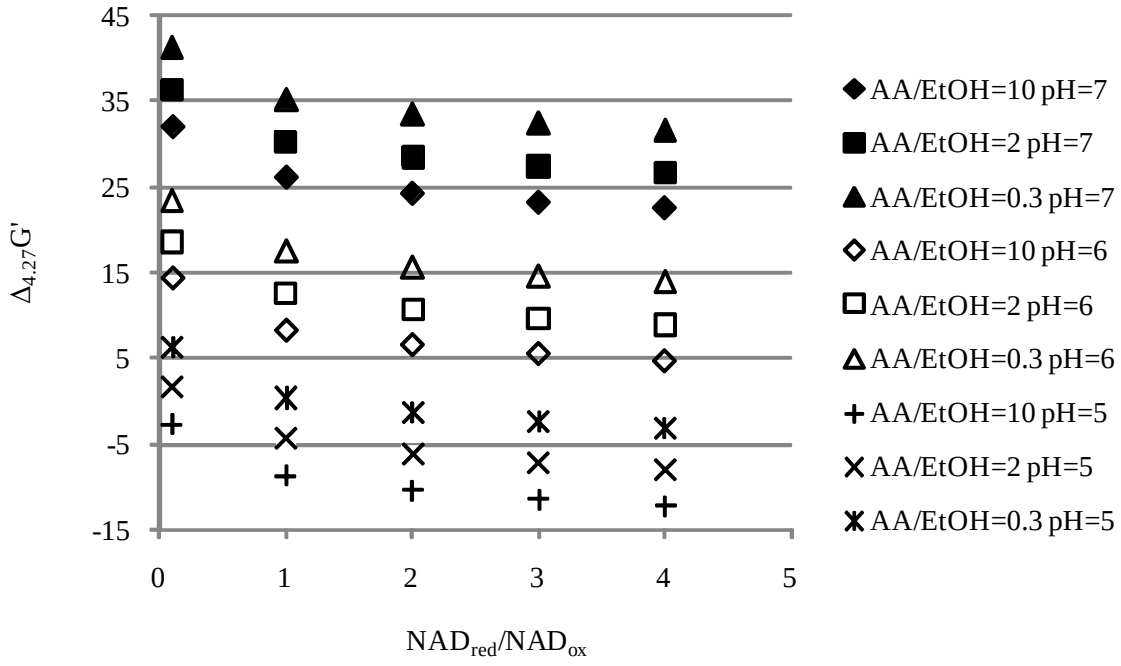

Figure 4-10.The transformed Gibbs free energy of reaction in kJ $mol^{-1}$for reaction 4.27 versus the change of $NADr_{ed}/NAD_{ox}$ ratios at different acetate to ethanol ratio (AA/EtOH) at pH 7, pH 6 and pH 5

4.6 Conclusions

The above analysis shows the effects of ionic strength, pH, and NAD_{red}/NAD_{ox} ratios on the transformed Gibbs free energy of some key reactions (and overall reactions) involved in the metabolic pathway. Ionic strength has only slight effects on the thermodynamic favorability of the reactions, whereas pH has a great effect. At standard conditions, electron production (reactions 4.5 and 4.6) is favorable at higher pH. For the intermediate acetyl-CoA synthesis steps (reactions 4.7 through 4.12), all Gibbs free energy of reaction values are either similar or lower at pH 5as compared to pH 7. The key thermodynamic bottleneck for acetyl-CoA synthesis appears to be reaction 4.7 although it is feasible that enzyme activities of later steps can lead to

other bottlenecks. For the acetate production, the key thermodynamic bottleneck is the reaction 4.14, especially at low pH. For the ethanol production, the bottleneck is likely the reaction 4.15 at high pH. More importantly, there is a possible conversion from acetic acid to ethanol and the pH and NAD_{red}/NAD_{ox} ratio play a crucial role on the conversion. At high pH (pH = 7), the conversion cannot occur in practice because the transformed Gibbs free energy is always positive at any combination of reasonable acetate/ethanol and NAD_{red}/NAD_{ox} ratios. However, lowering the pH can drive the transformed Gibbs free energy to negative and induce the conversion from acetic acid to ethanol. This is one potential method to increase the overall ethanol production. Also, if the pH is kept constant, the conversion may happen at higher NAD_{red}/NAD_{ox} ratios, but not at lower NAD_{red}/NAD_{ox} ratios. Thus, the acetate to ethanol conversion may be induced by decreasing the redox potential (E) of the reactor to have a high NAD_{red}/NAD_{ox} ratio.

Based on the above analysis, it is clear that altering the pH and redox potential of the system most likely can be used as a tool to promote the formation of the desired product. Although internal pH is difficult to control, adjusting the external pH may cause a lower internal pH. Since acetate production is generally considered to be growth-associated and ethanol production generally occurs when there is no cell growth, the above trends suggest that a strategy of adjusting the system pH and redox potential could be developed to promote either higher acetate formation (and thereby cell growth) or higher ethanol formation. A high pH environment may be maintained to overcome the potential bottlenecks for acetate production during cell growth phase, but a low pH environment with a low redox potential may be maintained to induce the conversion from acetate to ethanol and to maintain a preference for ethanol production relative to acetate production. Thus, such pH and redox potential modulation can not only

increase acetate production during growth phase, but also induce the conversion from acetate to ethanol during the non-growth phase, which would increase the overall production of ethanol.

In summary, the thermodynamic analysis for reactions involved in the acetyl-CoA metabolic pathway led to several findings regarding syngas fermentation.

- The pH, but not the ionic strength, has significant impact on several transformed Gibbs free energy ($\Delta_r G_T^{'}$) of reactions in the metabolic pathway.
- Electron production reactions are more favorable with increasing pH.
- A potential thermodynamic bottleneck for acetyl-CoA synthesis appears to be formate formation. This reaction only occurs when the formate concentration is negligible. Thus, formate must be scavenged rapidly.
- Acetyl-CoA synthesis reactions are more favorable with decreasing pH.
- A potential thermodynamic bottleneck for the conversion from acetyl-CoA to acetate appears to be the acetate formation reaction (reaction 4.14). This reaction is more favorable with increasing pH. In order to make reaction 4.14 proceed forward, the ATP/ADP ratio likely has to be small.
- A potential bottleneck for the conversion from acetyl-CoA to ethanol appears to be acetaldehyde formation (reaction 4.13). This reaction is more favorable as the pH decreases.
- Conversion of acetate to ethanol can happen at low pH (pH = 5), but is not as favorable at high pH (pH = 6 and 7), unless the ratio $NAD_{red}/NAD_{ox}$is increased.
- Increasing the NAD_{red}/NAD_{ox} ratio can greatly increase the driving force for both acetate and ethanol formation, with the likelihood that ethanol benefits more with an increasing ratio.

- Enhancement of syngas fermentation may be performed with adjusting pH and NAD_{red}/NAD_{ox} ratio of the media to promote the desired product.

With the thermodynamic analysis utilized in this Chapter based on the comparison of changing reaction conditions, it important to note that the analysis of the Gibbs free energy at the reaction site as a function of various conditions (pH, redox potential, gas composition) gives great insights as to whether the reaction will go in the forward or reverse direction at a given time during the fermentation. For a metabolic reaction to occur, a negative Gibbs free energy of the reaction is required. Thus, the thermodynamic analysis could be a tool for proposing adjustments to the media to favor or not favor a reaction towards promoting more ethanol formation. There is potential to adjust the reactor conditions to make the Gibbs free energy of reaction change from positive to negative or to make it more negative. For instance, thermodynamic analysis showed that the Gibbs free energy of acetate to ethanol conversion may vary positive or negative, depending on the redox potential and the pH. Thus, if the acetate to ethanol conversion can be induced by adjusting the reactor conditions, the overall ethanol production would be increased.

It should be noted that thermodynamic favorability is not the sole factor which determines whether or not a reaction occurs in practice; kinetics and transport phenomena must be considered. Therefore, reaction mechanistic factors such as kinetics and transport considerations could potentially prevent a reaction from occurring despite thermodynamic favorability. However, thermodynamic analysis provides a universally applicable understanding of the fermentation process which can later by adjusted with kinetics and transport parameters specific to each individual strains of bacteria. Thus, the key aspects of this chapter suggest that developing a combined pH and redox potential strategy can be used to enhance ethanol

production, with a lower pH and redox potential (associated with NADH) benefiting ethanol production. The focus of Chapters 5-7 involves the use of reducing agents, redox control, and pH control to confirm the insights developed in this chapter and to develop a strategy using the insights to enhance ethanol production.

5. Sulfide assessment in bioreactors with gas replacement

5.1 Introduction

From the literature review and the analysis in previous chapters, reducing agents and the associated redox potential may affect the process of syngas fermentation by not only maintaining an anaerobic environment, but also adjusting the redox potential of the media. Many biological processes have utilized the addition of sulfide constituents to affect the redox potential, remove residual oxygen, and/or provide a source of sulfur for metabolism. Sodium sulfide (Na_2S) or Na_2S combined with cysteine are often used as sulfide constituents. The redox level can be very important in biological processes since redox reactions are often critical for cell growth and product formation-- part of the reason may be due to the associated reducing equivalents (for example NAD_{red}/NAD_{ox}). Other agents used to affect redox levels include cysteine, titanium (III)-citrate, potassium ferricyanide, and methyl viologen (Bryant 1961; Rao 1987; Jee 1987; Sridhar 2001).

Many studies have involved the assessment of the effects of the addition of sulfur constituents on cell growth and product formation. However, as noted in Chapter 2, the effects of sulfide constituents and associated sulfide concentrations on growth and product formation have shown considerable variance. Although this variance can be a result of the types of cells utilized, varying experimental system designs have the potential for affecting the associated sulfide

concentrations evaluated. Whether used as a reducing agent or sulfur source, it is important to note that sulfide added to solution not only forms ions (HS^- or S^{2-}) but can also convert to hydrogen sulfide (H_2S) in the media. The degree of conversion depends upon the solution pH (Hansen, 1978). The converted H_2S may leave the bioreactor during the gas replacement and result in a change of sulfide concentration in the media. A preliminary study with the addition of 1% (V/V) cysteine-sulfide solution into batch and continuous bioreactors confirms this hypothesis and shows that sulfide concentrations change with time and are dependent upon the type of bioreactors (see Figure 5-1) (details of cysteine-sulfide solution and bioreactors are shown in section 5.2).

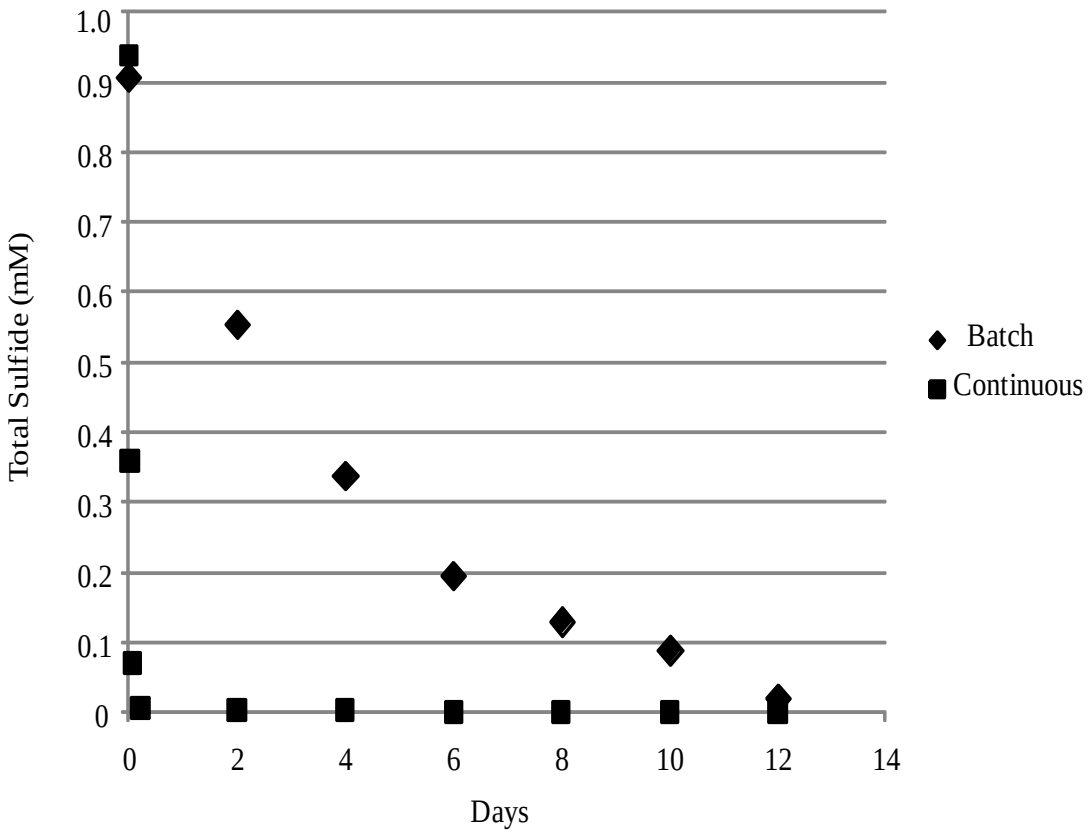

Figure 5-1.Sulfide concentration versus time in batch and continuous reactors

Since H_2S is a volatile compound, the potential loss of sulfide from the media can result in changing sulfide concentrations and potentially changing redox levels during the course of the experiment. This is in contrast to other reducing agents, such as cysteine, that remain in solution throughout an experiment. The loss of H_2S may have a significant effect on the fermentation process, leading to potential discrepancies among biological processes utilizing differing experimental designs. Thus, understanding the fate of sulfide in biological processes is critical, especially if the process involves continuous purging or intermittent replacement of the gas head space.

Since previous studies have not assessed the fate of sulfide in gas exchange bioreactors, this work explored the fate of sulfide in two bioreactors, one involving the continuous purging of the gas head space in a 1-liter bioreactor and one involving the intermittent purging of the gas head space in 100-ml bottles. The aim of this objective was to explore why and how the sulfide concentration changes and the associated effect on the redox potential.

In this work, models were developed that explained sulfide loss in bottle studies (batch reactors) and continuously gas-purged reactors. The results of this work lead to understanding the fate of sulfide during an experiment such that experiments can be designed to maintain constant sulfide levels for providing greater clarity when interpreting experimental results.

5.2 Materials and methods

5.2.1 Media and sulfide solutions

Although this study did not use cells, culture media was used to mimic the cellular environment. The media was made by adding 10 ml metals stock solution, 30 ml mineral stock

solution, 10 ml vitamin stock solution, 1 g yeast extract, and 10 g MES buffer to 950 ml distilled water. Trace metals stock solution contained (per liter) 0.2 g cobalt chloride, 0.02 g cupric chloride, 0.8 g ferrous ammonium sulfate, 1 g manganese sulfate, 0.2 g nickel chloride, 2 g nitrilotriacetic acid, 0.02 g sodium molybdate, 0.1 g sodium selenate, 0.2 g sodium tungstate, and 1 g zinc sulfate. The mineral stock solution contained (per liter) 4 g calcium chloride, 20 g hydrated magnesium sulfate, 10 g potassium chloride, 10 g phosphate Mono, and 80 g sodium chloride. The vitamin stock solution contained (per liter) 0.005 g aminobenzoic acid, 0.002 g d-Biotin, 0.005 g pantothenic acid, 0.002 g folic acid, 0.01 g MESNA, 0.005 g nicotinic acid, 0.01 g pyridoxin, 0.005 g riboflavin, 0.005 g thiamine, 0.005 g thioctic acid, and 0.005 g vitamin B12 (Rajagopalan, 2002). The media was titrated to pH 6.0 using 5N KOH prior to use. A Na_2S solution, containing 4 g of $Na_2S{\cdot}9H_20$ in 100 mL water, was freshly prepared for all experiments. The solution was prepared by adding 100 mL purified water into a serum bottle. The bottle was then boiled and purged with nitrogen to remove oxygen. Then, 4 g of sodium sulfide was added into the bottle in an anaerobic shell and sealed with a rubber septum and cap. In some cases, L-cysteine (4 g in 100 mL) was used alone or added to the sulfide solution to make a cysteine-sulfide solution. $Na_2S{\cdot}9H_2O$, hydrochloride acid and potassium hydroxide were purchased from EMD Chemicals (Gibbstown, New Jersey). All other chemicals were purchased from Sigma-Aldrich (St. Louis, Missouri).

5.2.2 Continuous 1-L and 3-L bioreactors

A BioFlo 110 Benchtop Fermentor with a 1-L working volume (New Brunswick Scientific, Brunswick, New Jersey) and 2-L head space was used for the continuous bioreactor

assessment involving batch liquid and continuous gas feed. This bioreactor was used for assessing the fate of sulfide and the corresponding redox potential in the bioreactor. After adding one liter of media, the bioreactor was autoclaved at 121 °C for 15 minutes and then purged with N_2 overnight to remove dissolved oxygen. Afterwards, 100 mL/min of syngas (30% H_2, 30% CO_2 and 40% CO) was continuously added to the bioreactor that was maintained at 37 °C. After the dissolved oxygen reading stabilized (with a value close to zero), 10 ml of the Na_2S solution was added to the media. Media and syngas were used to maintain consistency between the non-cellular work discussed in this chapter and the cellular studies outlined in Chapter 6.

At various time intervals, 1-mL of liquid was sampled through the sampling port and analyzed for the total sulfide concentration. The redox potential was continuously measured using an ORP probe with an Ag/AgCl reference electrode (Cole Parmer, Vernon Hills, Illinois). The response time of the ORP probe was approximately 250 ms. Labview (National Instruments, Austin, Texas) was used with a USB port data acquisition system to convert the output from the ORP probe to mV. All redox values were converted from the Ag/AgCl reference to the standard hydrogen electrode (SHE) reference assuming that a SHE reference is +222.3 mVcompared to an Ag/AgCl reference of 0 mV (Malazzo, 1978).

To assess the fate in different sizes of reactors, a BioFlo II Benchtop Fermentor with a 3-L working volume (New Brunswick Scientific, Brunswick, New Jersey) and a 2-L head space was also used for the continuous bioreactor assessment involving batch liquid and continuous gas feed. Similar operating conditions occurred with this reactor except 30 ml of the Na_2S solution was added to the media.

5.2.3 100-mL bottles

Serum bottles (total volume 288 ml) were used as batch bioreactors containing 100 ml of media and sealed with rubber septa. For all studies, 100 ml of media were added to the bottles and the bottles were continuously boiled and purged with nitrogen for 4 minutes to remove the oxygen in the media. Afterwards, the bottles were autoclaved at 121 °C for 10 minutes and then purged with syngas (30% H_2, 30% CO_2 and 40% CO) at ~1500 sccm for two minutes. Bottles were then pressurized with syngas at 20 psig.

For the experiments repeated in triplicate, 1 ml of Na_2S solution was added to the bottles. Bottles were placed in a shaking incubator at 150 rpm and 37 °C. During the experiments, bottles were regassed every two days by purging with syngas for one minute at ~1500 sccm and then pressurizing the bottles at 20 psig. The bottles were placed in a shaking incubator at 150 rpm and 37 °C. This regassing cycle was repeated five times and was used to mimic the cellular experiments. Before and after every regassing, 1-mL of liquid was withdrawn from the bottles by a syringe to take liquid analysis.

5.2.4 Liquid analysis

The total aqueous sulfide concentration (S^{2-}, HS^-, and H_2S) in all experiments was determined using Sulfide Vacu-Vials (CHEMetrics, Calverton, Virginia) which employ methylene blue chemistry. In an acidic solution, sulfide in a 1-mL liquid sample reacts with N, N-dimethyl-p-phenylene-diamine and ferric chloride to produce methylene blue. The resulting blue color absorbance at 660 nm is correlated to the sulfide concentration. The absorbance was

measured using a Shimadzu UV-1700 spectrophotometer (Shimadzu Scientific Instruments, Columbia, Maryland). According to the manufacturer, this method provides a detection limit of ~0.6 μM of total sulfide. From multiple measurements, we determined the accuracy to be approximately 2 μM. Once a measurement was obtained, the measured concentration was multiplied by 25 to obtain the sample concentration as a result of the dilution.

The pH of the samples was measured using an Oakton portable pH meter (Cole Parmer, Vernon Hills, Illinois) with an Accumet extra-long calomel combo pH electrode (Fisher Scientific, Pittsburgh, Pennsylvania).

5.3 Results

5.3.1 Continuous 1-liter bioreactor

As shown in Figure 5-2, the total sulfide concentration following the addition of 10 mL Na_2S solution into a pH 5.9 medium was approximately 0.9 mM. The injection of Na_2S occurred at time zero and the sulfide concentration decreased to zero in an exponential manner within approximately three hours. Thus, sulfide was stripped from the culture medium in a relatively short time compared to the typical operation of weeks or months for many syngas fermentation bioreactors.

With regards to the redox potential (E), the redox potential was initially stable at approximately -20 mV (SHE) prior to the injection of Na_2S. Following the injection of Na_2S, the redox potential rapidly decreased to -175 mV (SHE) and then increased to nearly the initial redox potential within three hours. The increase in redox potential corresponded to the decrease in sulfide concentration.

Additional experiments shown in Figure 5-2 show that the addition of 10 mL of cysteine, which was another reducing agent, rapidly lowered the redox potential to a relatively stable value of -80 mV (SHE). However, with the addition of cysteine-sulfide, the redox potential rapidly lowered to -190 mV (SHE) and then increased within three hours back to a value similar to the stable cysteine value. Similar to the Na_2S studies, the decrease in the sulfide concentration showed the same trend and the increase in redox potential correlated with a decrease in the sulfide concentration.

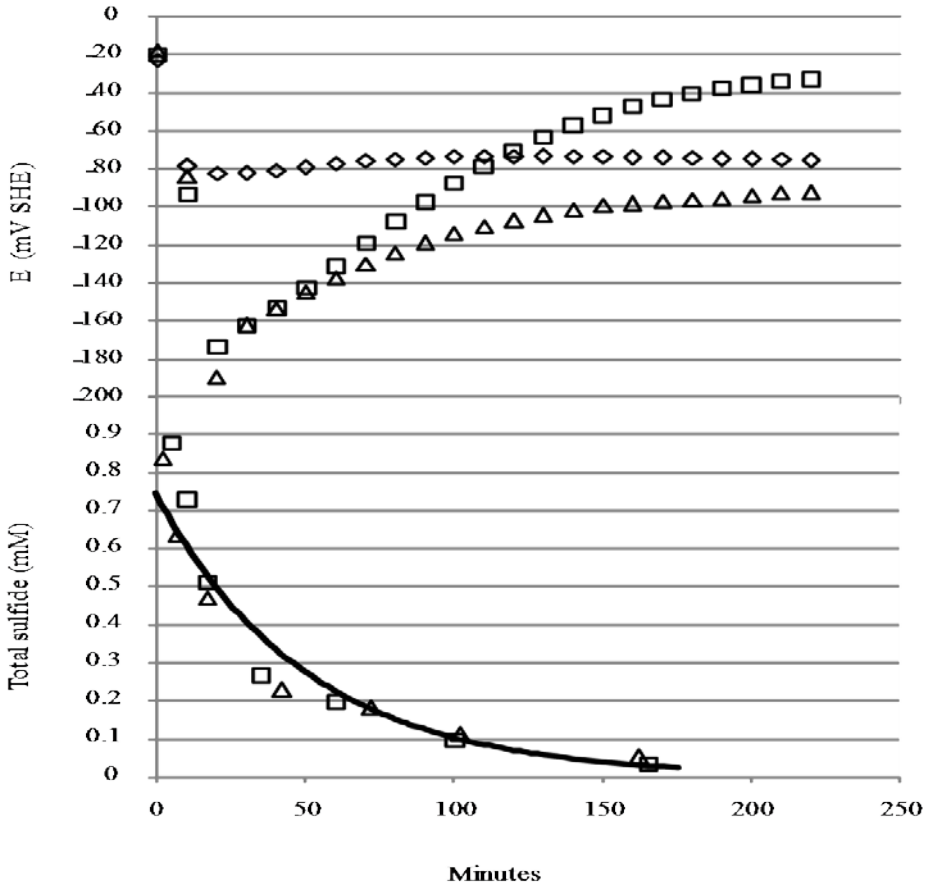

Figure 5-2.Top: Redox potential (E) in a continuous reactor following the injection of cysteine (open diamond), sodium sulfide (solid square), and cysteine-sulfide (solid triangle). The redox reference is a Standard Hydrogen Electrode (SHE). Bottom: Associated sulfide concentration profiles. The solid line represents the model of Equation 5.7 with k_La/V of 0.020 min^{-1}

The rapid sulfide loss for all of the above studies demonstrated that sulfide would be non-existent in a continuous reactor if sulfide was not replaced. Thus, interpretation of sulfide effects on a process would be in error.

5.3.2 100-ml bottles

During the 100-ml bottles studies, Na_2S with cysteine was added to the bottles and allowed to reach equilibrium. Following equilibrium, the head space was purged with fresh syngas as previously described. The sulfide concentration was then measured with time until a new equilibrium was established. Figure 5-3 shows an example of the total sulfide concentration with time for the above process in which time zero represents the equilibrium sulfide concentration just before purging. As shown, equilibrium took approximately 80 minutes to establish and the decrease in sulfide concentration showed an exponentially decaying trend.

The process of establishing equilibrium, regassing, and then obtaining a new equilibrium was repeated five times. As shown in the Figure 5-4 after each regassing, the sulfide concentration decreased to a new equilibrium concentration which was lower than the previous equilibrium concentration. After five gas replacements, the sulfide concentration decreased from an initial value of 0.9 mM to approximately 0.1 mM. Thus, gas replacement in bottle studies has a significant impact on the aqueous sulfide concentration. The decreasing concentration with time can have a significant impact on the interpretation of experimental results since the concentration is not maintained at a constant level. Although the redox potential was not measured, the redox potential should also change with changing sulfide concentration since such observations were noted in the continuous bioreactor studies.

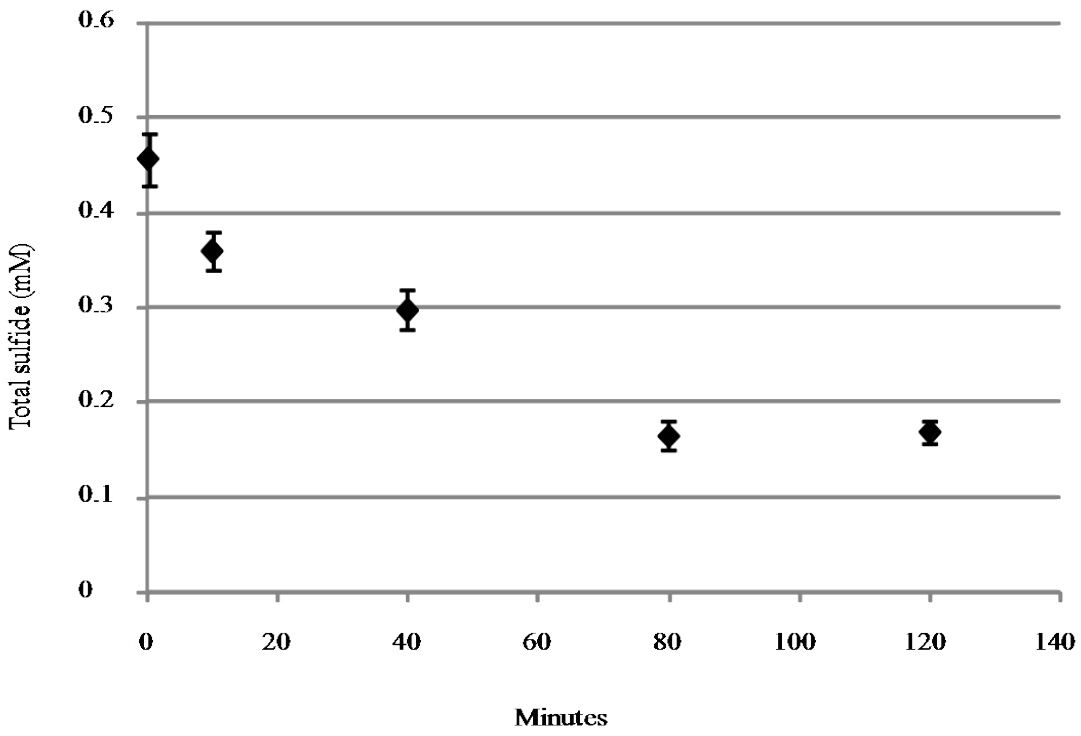

Figure 5-3.Sulfide concentration versus time in batch bioreactor following regassing. Error bars represent the standard error (n=3)

In comparison with the sulfide loss in the continuous bioreactor, the sulfide concentration remained in bottles studies for a longer time. For instance, these bottle studies represent gas replacement every two days. Thus, for this study, the sulfide concentration would change from 0.9 mM to 0.1 mM over five gas replacements (equivalent to ten days) whereas the sulfide concentration would be completely removed in the continuous reactor within three hours. Therefore, comparison between bottle studies and a continuous bioreactor would be difficult due to differing sulfide concentrations and redox potential, even if the initial sulfide concentrations were the same.

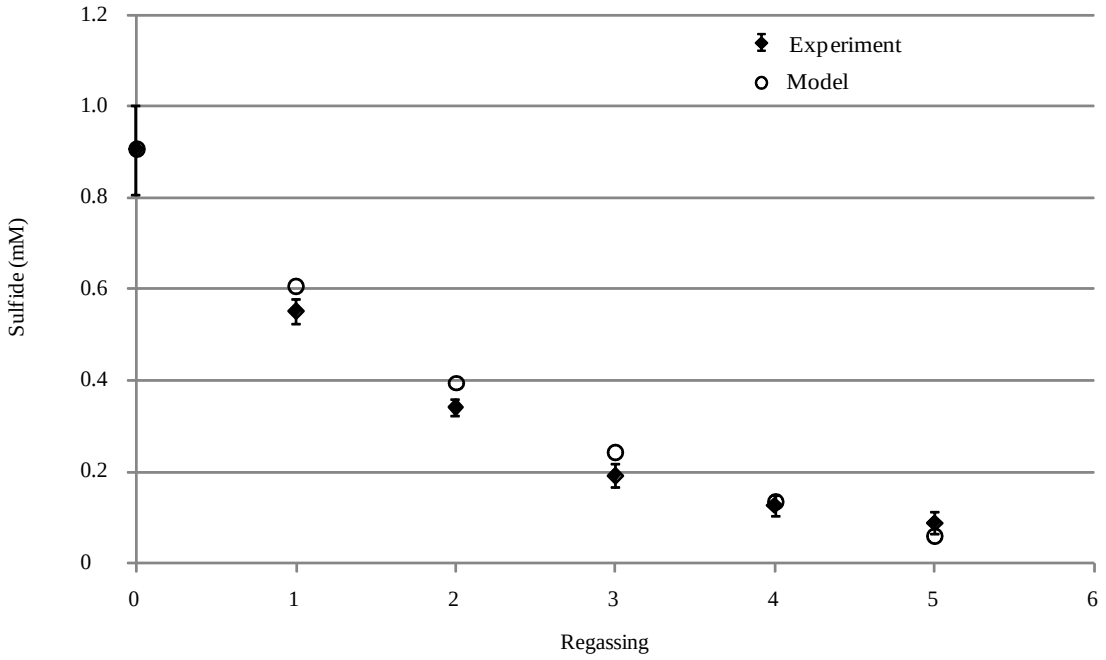

Figure 5-4.The equilibrium sulfide concentration and model predictions following each regassing. Error bars represent the standard error (n=3)

5.3.3 Continuous 3-liter bioreactor

When comparing two sizes of continuous reactors, Figure 5-5 shows that the trend of sulfide loss in the continuous 3-liter bioreactor followed a similar exponential decay as compared to the1-liter bioreactor, though the decrease of sulfide concentration was slower in the 3-liter bioreactor than in 1-liter bioreactor. As shown in Figure 5-5, the total sulfide concentration immediately following the addition of 30 mL Na_2S solution into the media was approximately 0.9 mM, then the concentration decreased to 0.1 mM within about 150 minutes. Compared with Figure 5-2, in which sulfide concentrations decreased from 0.9 mM to 0.1 mM within 100 minutes, the sulfide concentration change in the 3-liter bioreactor was slower than it was in the 1-L bioreactor, but both were much faster than the sulfide change in the batch bioreactor.

Another interesting finding was that the decay of sulfide concentration was similar at both pH 5.4 and 5.9, demonstrating that pH does not appear to play a dominate role in the sulfide stripping.

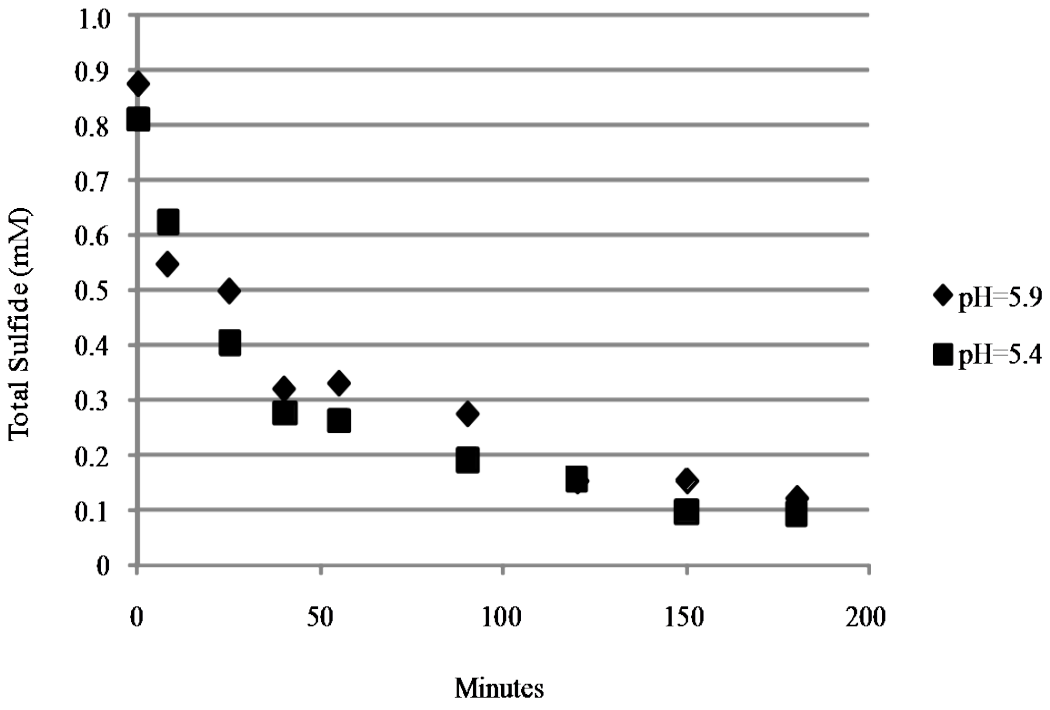

Figure 5-5.Sulfide concentrations after Na_2S addition into continuous 3-liter bioreactor

5.4 Discussion

As noted in the studies, the total sulfide concentration decreased with time as a result of continuous or intermittent purging with gas. As shown with the continuous bioreactor, it's important to recognize that the loss of sulfide can also result in a changing redox potential although the redox changes can be enhanced or tempered depending upon the experimental system (see Chapter 7 for redox potential control studies). Thus, cellular systems could be affected since the activity of some enzymes has been shown to be very sensitive to the redox

potential (Heo 2001; Van Dijk 1981). The important point is that previously noted discrepancies with sulfide studies may potentially be a result of sulfide and/or redox potential changes during an experiment and comparison of experimental studies would be difficult if sulfide losses occurred.

An understanding of the fate of sulfide following the addition of Na_2S to solution can provide insights into the interpretation of experimental results and can also help provide insights on how to develop bioreactors to maintain controlled levels of sulfide (and perhaps redox potential). Following the addition of Na_2S (initially forming S^{2-} in solution) to either the bottles or the continuous bioreactor, HS^- and H_2S can be formed in solution according to:

$$S^{2-}+H_2O \leftrightarrow HS^-+OH^- \quad (5.1)$$

$$HS^-+H^+ \leftrightarrow H_2S\ (aq) \quad (5.2)$$

where $H_2S(aq)$ represents the H_2S in aqueous solution. However, since S^{2-} does not exist in appreciable concentrations in water compared to the other sulfide species (Barbero 1982), it can be assumed that the total sulfide concentration $[S]_T$ in solution, as measured by the sulfide assay, is composed of only HS^- and H_2S (aq) concentrations. Thus:

$$[S]_T = [H_2S]_{aq} + [HS^-] = \left(1+\frac{1}{K_2[H^+]}\right)[H_2S]_{aq} \propto [H_2S]_{aq} \quad (5.3)$$

where K_2 is the equilibrium constant of Equation 5.2 and has a value of 6.65×10^6 M^{-1} at 37°C (Barbero 1982). As noted in Equation 5.3, $[S]_T$ is proportional to the aqueous concentration of

H_2S and the proportionality depends upon the solution pH. Equation 5.3 is useful in assessing the fate of total sulfide in both the continuous bioreactor and bottle studies. As part of the assessment, it's important to note that $[H_2S]_{aq}$ is a volatile species and can therefore transport between both the aqueous and gas phases according to:

$$H_2S\ (aq) \leftrightarrow H_2S\ (g) \tag{5.4}$$

where H_2S (g) represents the H_2S in the gas phase.

5.4.1 Continuous bioreactor

A material balance of $[H_2S]_{aq}$ is useful to show that changes in $[S]_T$ for the continuous bioreactor can be attributed to the loss of H_2S from solution. Assuming no other losses of $[H_2S]_{aq}$ except through transport via the gas-liquid interface, the material balance shows

$$\frac{d[H_2S]_{aq}}{dt} = \left(\frac{k_L a}{V}\right)_{H_2S} \left([H_2S]^*_{aq} - [H_2S]_{aq}\right) \tag{5.5}$$

where $[H_2S]^*_{aq}$ represents the H_2S aqueous concentration that is in equilibrium with the H_2S gas-phase concentration. The volumetric mass transfer coefficient for H_2S is k_La/V. For the continuous bioreactor studies, a high gas purge rate of syngas results in the approximation that $[H_2S]^*_{aq}$ is negligible since H_2S is not present in the purge gas.

Since $[S]_T$ is proportional to $[H_2S]_{aq}$ as shown in Equation 5.3 and $[H_2S]^*_{aq}$ is negligible, Equation 5.5 can be reduced to:

$$\frac{d[S]_T}{dt} = -\left(\frac{k_L a}{V}\right)_{H_s S} [S]_T \tag{5.6}$$

Integration of Equation 5.6 gives:

$$-\ln \frac{[S]_T}{[S]_{T0}} = \left(\frac{k_L a}{V}\right)_{H_2 S} t \tag{5.7}$$

where $[S]_{T0}$ represents that initial total sulfide concentration. Thus, a plot of $-\ln([S]_T/[S]_{T0})$ versus time would give a straight line with a slope of k_La/V if the premise that the above model via the stripping of H_2S completely explains the loss of sulfide from solution. For the Na_2S data in Figure 5-2, the plot did result in a nearly straight line (R^2=0.97) with a k_La/V of 0.020 ± 0.002 (std error) min^{-1}. Equation 5.6 using the regressed k_La/V value is shown in Figure 5-2. It is interesting to note that the sulfide loss is independent of pH according to Equation 5.6, which is consistent with the experimental results (Figure 5-5). As noted, sulfide loss decayed exponentially in both the 1-L and the 3-L reactors. Since mass transfer analysis depends greatly upon gassed power, superficial gas velocity, impeller geometry, and other reactor parameters (Wang 1979), it is beyond the purpose of this work to perform detailed analysis as to why the two reactors had different mass transfer coefficients. The key point is that sulfide is continuously lost in gas-continuous reactors.

The above analysis shows that H_2S loss from a continuously-purged bioreactor is a major issue when utilizing Na_2S. This loss, which can be very rapid, will not only lead to a diminishing sulfide concentration but also likely lead to an increasingly more positive redox potential, depending upon the presence or absence of other reducing agents. Varying bioreactor designs, which affect the H_2S mass transfer coefficient, will lead to varying rates of sulfide loss.

If desirable for experiments, it is possible to maintain a constant aqueous sulfide concentration ($d[S]_T/dt = 0$) in a continuous bioreactor if the net sulfide added between inlet and outlet streams is at a rate equivalent to $(k_La/V)[S]_T$. However, if Na_2S is continuously added, the effect of continuously added Na^+ on a cellular system should be assessed. The detailed analysis of a constantly-maintained sulfide concentration study in gas-continuous reactors is discussed in Chapter 6.

5.4.2 100-ml bottles

Unlike the continuous reactor in which the gas head space was continuously purged, the bottle studies involved an intermittent purging of the gas head space. With intermittent purging, the sulfide concentration will not disappear as rapidly as in a continuously purged bioreactor. Establishing a model to predict sulfide levels following each purging would be useful for knowing sulfide levels throughout an experiment (which is useful for comparisons among experiments) and for maintaining constant sulfide concentrations if desired. Following the initial injection of sulfide solution in a closed system such as a bottle, the sulfide species are distributed between the liquid and gas phases. The liquid phase contains HS^- and H_2S (S^{2-} is negligible as discussed above) and the gas phase contains only H_2S.

When the bottles are intermittently purged, any gas in the head space (including H_2S) is rapidly removed from the head space due to the purging. For this study, purging was for one minute at 1500 sccm with fresh syngas (gas residence time is approximately 188 ml/1500 sccm = 0.12 min). Since it was previously shown that equilibrium takes two hours for the bottles used in this study (Figure 5-3), it can be assumed that the sulfide species in the aqueous phase are essentially at the same concentrations before and after purging. Once the purging is stopped, a new equilibrium distribution of sulfide species occurs. In the liquid phase, equilibrium between HS^- and H_2S is reestablished. Equilibrium of H_2S is also established between both phases.

A model was developed to predict the equilibrium $[S]_T$ after each intermittent purging to confirm the above process. Following the initial injection of Na_2S and the establishment of equilibrium, $[S]_{T0}$ is present in the liquid phase. After the first purging, sulfide species are redistributed between the aqueous and gas phases and $[S]_{T1}$ is established (where the subscript "1" refers to the first purge). From a mole balance of the total sulfide species:

$$[S]_{T(n-1)}V_L = [H_2S]_{aq(n)}V_L + [HS^-]_{(n)}V_L + [H_2S]_{g(n)}V_G \tag{5.8}$$

where n represents the n^{th} intermittent purge. As a result of equilibrium

$$K_2 = \frac{[H_2S]_{aq(n)}}{[HS^-]_{(n)}[H^+]} \tag{5.9}$$

$$H_{H_sS} = \frac{[H_2S]_{aq(n)}}{[H_2S]_{g(n)}} \tag{5.10}$$

where H_{H2S} is the Henry's constant for H_2S at 37 ºC and has a value of 3.3 (Lide 1995). Therefore, all three sulfide species for the n^{th} purge can be calculated from $[S]_{T(n-1)}$ and the three relationships shown above, along with a knowledge of the pH, volumes, K_2, and H_{H2S}. Additionally, $[S]_{T(n)}$, which is the sum of $[H_2S]_{aq(n)}$ and $[HS^-]_{(n)}$, can also be calculated.

The predictions of $[S]_{Tn}$ after the initial addition of Na_2S are shown in the Figure 5-4 along with the experimentally measured data. As seen, the predictions are in excellent agreement with the measured data, demonstrating that aqueous sulfide concentrations (either total or individual species) can be predicted during the course of an experiment if intermittent gas purging occurs. If sulfide is appreciably consumed by the presence of cells in bottle experiments, the sulfide concentrations predicted by the model would be an upper estimate. If there is a desire to maintain a constant aqueous sulfide concentration, the model can be used to determine how much sulfide should be added after each gas purge. The application of a constantly maintained sulfide concentration in bottle studies is noted in Chapter 6.

When comparing sulfide concentrations between bottles and a continuously purged system, it is obvious that the sulfide will remain longer in the bottles. Thus, an understanding of the sulfide concentrations in an experimental system with time is critical if comparisons are to be made among different experimental systems. Varying experimental systems, such a varying bottle sizes or bioreactor types (bottle versus continuous), may be one reason as to why discrepancies of the effects of sulfide on cellular systems have been observed as previously noted. Although sulfide effects can vary with cellular type, it is still difficult to make comparisons between studies without assessing the fate of sulfide.

5.4.3 The relationship between redox potential and sulfide concentration

The redox potential is affected by reducing agents. From experimental results shown in Figure 5-2, it is clear that both the cysteine and sodium sulfide could each affect the redox potential separately. After injecting a sodium sulfide solution, the redox potential dropped immediately and then went back to the initial level, corresponding with the sulfide loss from 0.9 mM to zero in the reactor. After injecting a cysteine solution, the redox potential went to equilibrium. Upon injecting a cysteine-sulfide solution, the redox potential profile showed a combined effect of cysteine and sodium sulfide.

The correlation between redox potential and sulfide concentrations can be derived by the Nernst Equation:

$$E = E^0 - \frac{RT}{zF}\ln\left(\frac{a_{ox}}{a_{red}}\right) \tag{5.11}$$

where E is the redox potential, E^0 is the standard redox potential, R is the ideal gas constant, T is the temperature, z is the number of the transferred electrons involved in the oxidation-reduction reactions, F is the Faraday constant, a_{ox} is the activity of the oxidizing agent, and a_{red} is the activity of the reducing agent (cysteine, sulfide, etc). For this study, the activities will be approximated with concentrations relative to reference concentrations of 1M. Theoretically, the redox potential is the summation of all half-cell reduction reactions in the liquid. However, for studies in which only one strong reducing agent is changed (cysteine or sulfide) and the rest of the media stays approximately the same, Equation 5.11 can be arranged to the form of:

$$E = E^0 - \frac{RT}{zF}\ln\left(C_{ox}/1M\right) + \frac{RT}{zF}\ln\left(C_{red}/1M\right) = A + B\ln\left(C_{cys/sulfide}/1M\right) \quad (5.12)$$

Where $C_{cys/sulfide}$ is the concentration of the cysteine or sulfide reducing agent; A and B are constants.

In Figure 5-6, the redox potential as a function of Ln($C_{sulfide}$) from the data acquired in the Na_2S addition experiment shows that there is a correlation between the redox potential and the sulfide concentration that is consistent with the Nernst equation. The slope and intercept provides the parameters A and B.

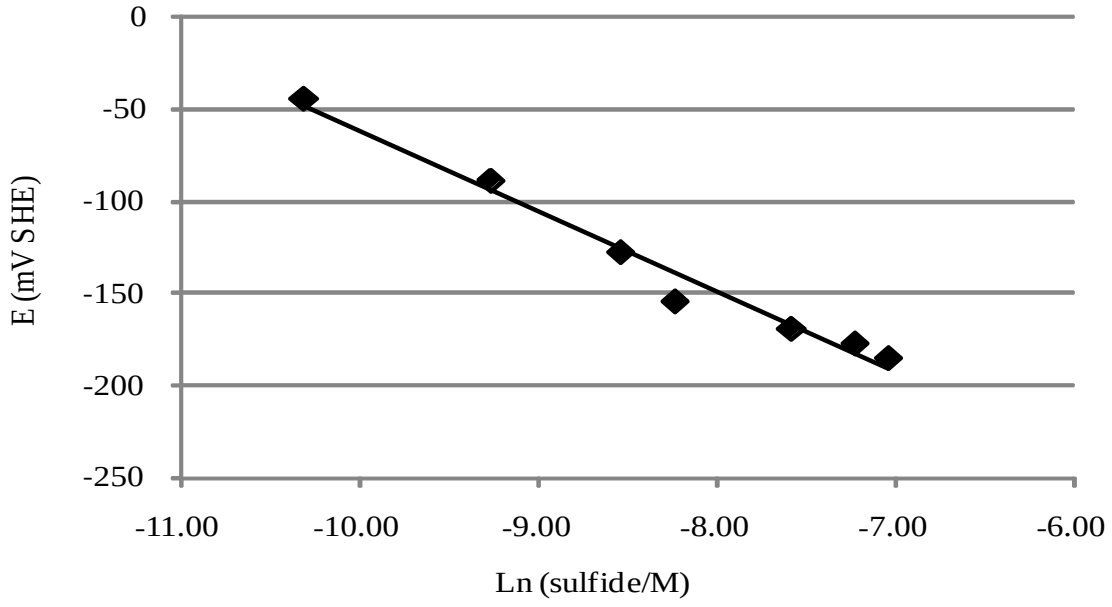

Figure 5-6.Plot of redox potential (E) versus Ln (sulfide/M). The straight line is the model by fitting the Nernst Equation (Equation 5.12)

The fitting of the Nernst Equation generates the straight line shown in Figure 5-6 and the corresponding equation is:

$$E\ (mV) = -496 - 43.36 \times \ln(Sulfide/M) \quad (5.13)$$

R^2 for this fitting is 0.9793 and the corresponding constants A and B are -496 mV and -43.36 mV, respectively.

The model of Equation 5.13 is useful in estimating the contributions of cysteine or sulfide to the redox potential—such a model would be beneficial for redox control studies. However, since this model is based on the assumption that only the concentration of one main reducing agent changes, care must be taken by estimating the redox level of different bioreactor systems since the values of A and B may change with varying media and redox conditions.

5.4.4 Mass transfer coefficient determination via the redox potential

A combination of Equations 5.7 and 5.12 can also be used to estimate the k_La/V for a reducing agent that transports between both the liquid and gas phase. Sulfide likely falls into this category but cysteine most likely does not. Following the changes in the redox potential (rather than following changes in the reducing agent concentration) can provide a measurement of the mass transfer coefficient. Substituting Equation 5.7 into Equation 5.12 where $[S]_T$ is the same as $C_{cys/sulfide}$ gives:

$$E = A + B\ln C_{red} = A + B(\frac{-k_La}{V}t + C_1) = (A + C_1) - B*\frac{k_La}{V}*t \quad (5.14)$$

where C_1 is the integration constant.

According to Equation 5.14, the redox potential resulting from sulfide loss should change linearly with time, and the positive slope should be equal to the product of (-B) and k_La/V. Thus, redox levels with time can be used with Equation 5.14 and a known value of B to obtain k_La/V for comparison with the earlier studies. Figure 5-7 shows the linear correlation between redox potential (E) and time when sulfide strips out of the media.

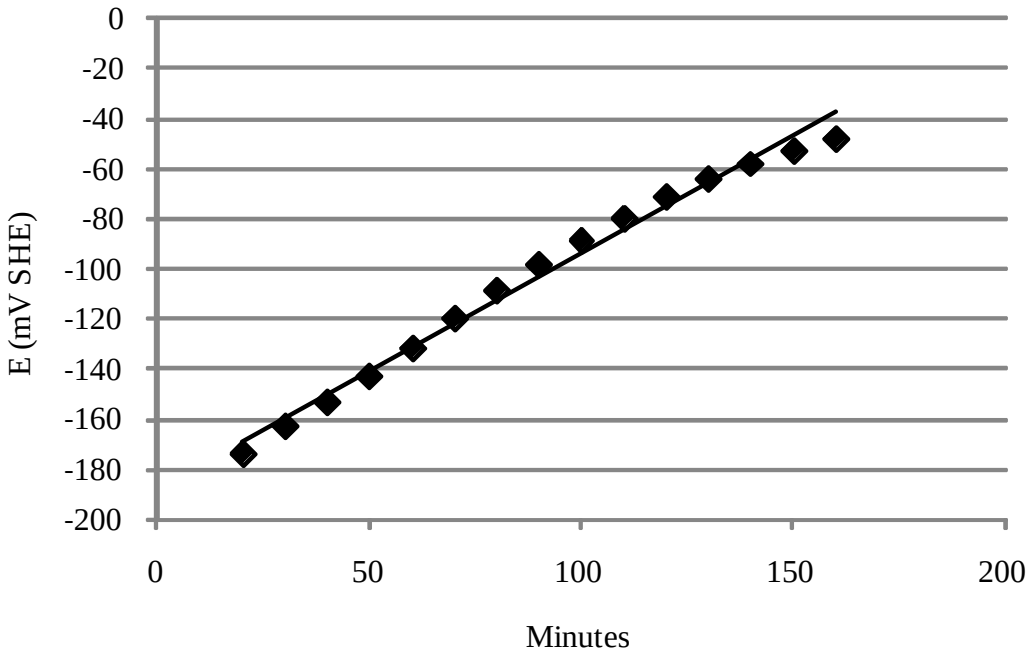

Figure 5-7.Redox potential (E) versus time when sulfide strips out of the media

From Figure 5-7, the linear fit with R^2=0.9874 gives:

$$-B*\frac{k_L a}{V} = 0.9366 mV/\min$$

Inserting the value of B previously determined gives:

$$\frac{k_L a}{V} = 0.021 \text{min}^{-1}$$

Thus, the mass transfer coefficient using the redox potential is similar to the value obtained from Figure 5-2, indicating the validation of both mass transfer and redox potential models.

5.5 Conclusions

The behavior of sulfide as a reducing agent was assessed in bioreactors with gas replacement. Models were developed that explained sulfide loss in the bioreactors of this study. Main achievements in this study include the following:

- Mass transfer plays a key role for sulfide loss in continuous reactors, whereas equilibrium is critical for sulfide loss in batch reactors.
- Sulfide loss in gas-continuous reactors is independent of pH.
- Models of sulfide loss can be used to understand the fate of sulfide during an experiment and can potentially be used to design experiments to maintain constant sulfide levels.
- The redox potential is associated with the concentration of reducing agents. Thus the sulfide loss in gas-replacement bioreactors will result in redox potential change.
- The redox potential can be used to assess the mass transfer coefficient for dominant reducing species that transfer between the liquid and gas phase.

It's important to note that care must be taken when designing and performing an experiment involving any volatile species that may be important to the process. Modeling volatile species,

such as what was done in this work, can provide insights towards designing appropriate experiments. Based on the sulfide model developed for the batch reactor, cellular experiments were carried out to demonstrate the maintenance of constant sulfide levels and the results are discussed in the next Chapter.

6. Sulfide and cysteine-sulfide effects on syngas fermentation

6.1 Introduction

As previously reviewed, many biological processes have utilized the addition of sulfide constituents, such as sodium sulfide or cysteine-sulfide, to improve anaerobic fermentation. However, many published articles have discussed the importance of sulfide effects on growth and product formation without assessing the fate of sulfide during the experiment. In Chapter 5, it is noted that sulfide added into the media cannot be maintained at a constant concentration with time in a gas-replacement system. Models developed show that sulfide is able to convert to volatile H_2S and diffuse out of the reactors with gas-replacement. Sulfide in gas-continuous bioreactors depletes within three hours due to the mass transfer of H_2S whereas the sulfide concentration in batch reactors decreases gradually due to the regassing of the reactors. Mass transfer plays a key role for sulfide loss in continuous reactors, whereas equilibrium following mass transfer plays a role for sulfide loss in batch reactors. Since sulfide is a reducing agent used in anaerobic fermentation, the loss of sulfide from the media results in a changing sulfide concentration which affects the redox potential during the course of the experiment. The effect of sulfide and/or changing redox potential may lead to potential discrepancies among biological processes utilizing differing experimental designs. Thus, it is necessary to wisely design an experiment to maintain the sulfide concentration to assess how sulfide can affect cell growth and

product formation during syngas fermentation. In addition, the effects of cysteine on anaerobic fermentation are also assessed.

6.2 Research objective

Based on the models of sulfide developed in Chapter 5, it's very feasible that many of the previous literature studies had changing sulfide concentrations, and possibly redox potential, during the course of an experiment. Therefore, an experiment was performed to assess sulfide effects on syngas fermentation in the presence of a constant sulfide concentration in 100-ml bottle studies. The objective was to explore how sulfide and cysteine-sulfide under controlled conditions can affect syngas fermentation.

The model noted in Chapter 5 was utilized to determine amounts of sulfide lost after each intermittent purging. Thus, an equivalent amount of the lost sulfide was added to maintain a constant sulfide concentration. In this Chapter, based on the sulfide loss model developed, an application of maintaining constant sulfide levels in 100-ml bottles is demonstrated for a cellular system using *Clostridium* P11 in which syngas (CO, CO_2, and H_2) is used to produce ethanol and acetic acid. The studies were performed to assess the effects of cysteine and sulfide on growth and product formation. The study in this Chapter with maintaining constant sulfide levels will provide greater clarity when interpreting experimental results. In addition to the bottle studies, insights regarding the maintenance of sulfide levels in a continuous reactor are also discussed.

6.3 Materials and methods

6.3.1 Media and sulfide solutions

The media was the same as outlined in Chapter 5. The media was titrated to pH 6.0 using 5N KOH prior to use and the pH was not controlled during the experiment. Na_2S solution and cysteine-sulfide solution were also the same as outlined in Chapter 5.

6.3.2 Bacterium

The bacterium used in the study was a *Clostridium* denoted as P11. P11 was kindly provided by Ralph Tanner from the University of Oklahoma and was isolated from the sediment of an agricultural settling lagoon. P11 produces ethanol and acetic acid from syngas. Before addition to the experimental system, P11 was passaged three times in the media noted above with an additional 1% vol/vol cysteine-sulfide solution. The inoculums for experiments conducted in this work were chosen when cells were during the exponential growth phase at the third passage.

6.3.3 Bottles

Serum bottles (total volume 288 ml) containing 100 ml of media were prepared the same as discussed in Chapter 5. For the experiments, a 10% vol/vol inoculum of P11 was added to the prepared bottles and these bottles were then pressurized with syngas (30% H_2, 30% CO_2 and 40% CO) at 20 psig. The bottles were placed in a shaking incubator at 150 rpm and 37 °C. These

bottles were regassed with syngas every two days and liquid samples were withdrawn using a syringe for measuring total sulfide concentration, the cell concentration, pH, ethanol concentration, and acetic acid concentration.

6.3.4 Continuous 1-L bioreactors

The gas-continuous bioreactor with a 1-L working volume outlined in Chapter 5 was used. The media preparation was also the same as outlined in Chapter 5. After media was autoclaved, 100 mL/min of syngas (30% H_2, 30% CO_2 and 40% CO) was continuously added to the bioreactor that was maintained at 37 °C. To assess the feasibility of maintaining the sulfide concentration in the gas-continuous bioreactor, a continuous Na_2S solution of 0.5 mL/min was added into the bioreactor through a Master flex L/S digital pump (Cole Parmer, IL).

6.3.5 Liquid analysis

The total aqueous sulfide concentration (S^{2-}, HS^-, and H_2S) in all experiments was determined using the method discussed in Chapter 5. In addition, samples were collected in 1-ml cuvettes and the optical density (OD) was measured at 660 nm using a Shimadzu UV-1700 spectrophotometer. The OD is proportional to the dry cell concentration (~ 0.43 dry g/ml per OD (Datar, 2004)). Samples with an OD greater than 0.4 units were diluted so that the OD was within the linear range of calibration. The pH of the samples were measured using an Oakton portable pH meter (Cole Parmer, Vernon Hills, Illinois) with an Accumet extra-long calomel

combo pH electrode (Fisher Scientific, Pittsburgh, Pennsylvania). Once the cell density and pH were measured, the samples from the bottles were centrifuged at 14,000 rpm for 10 minutes. The cell-free supernatant was then analyzed for ethanol and acetic acid using a Shimadzu 2014 Gas Chromatograph (Shimadzu Scientific Instruments, Columbia, Maryland) with a flame ionization detector and a Restek Porapak QS 80/100 Shimadzu 14A column (Bellefont, Pennsylvania). Nitrogen, utilized as the carrier gas, hydrogen, and air were maintained at flow rates of 35, 50, and 400 ml/min, respectively. The operating temperatures of 220, 200, and 250 °C were respectively maintained for the injection port, oven, and detector.

6.4 Results and discussions

6.4.1 Constant sulfide in 100-ml bottles with Na2S solution

At the beginning of the experiment, Na_2S solution was added and allowed to equilibrate. The total sulfide in solution was measured. From this, the sulfide distribution of HS^-, H_2S_{aq}, and H_2S_g was determined from Equations 5.8-5.10 as previously described in Chapter 5. After the first intermittent purge, the moles of lost sulfide would be equivalent to $[H_2S]_g V_g$. Thus, an equivalent amount of moles were added after purging to replenish the lost sulfide. Experiments with constant sulfide concentrations of 0, 0.9, 1.6, and 1.9 mM were performed in triplicate. Total sulfide concentrations were monitored throughout the experiment to validate the replacement of lost sulfide (Figure 6-1). For the sulfide experiments, the sulfide concentrations were maintained at 0, 0.9 ± 0.03, 1.6 ± 0.03, and 1.9 ± 0.05 mM. It is important to note that concentrations could be maintained via predictions just based on the initial sulfide addition and the volume of the gas and liquid.

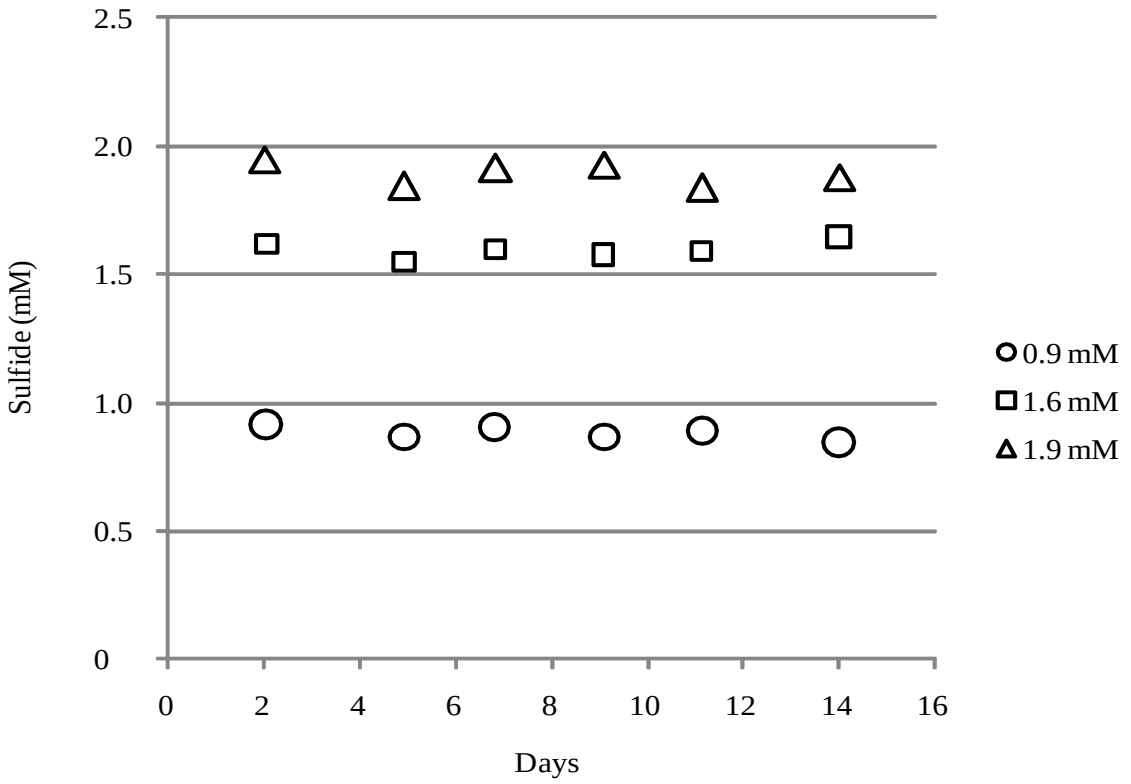

Figure 6-1.Measured average sulfide concentrations versus time in constant sulfide experiments using bottles

Figure 6-2 shows the cell concentration during the fermentation. As shown for all levels of sulfide, the cell concentration increased before Day 8, and then leveled off. The growth profiles suggest that lower sulfide levels lead to a slightly higher concentration of cells in the stationary phase. To compare whether average cell concentrations were statistically different as a result of sulfide levels, P-values (one-tail) were calculated between the average cell concentrations on Day 15 (P=0.29 for 0 and 0.9 mM, P=0.14 for 0.9 and 1.6 mM, P=0.057 for 1.6 and 1.9 mM). Assuming a basis of $\alpha_{1\text{-tail}}$=0.05 (90% confidence) that the average concentrations are different, the statistical analysis shows that the cell concentrations on Day 15 should not be considered significantly different at the 90% confidence level (i.e. P> $\alpha_{1\text{-tail}}$). Thus,

although the sulfide concentrations may appear to slightly affect cell growth, the effect is not statistically significant.

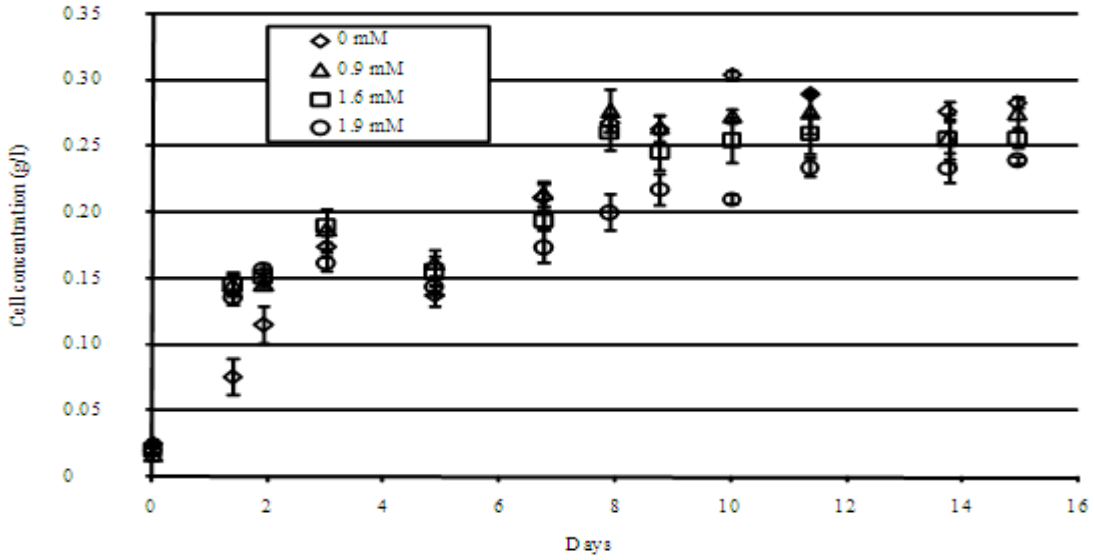

Figure 6-2.Cell concentration versus time at constant sulfide concentrations of 0, 0.9, 1.6 and 1.9 mM. Error bars represent the standard error (n=3)

The trends of product formation in Figures 6-3 and 6-4 show that the sulfide concentrations also appear to affect the formation of ethanol and acetic acid, especially as cells reach the stationary phase. On Day 15, the ethanol concentrations (with std error) were 0.9 ± 0.03, 1.2 ± 0.1, 1.6 ± 0.2 and 2.1 ± 0.1 g/l at sulfide levels of 0, 0.9, 1.6 and 1.9 mM, respectively. By comparing the ethanol concentrations on Day 15, the P-values (one-tail) were P=0.028 between 0 and 0.9 mM of sulfide, P= 0.066 between 0.09 and 1.6 mM of sulfide, and P=0.036 between 1.6 and 1.9 mM of sulfide. Assuming a basis of $\alpha_{1\text{-tail}}$=0.05 (90% confidence), the statistical analysis shows that the ethanol concentrations on Day 15 are significantly different at greater than the 90% confidence level (i.e. P< $\alpha_{1\text{-tail}}$) for the first and last comparisons. For the middle comparison, the confidence level is close at 87%. As for acetic acid, the concentrations

(with std error) at Day 15 were 5.2 ± 0.03, 4.6 ± 0.1, 4.1± 0.2 and 3.6 ± 0.1 g/l at sulfide levels of 0, 0.9, 1.6 and 1.9 mM, respectively. By comparing the acetic acid concentrations on Day 15, the P-values (one-tail) were P=0.004 between 0 and 0.9 mM of sulfide, P= 0.042 between 0.09 and 1.6 mM of sulfide, and P=0.035 between 1.6 and 1.9 mM of sulfide. Assuming a basis of $\alpha_{1\text{-tail}}$=0.05 (90% confidence), the statistical analysis shows that the acetic acid concentrations on Day 15 are significantly different at greater than the 90% confidence level (i.e. P< $\alpha_{1\text{-tail}}$) for all comparisons. The results indicate that ethanol production is favored at higher sulfide concentrations, but acetic acid production is favored at lower sulfide concentrations.

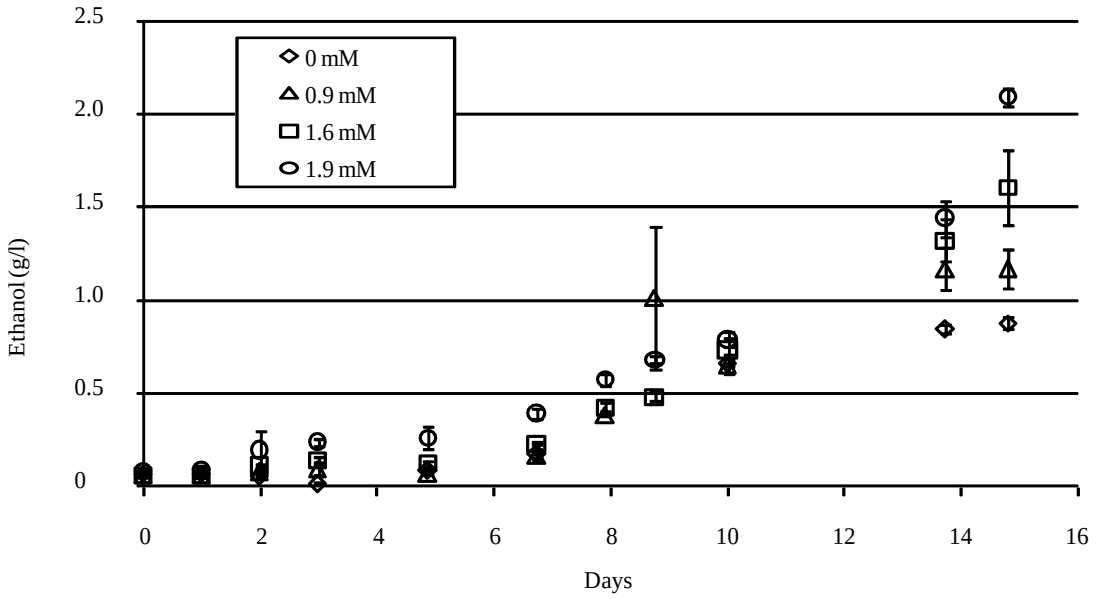

Figure 6-3.Ethanol concentrations versus time at constant sulfide concentrations of 0, 0.9, 1.6 and 1.9 mM. Error bars represent the standard error (n=3). Larger standard error bars for three of the concentrations were a result of one outlier for each triplicate experiment

The results related to product formation are consistent with sulfide being a reducing agent since ethanol is more reduced than acetic acid. In other words, an increasing concentration of sulfide would lead to a more negative (reducing) redox potential, leading to more ethanol and

less acetic acid. It should be noted that if sulfide was not replaced following purging, the results of this study would be difficult to assess since the sulfide concentration would continually decrease. For such a scenario, the sulfide concentration in one set of bottles would overlap sulfide concentrations in another set of bottles. Thus, the importance of assessing the fate of sulfide is evident.

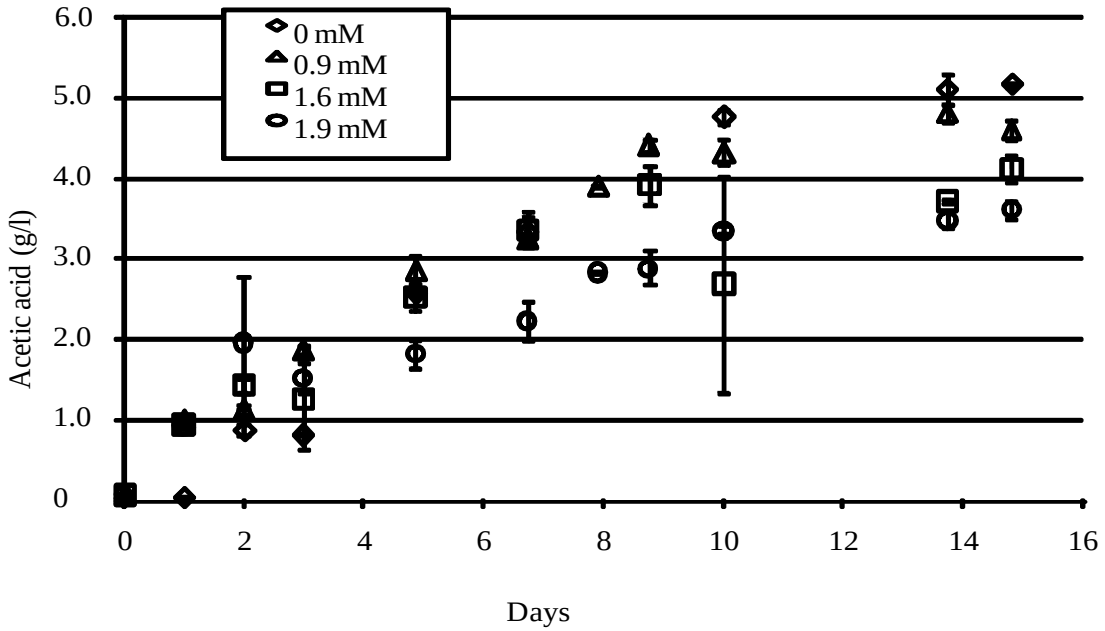

Figure 6-4.Acetic acid concentrations versus time at constant sulfide concentrations of 0, 0.9, 1.6 and 1.9 mM. Error bars represent the standard error (n=3). Larger standard error bars for three of the concentrations were a result of one outlier for each triplicate experiment

6.4.2 Constant sulfide in 100-ml bottles with cysteine-sulfide solution

Another experiment in which the sulfide concentration was maintained using a cysteine-sulfide solution, rather than sulfide solution, was also performed. Similar to the sulfide experiment discussed above, the cysteine-sulfide solution was added at the beginning of the experiment and allowed to equilibrate. The total sulfide in solution was measured. From this, the

sulfide distribution of HS^-, H_2S_{aq}, and H_2S_g was also determined. After every purge, the moles of lost sulfide were calculated and an equivalent amount of moles of lost sulfide were added using the cysteine-sulfide solution. Experiments with constant sulfide concentrations of 0.3, 1.5, and 2.7 mM were performed in triplicate. Total sulfide concentrations were measured throughout the experiment to validate the replacement of lost sulfide (Figure 6-5). For the sulfide experiments, the sulfide concentrations were maintained at 0.3 ± 0.03, 1.5 ± 0.04, and 2.7 ± 0.10 mM. Also, there is another group denoted as "NC" in which cysteine-sulfide was added initially but no cysteine-sulfide was added after gas purging. As discussed in Chapter 5, this would lead to a continual drop of the sulfide concentration with time. Figure 6-5 confirms this lost. The sulfide concentration of the NC group was initially 1.5 mM, but gradually decreased to 0 mM at day 10.

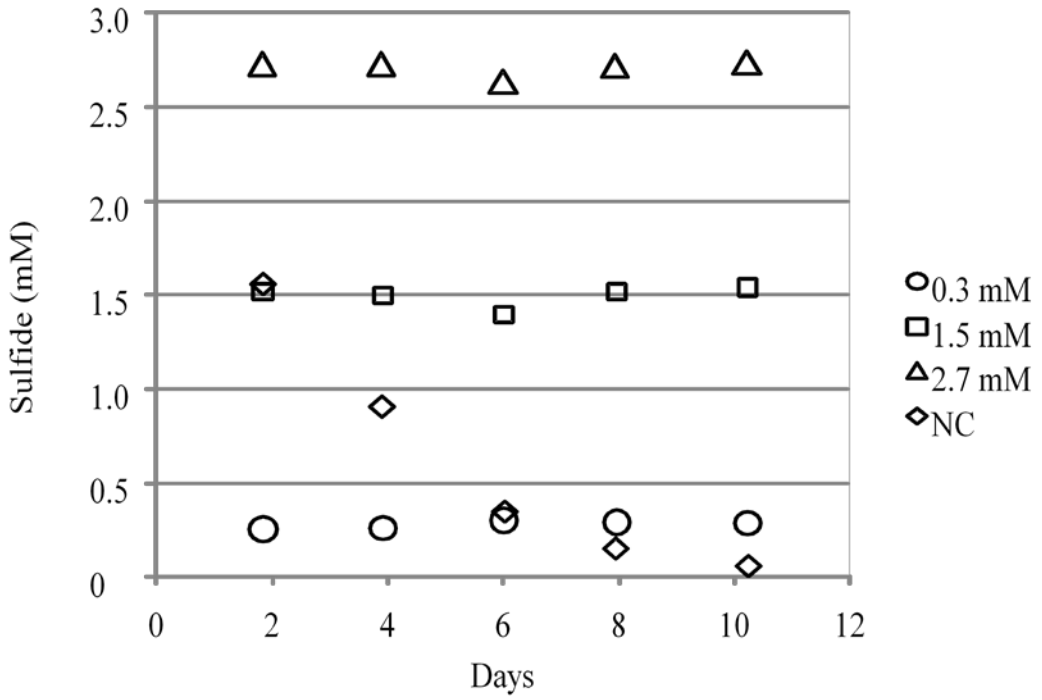

Figure 6-5.Measured average sulfide concentrations versus time in constant sulfide experiment using cysteine-sulfide solution. NC represents no additional sulfide additional after the start of the experiment

It should be noted that although H_2S can leave the bioreactors with regassing, cysteine would accumulate with the addition of cysteine-sulfide solution to maintain constant sulfide concentrations. If cysteine stayed in the media without any consumption, the cysteine concentration following the addition of cysteine-sulfide after each purging could be calculated based on the initial amount of cysteine added into the media and the amount added during the fermentation. Figure 6-6 shows the calculated profiles of cysteine concentration. As is evident, the difficulty with this type of experiment is that the sulfide concentration can be maintained but the cysteine concentration is not maintained. This can lead to difficulty in evaluating experimental data.

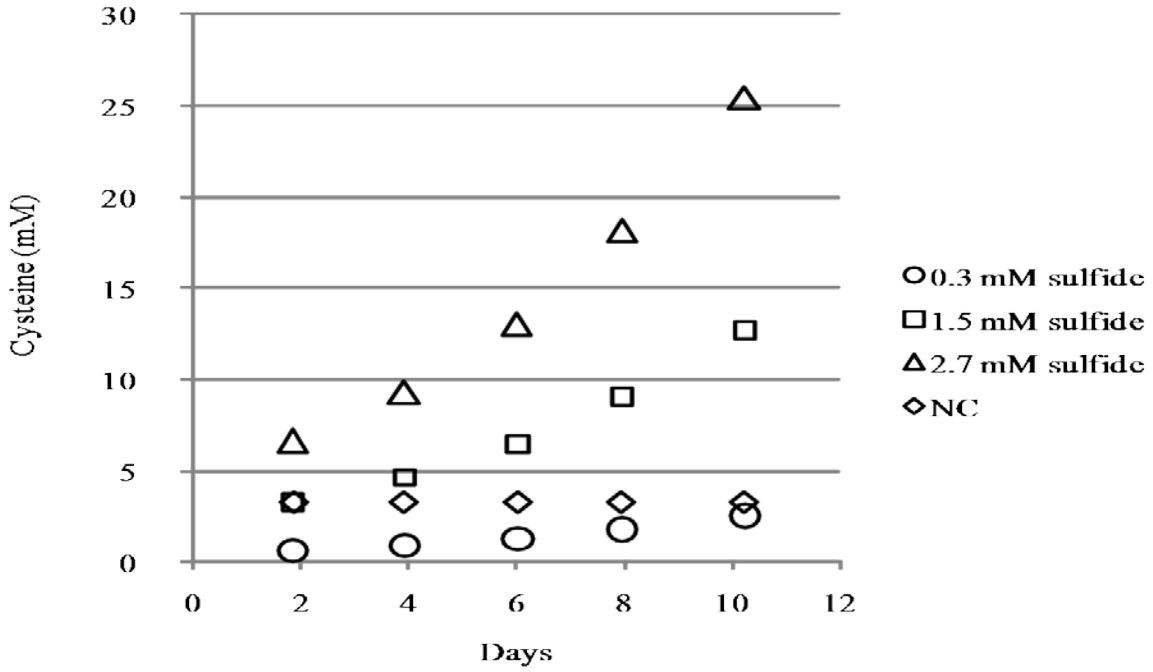

Figure 6-6. Calculated average cysteine concentrations versus time in constant sulfide experiment using cysteine-sulfide solution

Figure 6-7 shows the cell concentration during the fermentation. As shown in the figure, too much sulfide and cysteine had obvious negative effects on cell growth. There was almost no growth at all when sulfide concentration was controlled at 2.7 mM using cysteine-sulfide solution. Another obvious finding was that the group with the lowest sulfide (0.3 mM) had the greatest cell concentration (0.28 g/l at day 11), which was about double of the cell mass of the run with 0.15 mM (0.13 g/l at day 11) and the run with no sulfide added after the initial injection (0.15 g/l at day 11). The growth profiles likely suggest that lower sulfide levels leads to a higher concentration of cells in the stationary phase. This is in contrast to the study in which just sulfide was added (Figure 6-2). However, this conclusion is not solid because the changing cysteine concentrations of different groups may mislead the results. Also, it is noted that the trials with 0.15 mM sulfide and the trials with no additional sulfide had the same sulfide and cysteine levels before day 2. Then after day 2, the trials with no additional sulfide had decreasing sulfide concentrations (<0.15 mM) and constant cysteine (3.3 mM), whereas the run with 0.15 mM sulfide had constant sulfide concentrations (0.15 mM) and increasing cysteine concentrations (>3.3 mM). The similar growth profiles of these two runs may be due to sulfide, or due to cysteine, or due to the combined effects of both sulfide and cysteine. It is difficult to draw a solid conclusion from the experiment.

Figure 6-8 and 6-9 show the associated ethanol and acetic acid production. Besides the run with 2.7 mM sulfide, which had no growth at all, the other three groups had almost the same acetic acid production, but different ethanol production. Again, the results may be confounded by the combined effects of sulfide and cysteine. Thus, it is difficult to come to solid conclusions as compared to the sulfide only studies. Actually, the performance of the NC group, which had varying sulfide concentrations (1.5 mM to 0 mM) during the process, could lead to possible

biases in the analysis since the sulfide was not controlled. This bias provides a plausible reason as to why there could be conflicting reports in literature regarding the effects of sulfide on cellular systems. From Figure 6-7, cell growth of the NC group was very similar to the 1.5 mM study, which makes sense since cell growth occurred during the first several days and the initial sulfide concentration of the NC group was close to 1.5 mM. As for ethanol production (Figure 6.8), the NC group was close to 1.5 mM before day 8. But with the sulfide concentrations decreasing, ethanol production of the NC group was more like group 0.3 mM after day 8.

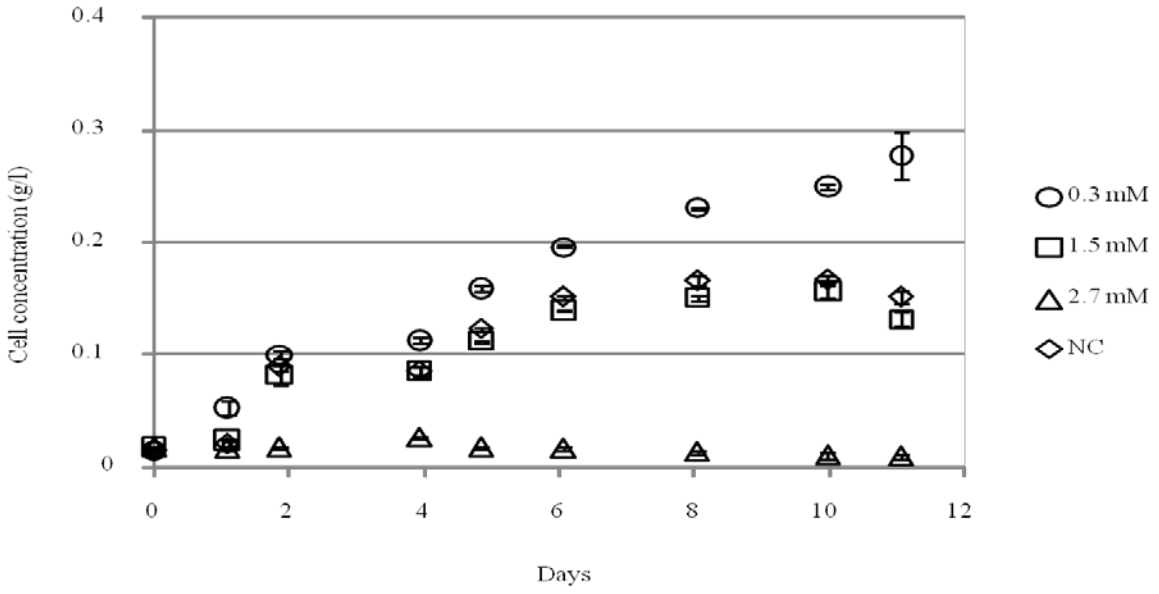

Figure 6-7.Cell concentration versus time at constant sulfide concentrations of 0.3, 1.5, and 2.7 mM, and at NC condition with using cysteine-sulfide solution. Error bars represent the standard error (n=3). NC represents no additional sulfide additional after the start of the experiment

Thus, different results may be concluded depending upon when the experiment was assessed. It is apparent that changing sulfide concentrations throughout an experiment can lead to different conclusions depending upon the time point of analysis. The studies with both sulfide

and cysteine addition demonstrate the importance of understanding the fate of chemicals within culture media and the associated implications when interpreting the experimental results.

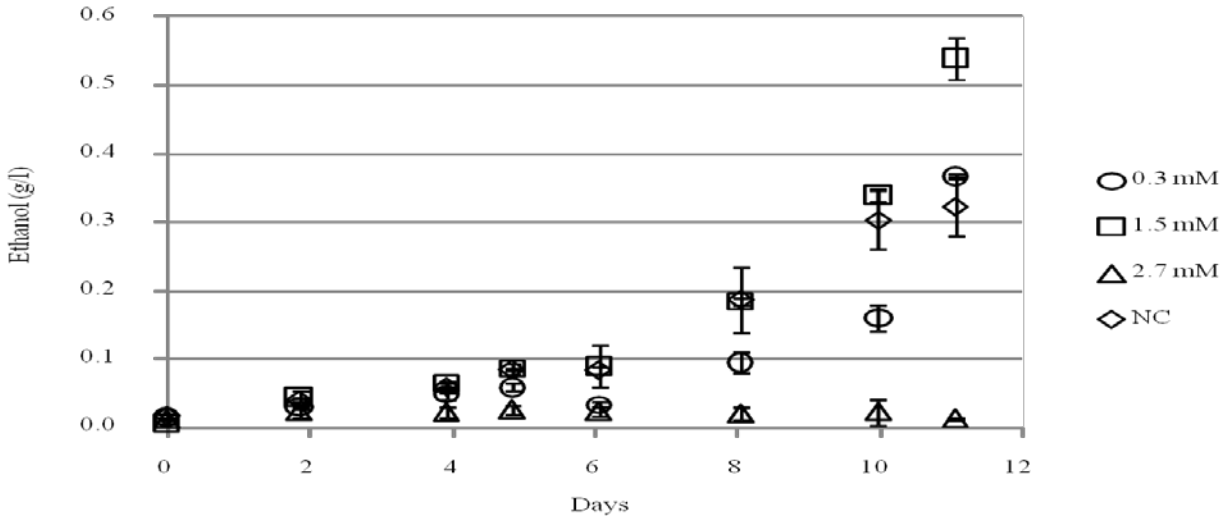

Figure 6-8.Ethanol concentrations versus time at constant sulfide concentrations of 0.3, 1.5, and 2.7 mM, and at NC condition using cysteine-sulfide solution as sulfide constitute. Error bars represent the standard error (n=3). NC represents no additional sulfide additional after the start of the experiment

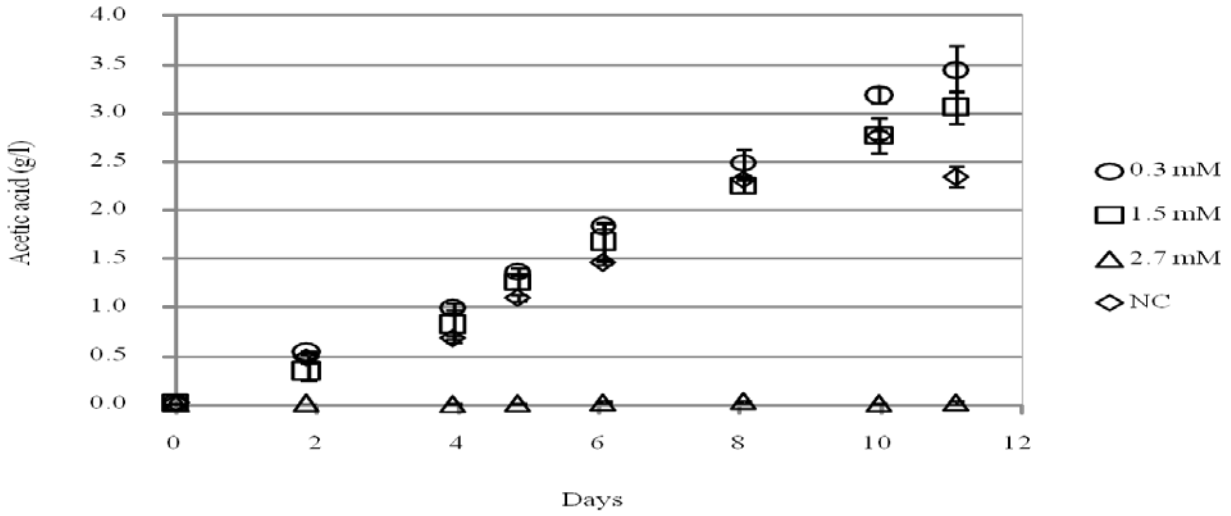

Figure 6-9. Acetic acid concentrations versus time at constant sulfide concentrations of 0.3, 1.5, and 2.7 mM, and at NC condition using cysteine-sulfide solution as sulfide constitute. Error bars represent the standard error (n=3). NC represents no additional sulfide additional after the start of the experiment

6.4.3 Constant sulfide in 1-L gas continuous bioreactor

Using the sulfide loss model developed in Chapter 5 for a continuous reactor, it is also possible to maintain a constant sulfide concentration in a gas-continuous bioreactor. If the net sulfide added between inlet and outlet streams is at a rate equivalent to the rate at which sulfide is lost, the sulfide concentration may be kept constant during the fermentation. The sulfide material balance used to develop a constant sulfide system is noted as:

$$\frac{dC(t)}{dt} = -k_L a \cdot C(t) + \frac{F \cdot C_s}{V_R} \qquad (6.1)$$

Here, C(t) is the sulfide concentration in the bioreactor, which is a function of time (t). The mass transfer coefficient is $k_L a$, F is the flow rate of the continuously added solution containing a Na_2S concentration (C_s), and V_R is the liquid volume of the reactor.

For a constant (i.e. *dC(t)/dt=0*) sulfide concentration of $C_R=C(t)$ to be maintained in the continuous reactor, Equation 6.1 shows that $C_R= FC_S/[(k_La)V_R]$. Note from this equation that C_R is directly proportional to F if all other parameters remain fixed. For the continuous reactor noted in Chapter 5, k_{La} was 0.02 min^{-1} for the 1-L liquid volume at the given reactor conditions. To assess a constant sulfide continuous reactor, it was decided to use a sulfide solution where C_S = 0.167 M, which is equal to 4 gm of Na_2S in 100 mL water. Based on these parameters, Figures 6-10 and 6-11 show the associated C_R as a function of time, obtained from Equation 6.1, following the initiation of sulfide being continuously fed into the reactor. Figure 6-10 is for a sulfide solution flow rate of 0.5 ml/min from which a steady-state sulfide concentration (C_R) of ~4 mM was achieved within 200 minutes. Similarly, Figure 6-11 shows the profile for a flow rate of 0.1

ml/min in which a steady-state sulfide concentration of ~0.8 mM was achieved within 200 minutes.

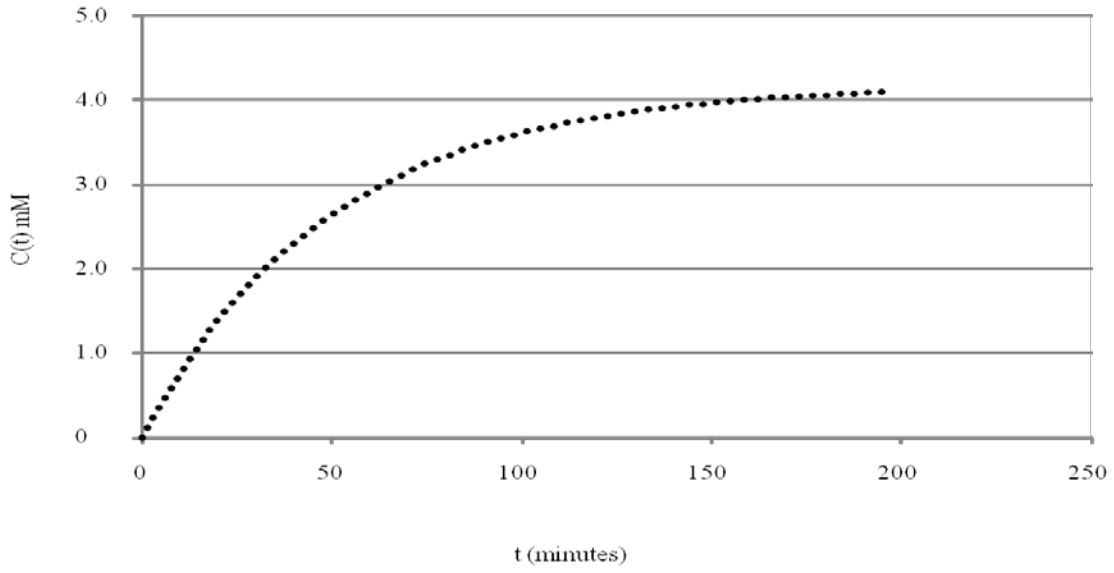

Figure 6-10.Sulfide concentration (mM) versus time (minute) when flow rate of the continuous sulfide solution is 0.5 ml/min. Model is based on Equation 6.1

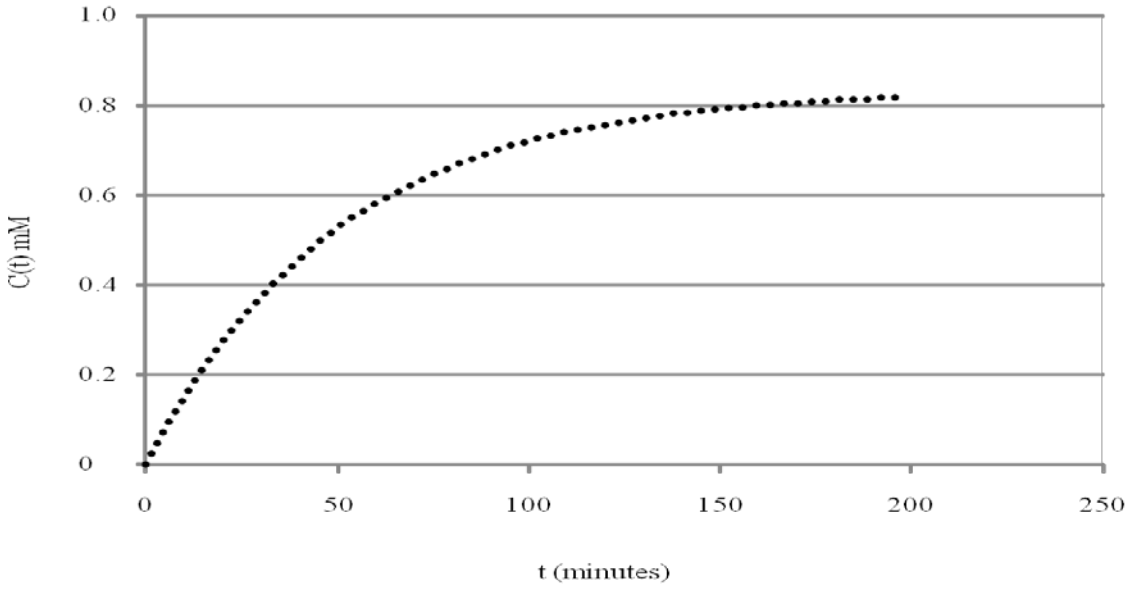

Figure 6-11.Sulfide concentration (mM) versus time (minute) when flow rate of the continuous sulfide solution is 0.1 ml/min. Model is based on Equation 6.1

To check the validation of the model shown in Figure 6-10, an experiment with a continuously fed Na_2S solution at 0.5 ml/min was conducted in the continuous 1-L bioreactor and the sulfide concentration was measured. In Figure 6-12, it's clear that the sulfide concentration increased gradually, and then reached a steady state. The steady state value was approximately 3.5 mM, which is 12.5% lower than the calculated value (4 mM) of Figure 6-10 at the specified flow rate. The error may due to the increasing total solution volume, or the possible sulfide loss while making Na_2S solution, or the possible utilization by the cells for metabolism. Although the steady state concentration of Figure 6-10 was a little higher, the dimensionless y-axis (sulfide/steady state sulfide) of Figure 6-10 and 6-12 is also shown in Figure 6-13 to show the predicted curvature in comparison with experimental data. The y-axis of Figure 6-13 shows the sulfide concentration relative to the steady state sulfide concentration for both the calculated values from model and the measured values from experiment. The similar curvature indicates a good agreement between the model and the experiment.

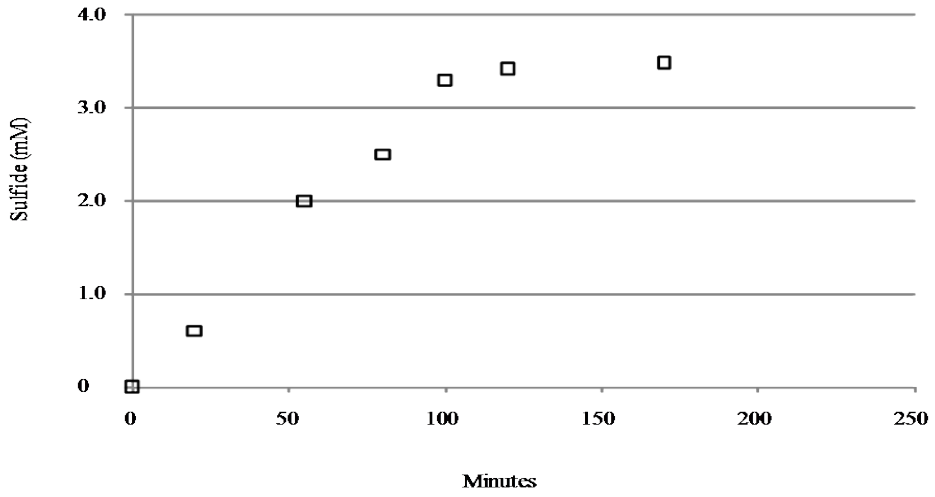

Figure 6-12.Measured sulfide concentration (mM) versus time (minutes) when continuous Na_2S solution with 0.5 ml/min was injected into gas-continuous bioreactor

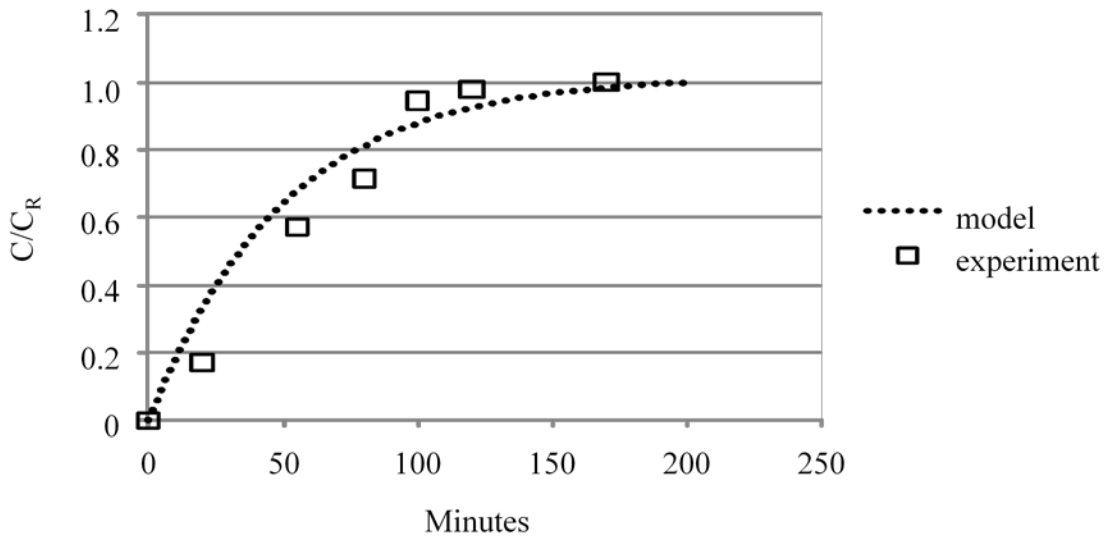

Figure 6-13.The dimensionless sulfide concentration of both the modeled and measured values versus time when a continuous Na_2S solution with 0.5 ml/min was injected into a gas-continuous bioreactor. The y-axis shows the sulfide concentration (C) relative to the steady state sulfide concentration (C_R). Model is based on Equation 6.1

With regards to sulfide addition, it should be noted that to maintain sulfide concentration, for example, at 0.5 mM, 72 ml of sulfide solution would need to be added every day, which accounts for a 7.2% volume increase. For a two-week fermentation, the volume change would be 1008 mL, which is more than the total volume of the original media. To reduce the flow rate to minimize volume changes, the sulfide concentration of the feed solution would have to be higher to obtain an equivalent constant sulfide concentration in the reactor. However, concentrated sulfide solutions can be problematic because a large amount of sulfide may convert to H_2S when making the solution or may convert to solid S and deposit in the bottle. Another concern regarding sulfide maintenance in a gas-continuous bioreactor is the accumulation of the ion associated with the sodium. If Na_2S is continuously added, the effect of continuously added Na^+ on a cellular system should be assessed. Thus, maintaining the sulfide concentration in a gas-continuous bioreactor has many challenges that need to be addressed properly in order to

correctly interpret the experimental conditions. Due to the problems of using sulfide in a continuous reactor to maintain a constant sulfide level that could potentially also control the redox potential, it was decided to focus on another method to control the redox potential. Redox potential control towards enhancing ethanol production is the focus of Chapter 7, along with pH control. As discussed in Chapter 4, pH and redox control are key possibilities for enhancing ethanol production. In Chapter 7, a redox control system using cysteine as the reducing agent and air as the oxidizing agent was designed and the experiments with controlled redox potential and pH were designed to assess the redox effects on cell growth and product formation.

6.5 Conclusions

Based on the sulfide model developed for the batch reactors in Chapter 5, cellular experiments were carried out to demonstrate how the maintenance of constant sulfide levels can affect syngas fermentation. Constant sulfide levels provided greater clarity when interpreting experimental results. Several key findings are listed following:

- The sulfide concentration may affect cell growth, but the effect appears slight.
- Ethanol production is favored at higher sulfide concentrations, but acetic acid production is favored at lower sulfide concentrations.
- Sulfide maintenance using cysteine-sulfide is confounded because of the accumulation of cysteine.
- Sulfide maintenance in a gas-continuous bioreactor is possible, but the increasing volume of the media and the accumulation of Na^+ ion are problematic. Thus, sulfide control in a continuous reactor is unrealistic when using sulfide addition.

The constant sulfide experiment in batch bioreactors shows an increasing concentration of sulfide which would lead to more ethanol and less acetic acid, probably resulting from a more negative (reducing) redox potential. Such results related to product formation are consistent with sulfide being a reducing agent since ethanol is more reduced than acetic acid. Thus, it would be beneficial to design a redox potential control system to run fermentations at the desired redox levels to assess how redox potential can affect the cell growth and product formation. This is the focus of Chapter 7.

7. Redox potential and pH effects on syngas fermentation

7.1 Introduction

In previous Chapters, two different aspects of the thermodynamic analyses were discussed. The first aspect dealt with the standard transformed Gibbs free energy which is related to concentrations of species associated with equilibrium conditions. However, cellular systems are in a dynamic state such that equilibrium concentrations of cellular systems are rarely met. The second aspect of the analysis dealt with the transformed Gibbs free energy which is related to concentrations of species at existing conditions. Since species concentrations are dynamic in cellular systems, the transformed Gibbs free energy can show how the thermodynamic conditions can change as a result of dynamic changes in the reactor conditions (e.g. pH, redox potential, and concentrations). At given concentrations of the reactants and products, the Gibbs free energy of the reaction shows the favorability of the reaction as to whether the reaction can go in the forward or reverse direction. For instance, if the transformed Gibbs free energy of some bottleneck reaction at a specific condition is adjusted from positive to negative, the reaction would become favorable in forming products. Although kinetics would dictate how fast the product is formed, the thermodynamics would suggest the favorable formation of the product. Thus, the analysis of the transformed Gibbs free energy can give insights on how reactor conditions can be adjusted to make the reactions favorable in the forward or reverse direction.

From the thermodynamic analysis in Chapters 3 and 4, the NAD_{red}/NAD_{ox} ratio greatly affects the reactions along the Acetyl-CoA metabolic pathway during syngas fermentation. As mentioned, the redox potential can impact the NAD_{red}/NAD_{ox} ratio. Generally, a more negative redox potential would be beneficial for both electron production and product formation. In Chapters 5 and 6, the research based on the addition of external reducing agents (cysteine-sulfide, cysteine, or sulfide) showed that varying the concentrations of reducing agents affected the cell growth and/or product formation, which may have resulted from the different levels of redox potential (although redox level was not measured). Redox potential is possibly an intrinsic factor associated with reducing equivalents (e.g. $NADH/NAD^+$) which are involved in the reactions along the metabolic pathways of syngas fermentation. Focusing on the redox potential, rather than on the concentration of reducing agents such as sulfide, may be a more beneficial assessment tool for developing methods to improve ethanol formation.

In addition, based on analysis of potential bottleneck reactions in Chapter 4, it is clear that altering the external pH of the system has the potential to impact the formation of the desired product. As previously noted, the pH at the reaction site (which would be somewhere between the internal and external pH) greatly affects the thermodynamics of many of the reactions. The adjustment of the external pH can potentially change the transformed Gibbs free energy of the reaction at the site of the reaction, leading to a possible change in the dynamic favorability of the reactions. Moreover, the pH and redox (E) dependency of conversion from acetate to ethanol suggests that a strategy of adjusting the system pH and E could be developed to promote higher ethanol formation. Since acetate production is generally considered to be growth-associated and ethanol production generally occurs when there is no cell growth, a high pH environment may be maintained to promote acetate production during the cell growth phase, but a low pH

environment may be maintained to induce the acetate to ethanol conversion during the non-growth phase as well as enhance ethanol production through the normal metabolic pathway. In this Chapter, experimental assessment of syngas fermentation was conducted via modulating the redox potential and pH.

7.2 Research objective

The aim of this objective was to explore how ethanol formation via syngas fermentation can be enhanced by adjusting the redox potential and pH. The purpose for the pH control is that the redox potential is likely associated with the pH. These two factors have to be assessed together. Experiments with controlled redox levels and pH were performed to assess whether control of the external redox potential (as compared to intrinsic control by cells) can be used to enhance the fermentation process. In the study, cysteine was used as the reducing agent for the redox potential control because cysteine is more stable in solution as compared to sulfide. Based on the thermodynamic analysis, the basic idea was to explore the effect of lowering the redox potential to promote both growth (and acetic acid production) and ethanol formation while keeping the pH high during growth and then lowering the pH to enhance ethanol formation. A hypothesis is that high acetate production can be achieved at higher pH during cells growth phase, but high ethanol production can be achieved at lower pH during the stationary phase. Also, lowering the pH and redox potential would induce the conversion from acetate to ethanol which was produced during the cell-growth phase, resulting in a higher overall ethanol yield and possibly a higher ethanol production rate.

7.3 Materials and methods

7.3.1 Media and redox solutions

The media was the same as outlined in Chapter 5. It was titrated to pH 6.0 using 5N KOH prior to use. Cysteine-sulfide solution outlined in Chapter 5 was initially used to remove residual oxygen and lower the redox potential when the experiment started. For redox control after the experiment started, a freshly-prepared cysteine solution, containing 4 g of L-cysteine in 100 mL water, was used. The preparation involved adding 100 mL purified water into a serum bottle. The bottle was then boiled and purged with nitrogen to remove oxygen. Then, 4 g of L-cysteine was added into the bottle in an anaerobic shell and sealed with a rubber septum and cap. L-cysteine was purchased from Sigma-Aldrich (St. Louis, Missouri).

7.3.2 Bacterium

The bacterium used in the study was a *Clostridium* denoted as P11. The cell preparation was the same as outlined in Chapter 6.

7.3.3 Continuous 1-L bioreactors

The gas-continuous bioreactor BioFlo-110 (New Brunswick Scientific, Brunswick, New Jersey) with a 1-L working volume outlined in Chapter 5 was used. The media preparation was also the same as outlined in Chapter 5. After the media was autoclaved, the bioreactor was

purged with 100 mL/min of N_2 overnight to remove the dissolved oxygen in the media. Then, syngas (30% H_2, 30% CO_2 and 40% CO) was continuously added to the bioreactor that was maintained at 37 °C. Syngas flow was initiated 1 hour before the addition of cells. Oxygen levels were continuously measured by the oxygen probe. At the beginning of the experiment, 10 mL cysteine-sulfide solution was added into the media to remove any residual oxygen and decrease the redox potential of the media. A 10% vol/vol inoculum of P11 was then added to the bioreactor. At various time intervals, 1 ml of liquid was sampled through the sampling port and analyzed for cell concentration, acetic acid concentration, and ethanol concentration.

7.3.4 Bottles

Serum bottles (total volume 288 ml) containing 100 ml of media were prepared the same as discussed in Chapter 5. For the experiments, a 10% vol/vol inoculum of P11 with OD 0.6 was added to the prepared bottles and these bottles were then pressurized with syngas (30% H_2, 30% CO_2 and 40% CO) at 20 psig. The bottles were placed in a shaking incubator at 150 rpm and 37 °C. These bottles were regassed with syngas every two days and liquid samples were withdrawn using a syringe for measuring pH, cell concentration, ethanol concentration, and acetic acid concentration. In one study, ionic strength in the bottle media was adjusted by adding different amounts of 3M KCl solution.

7.3.5 Liquid analysis

The pH, cell concentration, ethanol concentration and acetic acid concentration were measured as outlined in Chapter 6.

7.3.6 pH and redox potential control system

pH and redox potential were continuously measured using pH and ORP probes (Cole Parmer, Vernon Hills, Illinois). The pH of the media was controlled by the BioFlo-110 fermentor by adding 5 N HCl and/or 5 N KOH to maintain the desired pH. Redox potential was likewise controlled with air and the cysteine solution. Adding air to the system could be problematic because the bacteria are anaerobic. However, the effect of bubbling air through the media to control the redox potential had minimal effect on the oxygen concentration as the air flow rate was very low (0.1 mL/min) during the control time and the continuously measured oxygen level was always close to zero (< 1% saturation).

7.4 Results

7.4.1 Redox potential effects

A previous study showed that syngas fermentation using *Clostridium* P11 occurred mainly at redox potentials between -50 mV to -250 mV. Without redox control, the redox potential dropped to about -200 mV, suggesting that the cells had an internal mechanism for

adjusting the redox level (Frankman 2009). However, the redox level was not always maintained at a steady-state level such that the effect of controlling the redox potential at desired levels was not clear. In this work, three different redox potential levels were chosen at -100, -200 and -250 mV SHE to conduct experiments to assess how modulating the redox potential could affect the syngas fermentation. The pH was held constant at 5.8 for all runs. Other experimental conditions, such as temperature, gas flow rate, gas partial pressure, agitation, etc, were all held constant such that the redox potential was the only variable. Note that the redox potential was not necessarily at the desired level immediately upon inoculation; all runs started at the same redox potential of approximately -75 SHE, and then the potential was gradually adjusted to the desired redox potential between days 1 and 2. The gradual adjustment was to minimize any shock to the bacteria that could occur with rapid adjustments.

As illustrated in Figure 7-1, the redox potential and cell growth are clearly correlated. For each of the three runs shown, a more negative redox potential is indicative of faster cell growth. The experimental run at -100 mV grew slowly until reaching a cell mass of 0.19 g/l on day 8. It is unclear whether this was the peak cell mass since the experiment was terminated. The -200 and -250 mV bioreactors both reached a maximum cell mass of nearly 0.40 g/l, but the rates at which these cell mass levels were reached varied greatly. The -200 mV reactor grew steadily but did not reach peak cell mass until day 8. On the other hand, the -250 mV reactor reached peak cell mass by day 3. These results distinctly indicate that a more negative redox potential causes faster cell growth. From the thermodynamic analysis in Chapter 3, electrons required for cell growth may be from both CO and H_2, and pH and redox potential can affect the electron production. Since pH was the same from these three runs, the effect of pH can be eliminated. However, the more negative redox potential may boost the reactions.

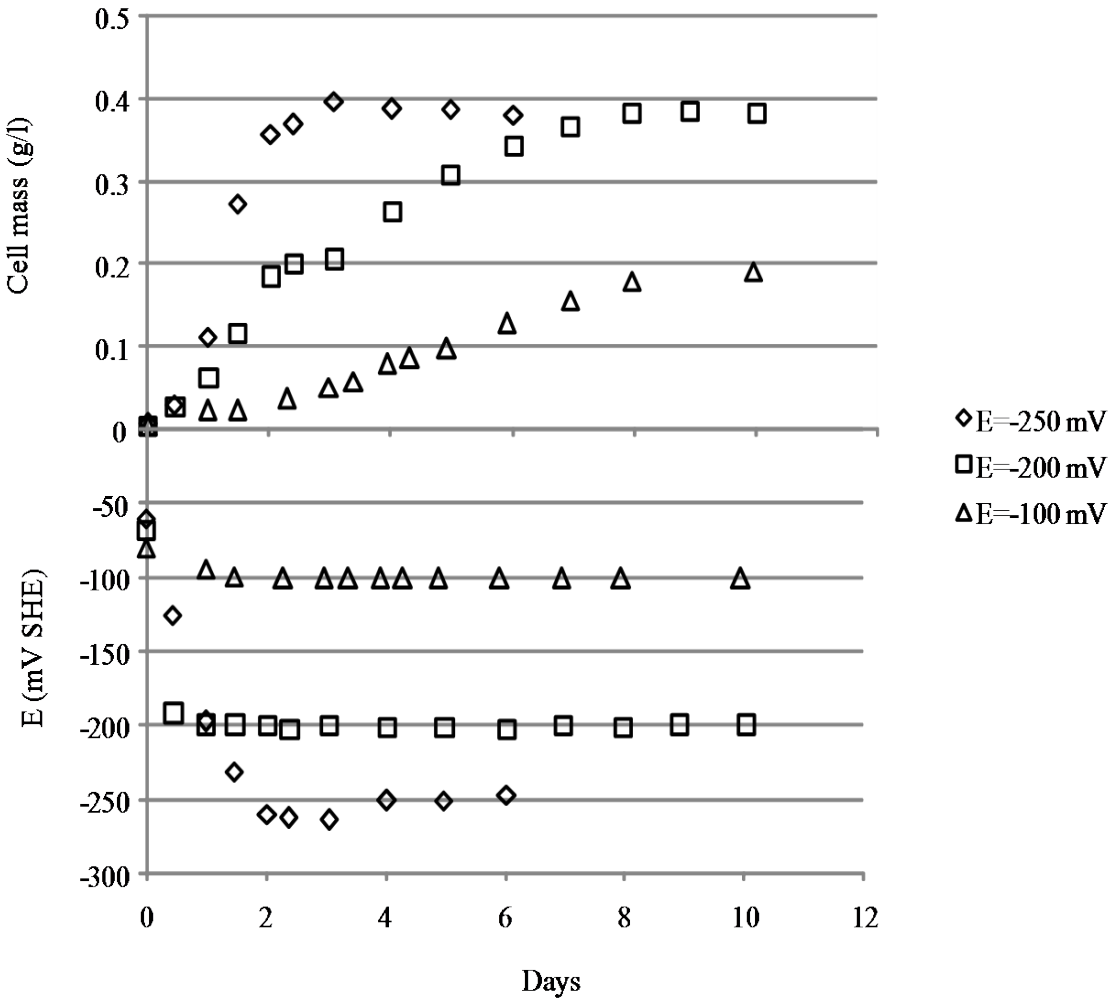

Figure 7-1.Cell concentration and the corresponding redox potential profiles at constant pH of 5.8

The redox potential also affected acetic acid and ethanol production. Figure 7-2 indicates that acetic acid production is higher at more negative redox potentials. The -250 mV run resulted in a maximum acetic acid concentration of over 5 g/l, while the -200 mV run maxed out at 3.5 g/l, and the -100 mV reactor only reached an acetic acid concentration of over 2 g/l. Interestingly, acetic acid concentration in the -250 mV reactor reached maximum on day 3 and subsequently decreased, while the -200 and -100 mV runs reached their maxima around day 10 or 11, and were increasing for the entirety of the experiment. On the other hand, the runs at -100

mV and -200 mV failed to produce any appreciable levels of ethanol, while the -250 mV run produced up to 5 g/l of ethanol.

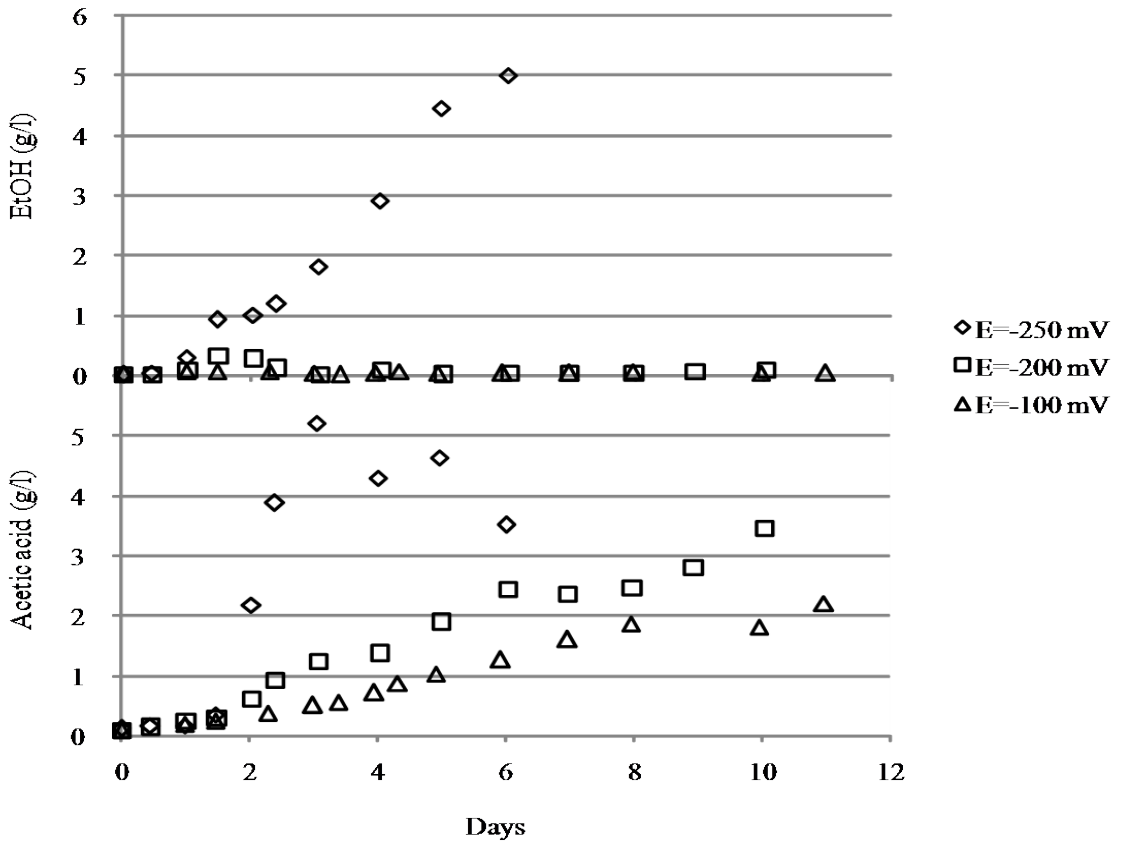

Figure 7-2.Ethanol and acetic acid production with varying redox potential at constant pH of 5.8

Another obvious finding regarding production is the concentration change of acetic acid. As seen, the acetic acid concentration decreased from 5 g/l to 3.5 g/l between day 3 to day 6 at a redox potential of -250 mV. Notably, during the same time, the ethanol concentration increased from 2 g/l to 5 g/l. It seems there was a conversion from acetic acid to ethanol although there was still some ethanol production independent of acetic acid conversion. The analysis of the conversion is discussed later.

7.4.2 pH effects – run 1

It was obvious from the redox potential experiments that a more negative redox potential resulted in better growth and more product formation. Thus, in this section, pH effects were assessed while the redox potential was controlled at the lowest level of – 250 mV. Figure 7-3 shows the measured pH profile for three separate experiments. All runs were performed in the gas continuous 1-L bioreactors and were maintained at -250 mV SHE. One reactor was maintained at pH = 5.8 for the duration of the experiment, and another was maintained at pH = 4.5 for the entire experiment. A third reactor was run at pH = 5.8 through the growth phase of the bacteria (until day 3), and was then gradually adjusted to pH = 4.5 by day 4, where it remained for the rest of the stationary phase.

Varying pH had a marked impact on cell mass (Figure 7-4). The run at pH 5.8 reached a maximum of nearly 0.4 g/l by day 3, while the run at pH 4.5 only reached a maximum of 0.18 g/l, and that was not until day 7. The third reactor followed the trend or cell growth at higher pH until the pH was adjusted around day 3, at which time there was a dip in cell mass from about 0.31 g/l to 0.27 g/l, indicating that changing pH likely killed some of the bacteria, but not very much. Once pH was stabilized at 4.5, cell growth resumed and reached a maximum of about 0.33 on day 6, similar to the pH 5.8 experiments. Likewise, a higher pH was shown to be more beneficial for acetate production, as both the run at pH = 5.8 and the run with variable pH (5.8/4.5) reached maxima of 5.2 and 5.7 g/L acetate, respectively, while the run at pH = 4.5 never even reached acetate concentrations of 1 g/L. It is also important to note that acetate concentration decreased in all runs with growth at pH 5.8 after the bacteria reached the stationary phase. One hypothesis is that during the stationary phase acetate is converted to ethanol, thereby decreasing acetate concentrations and increasing ethanol production.

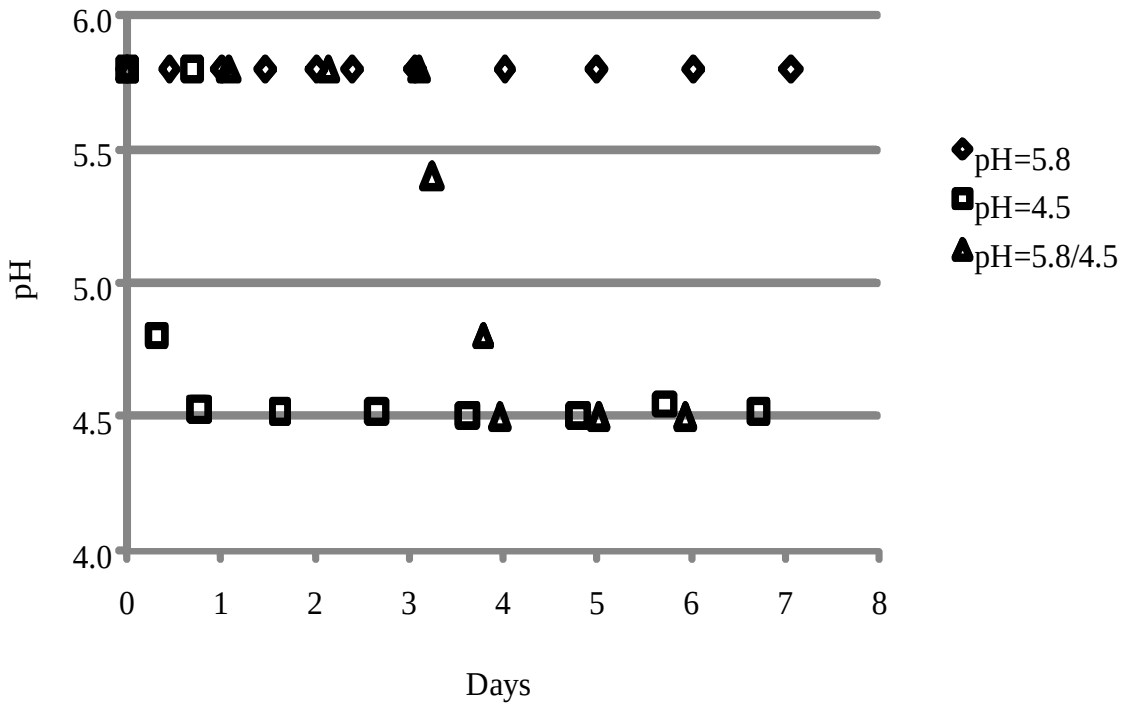

Figure 7-3.pH profiles of experiments at constant redox potential of -250 mV

Figure 7-4 also shows that a higher pH yielded greater ethanol concentrations. The run with pH 5.8 yielded a maximum ethanol concentration of 5 g/l, while the run at pH 4.5 yielded a maximum of 4 g/l. However, even though the run at pH 5.8 yielded a higher overall ethanol concentration than the run where pH 4.5, it was at a lower ethanol amount per cell mass because the cell concentration at pH 5.8 was much higher than it was at pH 4.5. In addition, comparison of the different ethanol production rates allows for a better understanding of which pH is actually more favorable for ethanol production. Inspection reveals that at pH 5.8, the rate of ethanol production during the non-growth phase was approximately 2.8 g/day/g-cell, while at pH 4.5, the rate was 4.9 g/day/g-cell. This indicates that the high ethanol concentrations in the run at higher pH was due primarily to the fact that it had greater cell mass, and that lower pH is actually more favorable for ethanol production.

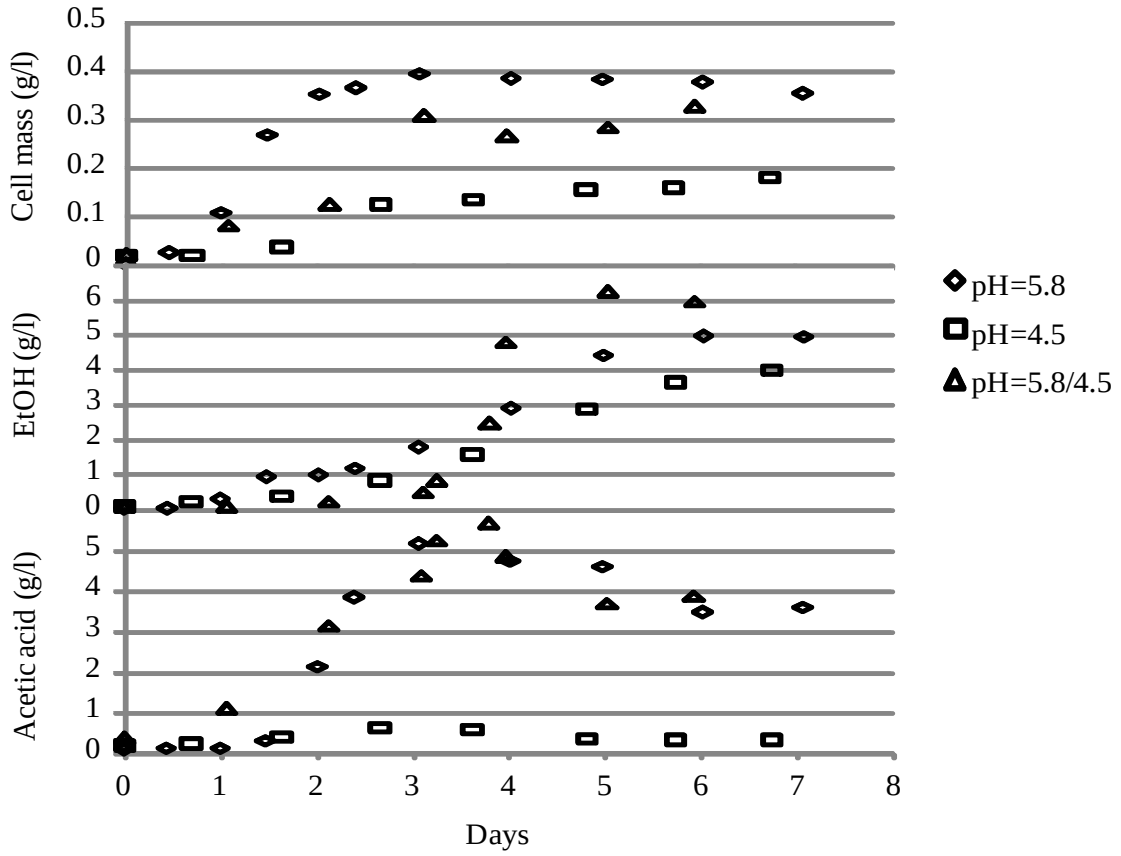

Figure 7-4.Cell growth, ethanol production and acetic acid production with controlled pH associated with Figure 7-3 at a constant redox potential of –250 mV

The above findings of the two-stage experiment showed that a greater cell mass occurred at higher pH and a higher rate of ethanol production occurred at lower pH. Accordingly, maximum ethanol production was attained by the run in which the pH was switched from 5.8 to 4.5. This run reached ethanol concentrations of over 6.3 g/L on day 5, while the run at pH = 5.8 maxed out at 5 g/L on day 6, and the run at pH = 4.5 reached 4 g/L on day 7. Another interesting finding is the rapid rise in the ethanol concentration following the pH switch (day 3 to 4). During that time, the ethanol concentration changed from 0.3 g/L to 5 g/L. As seen, the drop in the pH provided a more rapid increase in the amount of ethanol produced as compared to the run in which the pH was maintained at pH 5.8 (Note that the cell concentration was similar).

Even more significant than the total ethanol concentration in solution is the specific rate of ethanol production. As far as the ethanol rate is concerned, the run at pH 5.8 had the lowest ethanol production rate of 2.8 g/day/g-cell, while the run at pH 4.5 came next with a rate of 4.9 g/day/g-cell. The reactor in which the pH was switched between the growth and stationary phases reached an ethanol production rate of 5.3 g/day/g-cell. Although this rate was only slightly higher than the rate at pH 4.5, the amount of cells was much great—this would lead to higher volumetric ethanol yields. These results clearly indicate that the strategy of pH adjustment is beneficial for initially promoting higher cell growth followed by higher ethanol production.

Table 7-1 summarizes the production parameters at varying pH levels. For each of the three runs, this table lists the production phase of ethanol, the average cell concentration over that same time period, the shift in ethanol concentrations during the production phase, and the rate of ethanol production over the same time period. The run with variable pH is once again confirmed to be the most productive run, both in terms of total cell mass and total ethanol concentration (along with an increased rate of ethanol production). In fact, the rate of ethanol production of the run with variable pH is 108% of the rate at pH 4.5 and 190% of the rate at pH 5.8.

Table 7-1.The average cell concentration, ethanol concentration, and the specific ethanol production during the production phase at varying pH levels

Run	Production phase (day)	Cell concentration (g/l)	EtOH (g/l)	R_{EtOH} (g/day/g-cell)
5.8	3.1 to 6	0.39	1.8 to 5.0	2.8
4.5	3.6 to 6.7	0.16	1.6 to 4.0	4.9
5.8/4.5	3.8 to 6.0	0.30	2.5 to 6.0	5.3

Moreover, it is also interesting to compare the product concentration relative to the cell concentration. In Figure 7-5, the amount of acetate per cell was higher at pH 5.8 (including the run in which the pH was changed to 4.5 after Day 4) than at pH 4.5, indicating that higher pH is better for acetate production. When cells were at the non-growth phase (after day 5), the acetate/cell ratio for some runs decreased due to the apparent conversion of acetate.

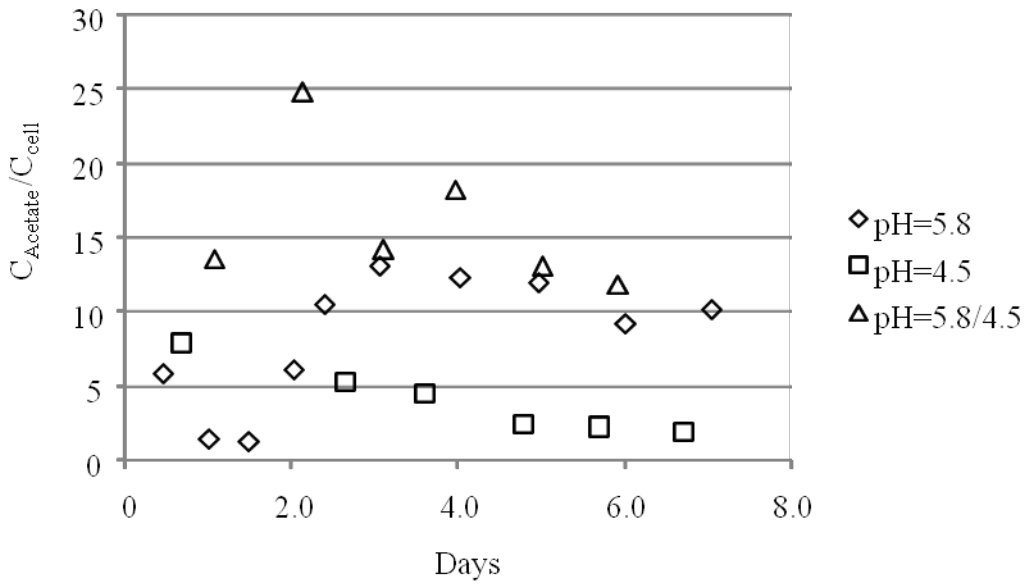

Figure 7-5.Ratio of acetate concentration ($C_{Acetate}$) to the cell concentration (C_{cell}) associated with pH at constant redox potential of -250 mV

A similar graph was plotted for the ethanol concentration relative to the cell concentration (Figure 7-6). From the figure, the run with constant pH 4.5 had a consistently high ratio of ethanol concentration to cell concentration throughout all the days. The run with constant pH 5.8 had the lowest ratio of ethanol concentration to cell concentration throughout. An interesting finding is the ratio at day 4 for the pH switch run. From day 3 to day 4, the ratio jumped from almost zero to a high level with a pH drop from 5.8 to 4.5. The high level was consistent with the pH 4.5 run. However, the advantage of the pH switch is that the amount of

ethanol formed is the highest since the cell concentration is much higher for the pH switch as compared to pH 4.5.

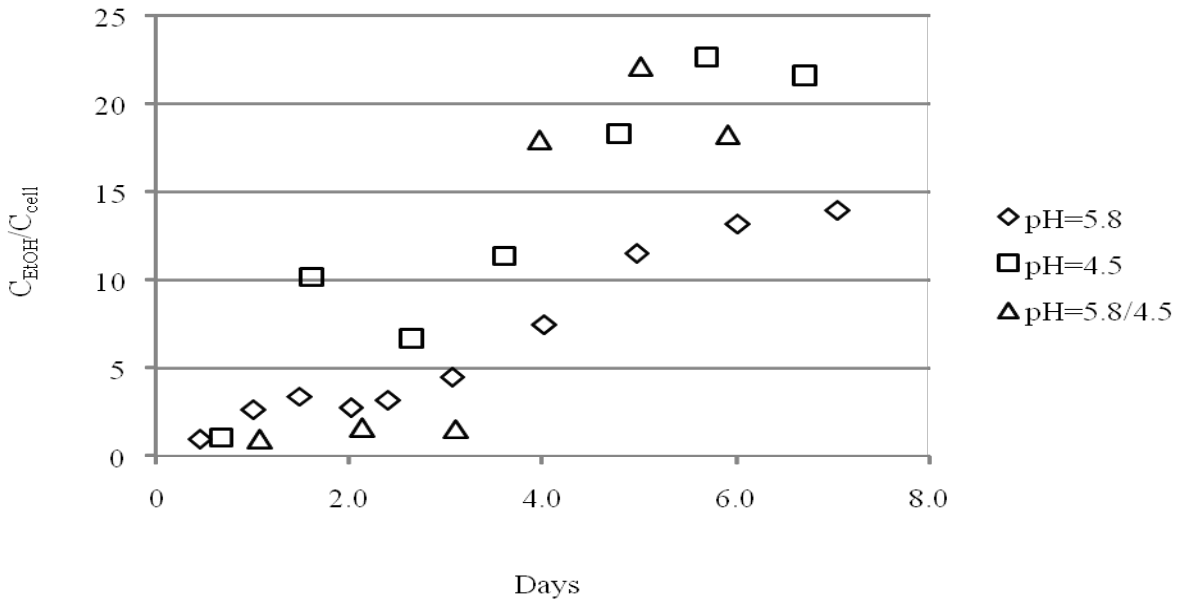

Figure 7-6.Ratio of the EtOH concentration (C_{EtOH}) to the cell concentration (C_{cell}) associated with pH at constant redox potential of -250 mV

7.4.3 pH effects – repeat run

Another set of experiments with the same pH control as Figure 7-3 was conducted to verify the results. Figures 7-7and 7-8 show the measured pH profiles, cell growth, ethanol concentration, and acetic acid concentration of the repeat experiments. The results shown in Figure 7-8 are similar to the results from Figure 7-4 with different growth and production affected by varying the pH. Both runs in which the growth phase was at pH 5.8 had the highest final cell concentration, although the run with pH switch (5.8/4.5) had the highest ethanol concentration.

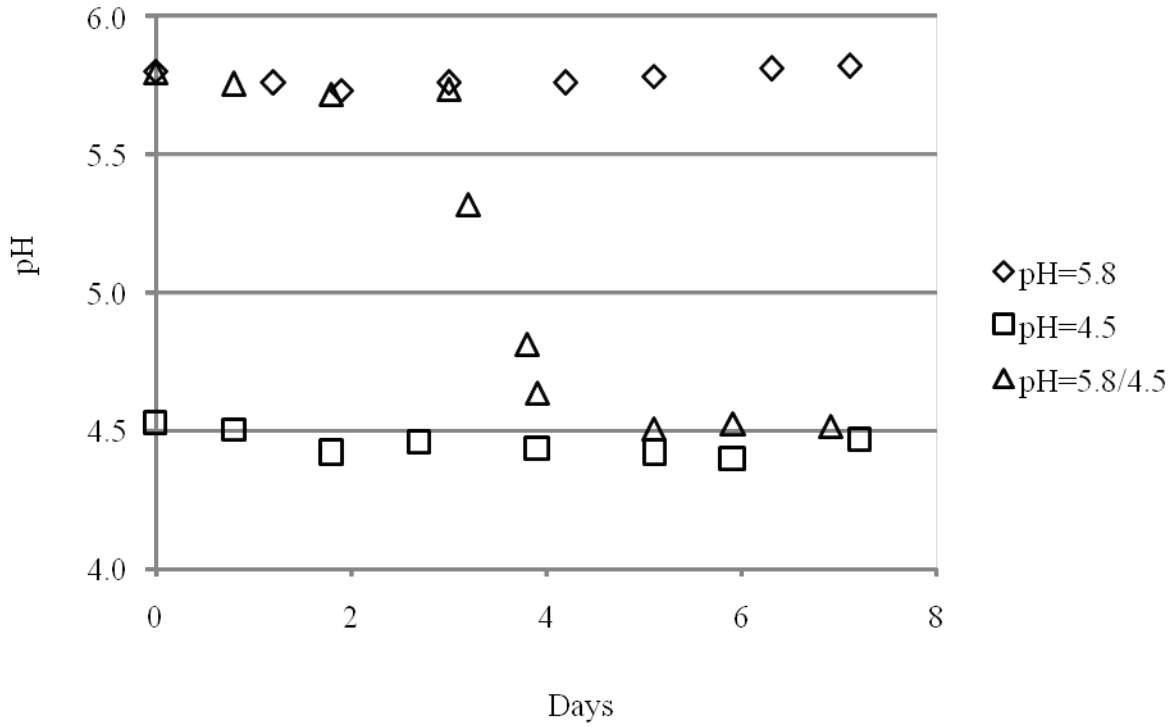

Figure 7-7.pH profiles of repeat pH effects experiments at constant redox potential of -250 mV

Also, the induction of ethanol production during the pH drop was observed. Similar to the previous run, the product formation relative to cell formation was compared in Figure 7-9 and 7-10 and similar conclusions can be derived. In Figure 7-9, when cells were in the growth phase, the amount of acetate per cell mass was higher at pH 5.8 (including the run in which the pH was changed to 4.5 after Day 4) than at pH 4.5, indicating that higher pH is better for acetate production. When cells were at the non-growth phase (after day 5), the decreasing ratios of acetate to cell mass, likely due to acetate conversion, were also observed for some runs.

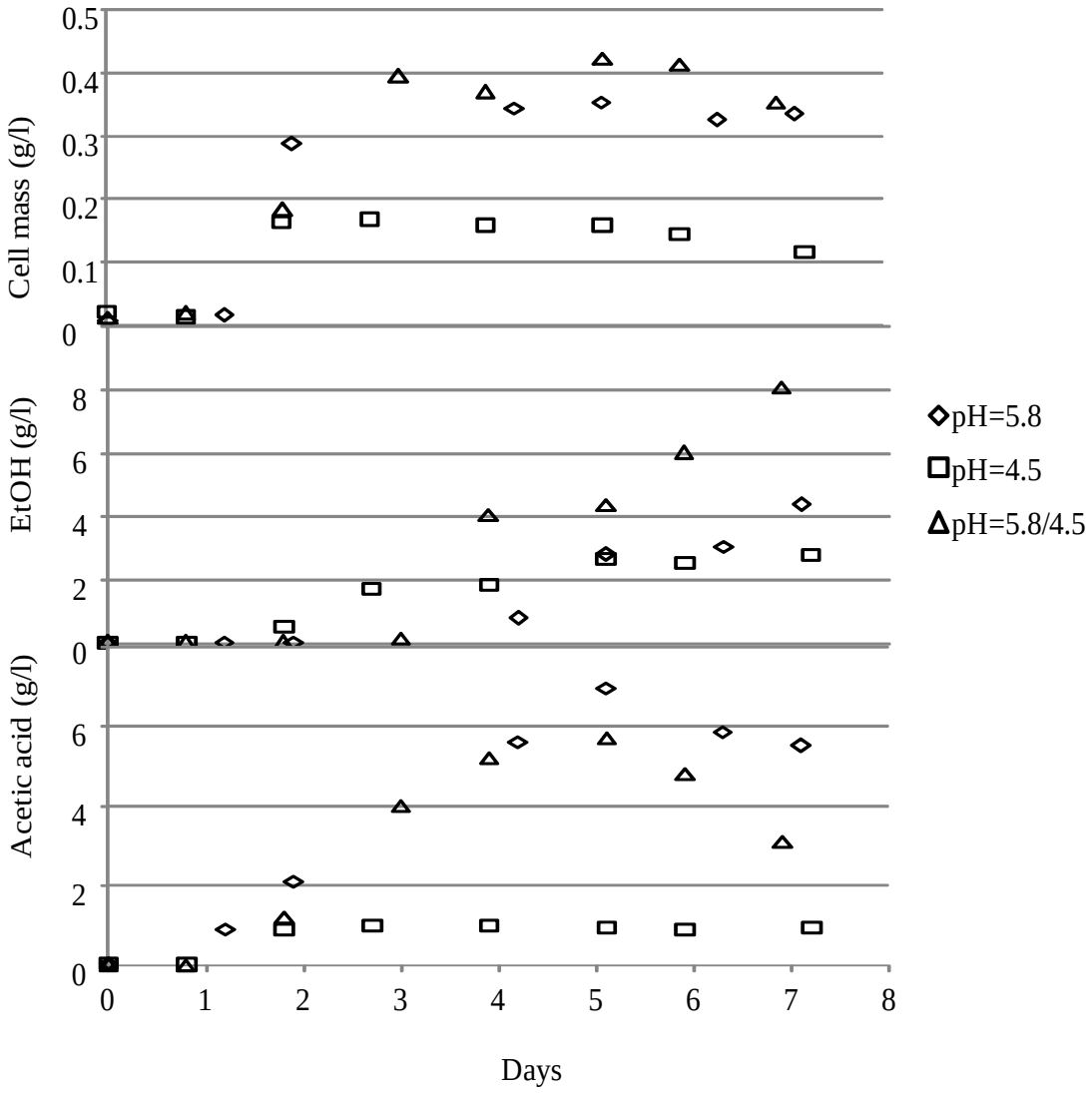

Figure 7-8.Cell growth, ethanol production and acetic acid production associated with pH at constant redox potential of –250 mV

As for the ethanol concentration relative to the cell concentration (Figure 7-10), the run with constant pH 4.5consistently had the highest ratio of ethanol concentration to cell concentration, whereas the run with constant pH 5.8 had the lowest ratio of ethanol concentration to cell concentration throughout. Also, for the run with pH switch, the ratio of ethanol concentration to cell concentration was initially very low before the pH switch, but it increased rapidly after the pH switch to approach the run with pH 4.5. Again, it should be noted that the

run with the pH switch had a higher cell mass so the ethanol productivity would be higher for the pH switch as compared to pH 4.5.

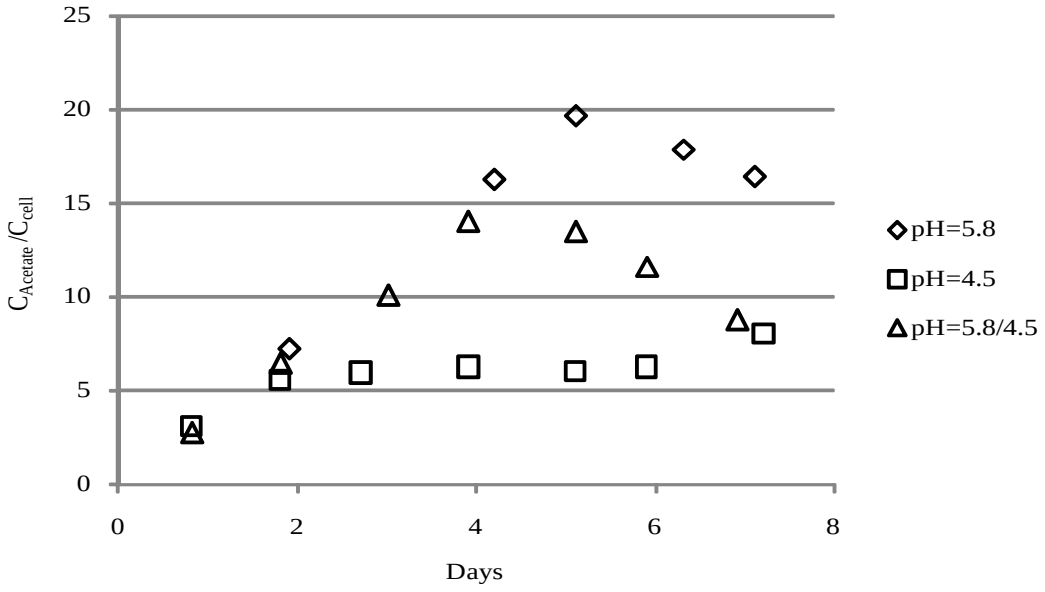

Figure 7-9.Ratio of acetate concentration ($C_{Acetate}$) to the cell concentration (C_{cell}) associated with pH at constant redox potential of -250 mV (repeat experiment)

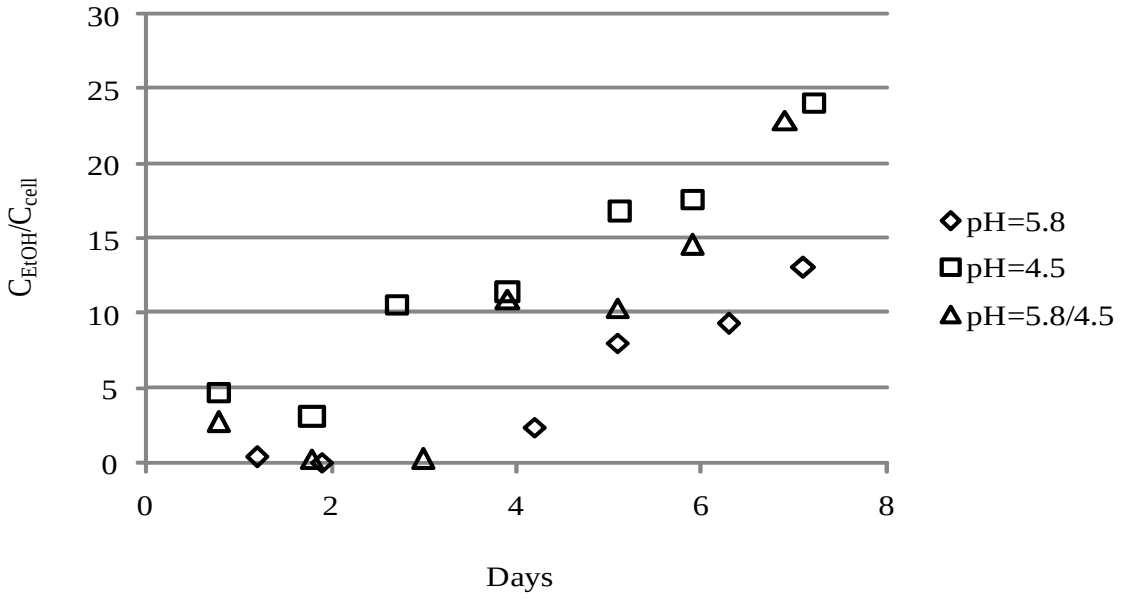

Figure 7-10.Ratio of the EtOH concentration (C_{EtOH}) to the cell concentration (C_{cell}) associated with pH at constant redox potential of -250 mV (repeat experiment)

The results of the repeat experiment of varying pH levels were calculated and summarized in Table 7-2. Although the values in Tables 7-1 and 7-2 were not exactly the same, the trends and conclusions were consistent between the experiments. Basically, the run with pH 5.8 during the growth phase followed by a switch to pH 4.5 during the non-growth phase resulted in the best cell growth and ethanol production.

Table 7-2.The average cell concentration, ethanol concentration, and the specific ethanol production during the production phase at varying pH levels for the repeated pH effects experiment

Run	Production phase (day)	Cell concentration (g/l)	EtOH (g/l)	R_{EtOH}(g/day/g-cell)
5.8	4.2 to 7.1	0.35	0.82 to 4.4	3.5
4.5	1.8 to 5.1	0.15	0.51 to 2.68	4.2
5.8/4.5	5.1 to 6.9	0.40	4.37 to 8.1	5.1

The results of the above two pH effects experiments and the statistics are summarized in Table 7-3. It clearly shows that the two-stage pH experiment achieved the aim of maintaining high cell growth while obtaining higher ethanol production. Also, the specific ethanol production rate of the two-stage pH experiment is higher than other two runs, although the rate of pH 5.8/4.5 is not significantly different than the rate of pH 4.5. Additionally, the actual amount of ethanol is greatly higher for pH 5.8/4.5 since the cell concentration is higher.

Table 7-3.Summarized results of the maximum cell concentration, maximum ethanol concentration, and the specific ethanol production rate of pH effects experiment

Run	Cell concentration (g/l)	EtOH (g/l)	R_{EtOH}(g/day/g-cell)
5.8	0.37±0.03	4.6±0.57	3.2±0.49
4.5	0.16±0.01	3.6±0.57	4.6±0.49
5.8/4.5	0.35±0.07	7.0±1.41	5.2±0.14

7.4.4 Acetate to Ethanol conversion

The conversion from acetate to ethanol was observed in several runs. From Figures 7-4 and 7-8, acetate conversion was clearly evident when the pH was switched from 5.8 to 4.5. Some conversion was also noted at pH 5.8 but it wasn't as much as the run with the pH switch. Figures 7-5 and 7-9 show a clearer picture of the conversion. For the pH 4.5 run, some conversion appeared to occur but it was difficult to discern due to the low amounts of acetate. These results show that in the presence of large amounts of acetate, the lower pH appeared to have a greater conversion. As for the effects of redox potential on conversion, the conversion was only observed at a very negative redox potential of -250 mV (Figure 7-2, 7-4 and 7-8), but not at redox potentials of -200 mV and -100 mV (Figure 7-2). In the runs with acetate conversion, some ethanol was produced from gas substrate during the non-growth phase as well as produced from the acetate conversion.

The experimental results were in agreement with the thermodynamic analysis in Chapter 4, in which the conversion from acetate to ethanol can be induced by changing the experimental conditions. It should be noted that the conversion analysis is best understood during the non-growth phase when acetate is generally not produced since the production (and potential conversion) of acetate during the growth phase would be difficult to distinguish. As noted in Chapter 4, it was shown that conversion changed from thermodynamically unfavorable to thermodynamically favorable as the NAD_{red}/NAD_{ox} ratio increased, the acetic acid to ethanol concentration increased, and the pH decreased. As is evident, a lower pH and lower redox (likely correlated with a higher NAD_{red}/NAD_{ox}) led to greater conversion conditions. Thus, similar to the thermo analysis, there are likely conditions in which conversion is favored and it is not favored.

Although the analysis is complicated since the internal pH is not the same as the external pH, the reviewed literature (Chapter 2) showed that there is a possibility that the internal pH can be affected by the external pH, even though the internal pH has some resistance to external pH changes. Thus, it is reasonable that the internal pH could decrease if the reactor pH decreased from 5.8 to 4.5.

7.4.5 Ionic strength effects

The thermodynamic analysis discussed in Chapter 4 showed that ionic strength may have some effects on syngas fermentation, though the effects are slight. To validate the thermo analysis, it is valuable to assess how the ionic strength affects the ethanol production during syngas fermentation. Therefore, experiments were conducted in bottles. Since ethanol production generally occurs during the non-growth phase, different amounts of KCl solution were added into the media to affect the ionic strength (which was calculated following the addition of KCl) after cells stopped growing. Figure 7-9 shows the cell growth and pH profiles of the experiment and Figure 7-10 shows the production profiles. For all experiments, ionic strength was adjusted at day 5, when cells already stopped growing. Since all experiments had the same conditions during the growth phase, it is reasonable that all runs had similar cell growth, pH, and acetic acid profiles prior to day 5.

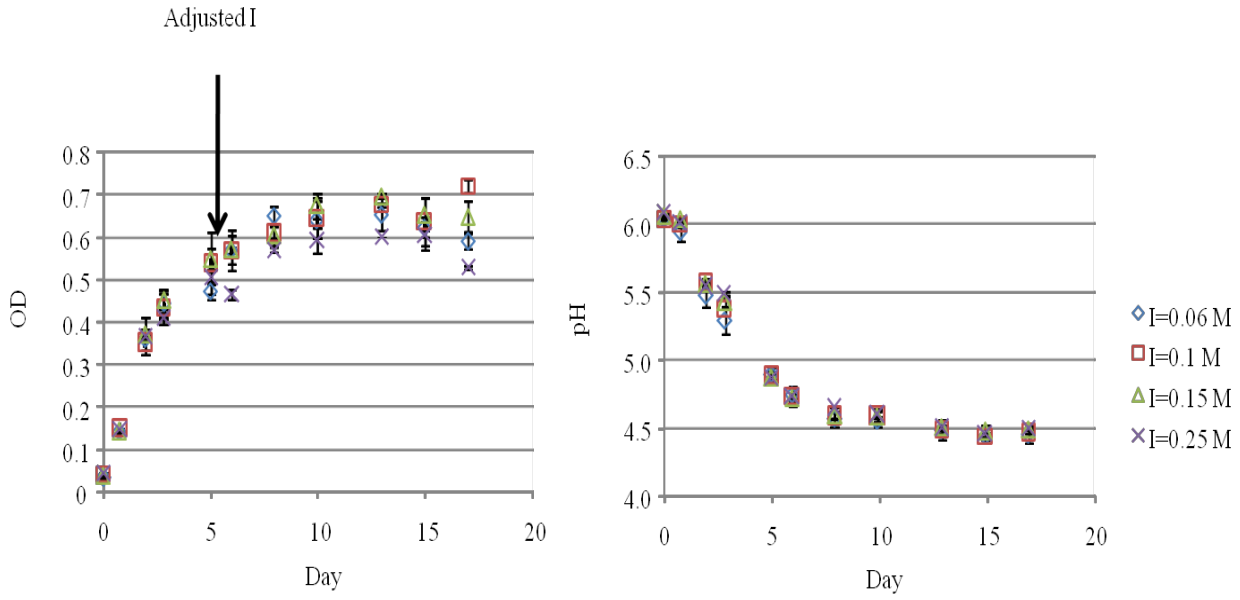

Figure 7-11.Cell growth (left) and pH (right) profiles of the ionic strength effects experiments. Four different levels of ionic strength (0.06 M, 0.1 M, 0.15 M and 0.25 M) were obtained by adding different amounts of KCl solution. Error bars represent the standard error (n=3)

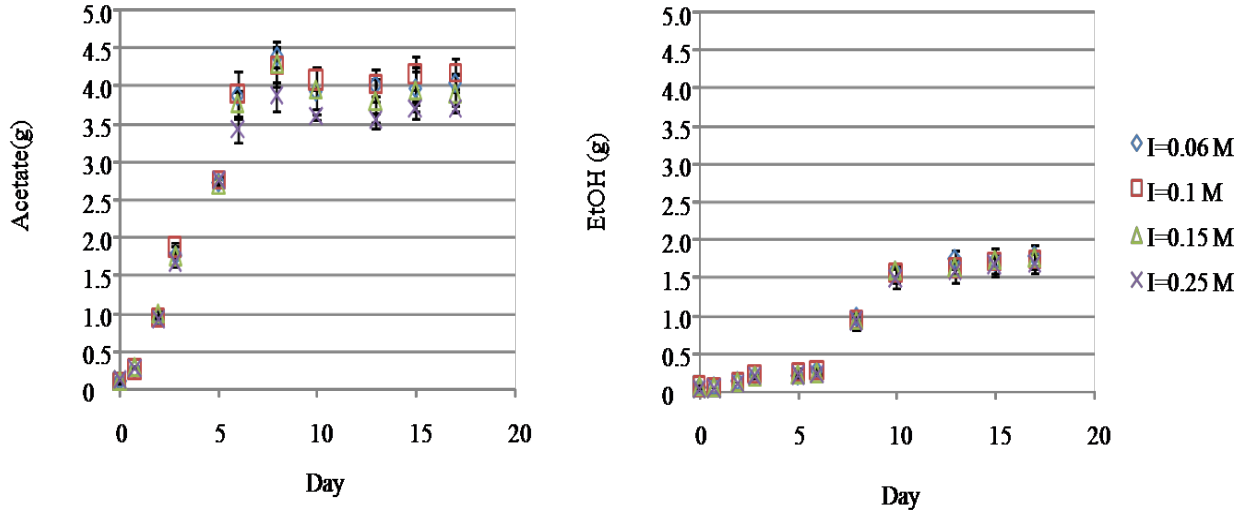

Figure 7-12.Acetate (left) and ethanol (right) profiles of the ionic strength effects experiments. Four different levels of ionic strength (0.06 M, 0.1 M, 0.15 M and 0.25 M) were obtained by adding different amounts of KCl solution. Error bars represent the standard error (n=3)

As for ethanol production, no significant difference was observed for different ionic strengths. The results are consistent with the thermodynamic analysis which shows that ionic strength only has negligible effects on syngas fermentation.

7.4.6 NADH/NAD+ measurements

Although it is shown in the literature that a more negative redox potential would result in a higher NADH/NAD^+ ratio, it is still beneficial to experimentally measure the real NADH/NAD^+ ratio during syngas fermentation. Such measurements were tried in the laboratory. From the measurements, the error for the same sample using the same preparation method was larger than 30%. Such a great error may result from the random error or from the high oxygen sensitivity of NADH and NAD^+ when they are exposed to the air. The poor repeatability of such measurements made the results not solid. Thus, the results are not presented here. In the future, the repeatability of such measurements should be improved to provide more reasonable results.

7.5 Discussion

It is obvious from the metabolic pathway analysis (Chapter 4) that changing the pH and redox potential (NADH/NAD^+) affects the thermodynamics of syngas fermentation—in many cases from the unfavorable to favorable formation of products. In Chapter 3 and 4, the thermodynamic models showed how these factors quantitatively influenced the reactions involved. An advantage of looking at the transformed Gibbs free energy ($\Delta_r G_T^{'}$), instead of the

standard transformed Gibbs free energy ($\Delta_r G'^0_T$), is that the analysis is not dealing with equilibrium conditions at the end-point state, but is addressing the favorability of the reactions during any fermentation condition that occurs throughout time. The values of ($\Delta_r G'_T$) depend upon the reactor conditions and the concentration ratios of the reactants to products at any point in time. In some cases, a reaction may be favorable ($\Delta_r G'_T$<0). In other cases, a reaction can be unfavorable ($\Delta_r G'_T$>0). For instance, the favorability of electrons produced from H_2 varies with pH. In some instances it is favorable and in other instances it is not. Similarly, the bottleneck reactions of acetate and ethanol production can potentially become favorable or unfavorable by adjusting the redox potential (E) and pH. Also, making the redox potential (E) more negative and lowering the pH can lead to the favorable conversion of acetate to ethanol, resulting in a higher overall ethanol production. Although the external pH is not exactly the same as the pH at the site of the reaction, the change of reactor pH is believed to affect the internal pH as discussed in the literature review. In this Chapter, experiments with varying experimental conditions (external pH and redox potential) were conducted for the enhancement of the ethanol production.

The most readily apparent conclusion from the redox potential experiment is that a more negative redox potential is generally more advantageous with regard to essentially every aspect of the syngas fermentation process. More negative redox potentials yield higher cell mass, higher acetic acid production, and higher ethanol production. Upon inspection of the three different redox potentials investigated in this study, there appears to be no advantage to maintaining a more positive redox potential. Therefore, syngas fermentation systems should be operated at a more negative redox potential in order to promote both cell growth and product formation.

A possible explanation for why redox potential so strongly affects the cell growth and product formation lies in thermodynamics. A more reduced system (i.e. more negative redox

potential) will of necessity have a higher $NADH/NAD^+$ ratio (Lee 2008). Furthermore, at many points along the acetyl-CoA pathway, NADH is utilized as a reactant. Acetic acid production requires utilization of 3 NADH molecules, while ethanol production requires the use of 5 NADH molecules. Therefore, having a higher $NADH/NAD^+$ ratio would help favor these reactions in the forward direction, since NADH is a reactant in these reactions. Thermodynamic analysis of the acetyl-CoA pathway showed that having a high $NADH/NAD^+$ ratio can significantly decrease the Gibbs free energy of a given reaction, thereby increasing its thermodynamic favorability. For some runs in which no ethanol production was observed (Figure 7-2), it is possible that some metabolic reactions did not happen because they were thermodynamically unfavorable at the higher redox potential (resulting in a potentially lower $NADH/NAD^+$ ratio). Unlike previous studies, this work was able to show that ethanol formation was not favorable above a redox potential of -200 mV. Although the $NADH/NAD^+$ ratio was not measured during this study, it would be beneficial in future studies to measure the ratio as a function of the redox potential to help assess the conditions in which the thermodynamics changed from unfavorable to favorable for ethanol formation.

As for the pH effects, one unique aspect of the changing pH study is the investigation of differing pH levels at a controlled redox potential. By holding the redox potential constant while varying pH, this experimental design ensured that the observed effects were indeed due to the difference in pH, and not to a combination of pH and redox potential. Accordingly, it is clear that a higher pH is more favorable for cell growth and acetic acid production. Since acetic acid production is associated with ATP production and cell growth requires ATP, the ATP produced from acetic acid production would promote additional cell growth, thereby increasing the cell mass concentration of the system. Acetic acid production tends to lower the pH because it is an

acid, so maintaining a higher pH also keeps the equilibrium in such a position that acetic acid production is still favorable.

While higher pH is more favorable for cell growth and acetate formation, it is just as easily apparent that a lower pH is desirable for ethanol formation. In the opposite manner from that described above, a lower system pH will inhibit acetic acid formation, thereby promoting ethanol production. Furthermore, when the redox potential is very negative and the pH is low, acetic acid produced during cell growth phase can actually be converted to ethanol, thereby increasing the overall ethanol production.

The experimental results concur with the thermodynamic analysis discussed in Chapters 3 and 4. From the analysis of $\Delta_r G_T^{'}$, reactions can be unfavorable or favorable at a certain condition. A more negative redox potential (with higher NADH/NAD^+ ratio) is obviously better for the fermentation because it increases the favorability of the metabolic reactions. As for pH effects, it is much more complicated. A higher pH is better for the favorability of the bottleneck reactions of acetate formation, but lower pH is better for the favorability of the bottleneck reactions of ethanol formation. Although there may be a pH gradient across the cell membrane, the modulation of external pH can potentially affect the internal pH as shown in the literature review. Thus, a rational design of adjusting the reactor conditions, such as redox potential and pH, can lead to the modulating of reaction conditions towards favorable or unfavorable conditions (or more favorable conditions), with the purpose of increasing the product formation.

The trends in the effect of pH on cell growth and product formation led to the design of the experiment with variable pH in order to maximize ethanol production. Clearly, if the advantages of both high and low pH could be utilized in one run, it would significantly contribute to enhancing ethanol production. Accordingly, one run in the pH experiment was

started at a higher pH (pH = 5.8) in order to take advantage of the more rapid cell growth to reach a peak cell mass greater than that which could be obtained at lower pH. Once the growth phase was completed, lowering the pH to 4.5 enabled a higher rate of ethanol production which comes with lower pH to be utilized with the higher cell mass concentration that was initially found only in systems with high pH. As described above, this process yielded both higher overall ethanol concentrations and a greater rate of ethanol production than in either of the runs where pH was held constant throughout the experiment in its entirety. Clearly, a strategy of adjusting the pH during the course of a run can greatly impact and enhance the efficiency and overall yield of ethanol production. It is important to note that a low redox potential was important in combination with the pH adjustment.

Industrially, some methods may be applied for increasing the cell growth, resulting in an increase of acetate production during the cell growth phase. Since ethanol is the main objective, the produced acetate is a by-product and the removal and/or separation from ethanol may add to the cost. If the conversion from acetate to ethanol can be induced by adjusting the reactor conditions, it would lead to not only higher overall ethanol production, but also a lower by-product. Obviously, the economics of ethanol versus acetate would need to be considered to determine the best strategy.

Also recall that electron production from both CO and H_2 is more favorable at higher pH and CO is more favorable than H_2 as an electron source, as described in Chapter 3. Since enzymes associated with electron production are likely membrane-bound, the reactor pH may affect the reactions more directly (Drake 2005). Although CO cannot be completely converted to carbon in product due to the strong favorability as an electron source, it is wise to run experiments at higher pH such that the thermodynamics would be more favorable for H_2 to be

used as an electron source. Therefore, this would reduce the dependency of CO as an electron source, and thus increase the carbon utilization efficacy of CO. Thus, running experiments at high pH during the growth phase would make not only better growth, but also would have possibly higher CO utilization efficiency. Then, to achieve high ethanol production during the non-growth phase, the fermentation needs to be changed to low pH. At such pH conditions, H_2 as an electron source may not be possible, such that CO must be used for generating electrons. Thus, to achieve high ethanol production, the pH should be maintained at low pH although the loss of some CO to electron production is inevitable since electron production from H_2 is less favorable at low pH. Thus, it is advantageous to perform a pH switch to maximize the CO conversion efficiency so that H_2 can at least potentially be utilized at the higher pH for electron production during the growth phase. Therefore, the two-stage pH strategy of syngas fermentation would result in higher cell growth, higher ethanol production, and possibly higher CO conversion efficiency to product.

7.6 Conclusions

Several conclusions were derived from the experiments and analysis:

- A more negative redox potential is good for cell growth, acetic acid production and ethanol production.
- Ethanol cannot be produced above a redox of -200 mV.
- A higher pH is good for cell growth and acetic acid production.
- A lower pH is good for ethanol production.

- Acetic acid may be converted to ethanol during fermentation. Such conversion occurs more easily at a more negative redox potential. This is confirmed by thermodynamics.
- Fermenting at a low redox potential combined with a two-stage pH strategy would enhance cell growth and ethanol production. It is also likely that CO conversion efficiency would be better than runs at controlled low pH during the entire fermentation.

8. Conclusions and future work

This work assessed the thermodynamic, sulfide, redox potential and pH effects on syngas fermentation based on both theoretical modeling and laboratory experiments. The study provided great insights of how varying experimental conditions can affect syngas fermentation. The main conclusions of this work and several suggestions of future work are listed below.

8.1 Conclusions

8.1.1 Thermodynamic analysis

- $\Delta_r G_T^{'}$ for the reaction of electron production from CO is negative (thermodynamically favorable) for typical fermentation conditions.
- $\Delta_r G_T^{'}$ for the reaction of electron production from H_2 can vary between thermodynamically favorable and unfavorable depending upon the fermentation conditions.
- Electron production from CO is always more thermodynamically favorable compared to electron production from H_2 and this is independent of pH, ionic strength, gas partial pressure, and electron carrier pairs. Therefore, CO conversion efficiency to

product will be sacrificed during syngas fermentation since some of the CO will make electrons at the expense of product and cell mass formation.

- The pH, but not the ionic strength, has significant impact on several transformed Gibbs free energies ($\Delta_r G_T^{'}$) of reactions in the metabolic pathway.
- Electron production reactions are more favorable with increasing pH.
- A potential thermodynamic bottleneck for acetyl-CoA synthesis appears to be formate formation. This reaction only occurs when the formate concentration is negligible. Thus, formate must be scavenged rapidly.
- Acetyl-CoA synthesis reactions are more favorable with decreasing pH.
- A potential thermodynamic bottleneck for the conversion from acetyl-CoA to acetate appears to be the reaction from acetyl-P_i to acetate. This reaction is more favorable with increasing pH. In order to make this reaction proceed forward, the ATP/ADP ratio must likely be small.
- A potential bottleneck for the conversion from acetyl-CoA to ethanol appears to be the reaction from acetyl-CoA to acetaldehyde. This reaction is more favorable with decreasing pH.
- The different dependency of pH on acetic acid and ethanol formation leads to potential application on syngas fermentation with adjusting pH of the media to promote the desired product.
- Increasing the NAD_{red}/NAD_{ox} ratio can greatly increase the driving force for both acetate and ethanol formation, with the likelihood that ethanol benefits more with an increasing ratio.

- Conversion of acetate to ethanol is more likely at more negative redox potential and low pH as compared to more positive redox potential and high pH.

8.1.2 Sulfide, redox potential and pH research

- Sulfide loss happens in both continuous and batch reactors. Mass transfer plays a key role for sulfide loss in continuous reactors, whereas equilibrium is critical for sulfide loss in batch reactors. The loss of sulfide results in the change of the associated redox potential of the media, which may affect the fermentation.
- Sulfide loss in gas-continuous reactors is independent of pH.
- Models of sulfide loss can be used to understand the fate of sulfide during an experiment and can potentially be used to design experiments to maintain constant sulfide levels.
- The redox potential can be used to assess the mass transfer coefficient for dominant reducing species that transfer between the liquid and gas phase.
- The sulfide concentration may affect cell growth, but the effect appears slight.
- Ethanol production is favored at higher sulfide concentrations, but acetic acid production is favored at lower sulfide concentrations.
- Sulfide maintenance using cysteine-sulfide is confounded because of the accumulation of cysteine.
- Sulfide maintenance in a gas-continuous bioreactor is possible, but the increasing volume of the media and the accumulation of Na^+ ion are problematic. Thus, sulfide

control in a continuous reactor is unrealistic when using sulfide addition.

- Control of the redox potential, instead of reducing agent concentrations, is a more efficient method for addressing enhancements in growth and product formation.
- A more negative redox potential is good for cell growth, acetic acid production and ethanol production.
- A higher pH is good for cell growth and acetic acid production.
- A lower pH is good for ethanol production, but less favorable for acetic acid production.
- Acetic acid may be converted to ethanol during fermentation. Such conversion occurs more easily at a lower pH and more negative redox potential.
- Designing experiments with a low redox potential along with a two-stage pH process will enhance both cell growth and ethanol production.

8.2 Future work

Research of syngas fermentation is still in the beginning phase and a lot of issues need to be addressed before commercialization. Key bottlenecks include lower cell concentration, lower ethanol production, and lower carbon utilization efficiency. In this work, for example, a cell concentration of 0.4 g/l and ethanol concentration of 6 g/l were achieved. The highest ethanol production rate was 5.3 g/day/g-cell. Obviously, this level is far from commercialization. In the future, a lot of research, such as metabolic engineering, media optimization, and reactor design, should be continued to increase the cell concentration and ethanol production rate.

In addition, this study showed that all CO to product conversion cannot be achieved because part of the CO tends to be used for electrons. Thermodynamically, it is impossible to make electron production from H_2 more favorable than electron production from CO. Thus, to maximize the gas utilization, multiple-stage bioreactors or gas-recycling systems need to be incorporated. Moreover, to make H_2 the preferred electron source, research about kinetics or metabolic engineering may be applied to achieve the aim. For instance, if the gene for CO to CO_2 conversion for electron production is knocked out, H_2 would be forced to become the primary electron source. Thus more CO would be converted to product, which would increase the carbon to product utilization efficiency.

This study analyzed the thermodynamics of the reactions along the Acetyl-CoA metabolic pathway, which provided the relative thermodynamic favorability of each reaction. However, thermodynamic favorability is not the sole factor which determines whether or not a reaction occurs in practice; kinetics must also be considered. For example, kinetics analysis may be conducted for the bottleneck reactions. If the reactions following the bottleneck reaction can be accelerated, the rapid removal of the reactant, which is the product of the previous bottleneck reactions, would increase the favorability of the bottleneck reaction. It would also be beneficial to look at the enzyme levels of the bottleneck reaction and surrounding reactions to determine whether methods need to be employed to enhance levels.

In this study, redox potential was shown to play an important role in syngas fermentation with more negative redox potential providing higher cell growth, acetic acid production, and ethanol production. However, this study just assessed the redox potential as low as -250 mV (SHE) because the reducing power of cysteine is not very strong. In the future, studies at a more negative level than -250 mV may be beneficial to thoroughly understand the redox potential

effects on syngas fermentation. Some potential stronger reducing agents include sodium thiosulfate and titanium citrate.

Concentrations of nucleotides, such as NADH, NAD^+, ATP, ADP, etc, have shown the possibility to affect the reactions on the Acetyl-CoA metabolic pathway through thermodynamic analysis. In this study, NADH/NAD^+ effects were indirectly adjusted by modulating the redox potential of the media. In the future, a direct correlation between nucleotides and syngas fermentation would be beneficial to provide more insights on the process, which requires more accurate and precise experimental methods to determine the nucleotide concentrations.

8.3 Conclusions

The great energy demand and environmental concerns increase the interest of ethanol as one of the alternative fuels to fossil fuel. Currently, work in ethanol production is exploring the fermentation of syngas (primarily CO, CO_2, and H_2) following gasification of cellulosic biomass. The syngas fermentation by clostridium microbes, such as *Clostridium* P11 in this study, utilizes the Wood-Ljungdahl metabolic pathway. This work showed the approaches of both theoretical modeling and laboratory experiments with the aim of enhancing ethanol conversion during syngas fermentation. In Chapters 3 and 4, thermodynamic analysis of the reactions involved in the metabolic pathway was conducted. It explored the relative thermodynamic favorability of the electron production from H_2 and CO. Also, the thermodynamics of the metabolic pathway steps were assessed and the potential thermodynamic bottleneck steps were determined. Based on the analysis of the bottleneck reactions, studies of redox potential and pH were explored trying to enhance the syngas fermentation. Chapters 5 and Chapter 6 assessed the fate of the reducing

agent cysteine-sulfide in the bioreactor and the associated effects on the syngas fermentation. In Chapter 7, controlling the redox potential and pH, rather than reducing agent concentrations, was explored for improving ethanol production during syngas fermentation. Although much work still remains to be done, this work provides significant insights on enhancing the syngas fermentation process via *Clostridium* P11 and identifies key thermodynamic issues.

REFERENCES

Abrini, J., Naveau, H., and Nyns, E. J. (1994).“Clostridium autoethanogenum, Sp-Nov, an anaerobic bacterium that produces ethanol from carbon-monoxide.” Archives of Microbiology **161(4)**: 345-351.

Alberty, R. A. (1997). “Apparent equilibrium constants and standard transformed Gibbs energies of biochemical reactions involving carbon dioxide.” Archives of Biochemistry and Biophysics **348(1)**: 116-124.

Alberty, R. A. (2000).“Calculation of equilibrium compositions of large systems of biochemical reactions.” Journal of Physical Chemistry B **104**: 4807-4814.

Alberty, R. A. (2001). "Effect of temperature on standard transformed Gibbs energies of formation of reactants at specified pH and ionic strength and apparent equilibrium constants of biochemical reactions." Journal of Physical Chemistry B **105(32)**: 7865-7870.

Alberty. R. A. (2003) “Thermodynamics of biochemical reactions” John Wiley & Sons, Inc. Hoboken, New Jersey.

Ball, D. W. (2003) “Physical chemistry” First Edition, Brooks/Cole, Pacific Grove, California.

Balusu, R., and Paduru, R. R. (2005).“Optimization of critical medium components using response surface methodology for ethanol production from cellulosic biomass by Clostridium thermocellum SS19.” Process Biochemistry **40(9)**: 3025-3030.

Barbero, J.A., McCurday, K. G., and Tremaine, P.R. (1982) “Apparent molar heat capacities and volumes of aqueous hydrogen sulfide and sodium hydrogen sulfide near 25 ºC: the temperature dependence of H2S ionization.” Canadian Journal of Chemistry **60**: 1872-2880.

Baronofsky, J. J., and Schreurs, W. J. A. (1984). “Uncoupling by acetic-acid limits growth of and acetogenesis by Clostridium-thermoaceticum.”Applied and Environmental Microbiology **48**(6): 1134-1139.

Bilgen S, Kaygusuz K, and Sari A. (2004). “Renewable energy for a clean and sustainable future.” Energy Sources **26(12)**:1119-1129.

Blanch, H. W., and Clark, D. S. “Biochemical engineering.” (1997) Marcel Dekker, New York.

Bryant, M. P., Robinson, I. M. (1961). “An improved nonselective culture-medium for ruminal bacteria and its use in determining diurnal-variation in numbers of bacteria in the rumen.” Journal of Dairy Science **44**: 1446-1456.

Datar, R. P., Shenkman, R. M., Cateni, B. G., Huhnke, R. L., and Lewis, R. S. (2004). "Fermentation of biomass-generated producer gas to ethanol." Biotechnology and Bioengineering **86(5)**: 587-594.

Dayton, D.C and Spath, P.L (2003)."Preliminary screening —technical and economic assessment of synthesis gas to fuels and chemicals with emphasis on the potential for biomass-derived syngas." Golden, Colorado 80401-3393: National Renewable Energy Laboratory.

Desvaux, M. (2001). "Kinetics and metabolism of cellulose degradation at high substrate concentrations in steady-state continuous cultures of Clostridium cellulolyticum on a chemically defined medium." Applied and Environmental Microbiology **67**: 3837-3845.

DOE (2005), Department of Energy, US. http://zfacts.com/metaPage/lib/DOE-2005_Ethanol-Energy-z.pdf

DOE (2010), Department of Energy, US. Http://tonto.eia.doe.gov/kids/energy.cfm?page=biofuel_home-basics#biofuel_ethanol_home-basics

Drake, H. L., and Daniel, S. L. (2004) "Physiology of the thermophilic acetogen Moorella thermoacetic." Research in Microbiology **155(6)**, 422-436.

Dry, M.E. (2002). "The Fischer-Tropsch process: 1950-2000." Catalysis Today, **71(3-4)**: 227-241.

Energy Information Administration (2010), Http://www.eia.doe.gov/emeu/mer/pdf/pages/sec9_3.pdf

Frankman A. W. (2009), "Redox, pressure and volume effects on syngas fermentation." in Master dissertation of Department of Chemical Engineering, Brigham Young University, Provo, UT.

Gaddy, J. L. (1997)."Clostridium strain which produces acetic acid from waste gases." US Patent: 5593886

Geller, H. (2001)."Strategies for reducing oil imports: Expanding oil production vs. increasing vehicle efficiency." Washington D.C: American Council for an Energy-Efficient Economy. Report E011.

Girbal, L., Croux, C., Vasconcelos, I., and Soucaille, P. (1995). "Regulation of metabolic shifts in Clostridium acetobutylicum ATCC 824." FEMS Microbiology Reviews **17(3)**: 287-297.

Goldberg, R. N., and Tewari, Y. B. (1991). "Thermodynamics of the disproportionation of adenosine 5'-diphosphate to adenosine 5'-triphosphate and adenosine 5'-monophosphate. I. Equilibrium model," Biophysical Chemistry **40**, 241-261.

Gottschalk, J. C., and Morris, J. G. (1981). “The induction of acetone and butanol production in cultures Clostridium acetobutylicumby elevated concentrations of acetate and butyrate.” FEMS Microbiology Letters **12**: 385-389.

Guedon, E. (1999). “Carbon and electron flow in Clostridium cellulolyticum grown in chemostatcultrue on synthetic medium.” Journal of Bacteriology **181**: 3262-3269.

Guedon, E. (2000). “Relationships between cellobiose catabolism, enzyme levels, and metabolic intermediates in Clostridium cellulolyticum grown in a synthetic medium.” Biotechnology and Bioengineering **67**: 327-335.

Hansen, M. H., Ingvorsen, K., and Jorgensen, B. B. (1978) “Mechanisms of hydrogen-sulfide release from coastal marine-sediments to atmosphere.” Limnology Oceanograph.**23:** 68-76.

He, B. Q., Jian, X. W., Hao, J. M., Yan, X. G., and Xiao, J. H. (2003). “A study on emission characteristics of an EFI engine with ethanol blended gasoline fuels.” Atmospheric Environment **37(7)**: 949-957.

Heiskanen, H., I. Virkajarvi, and Viikari L. (2007). “The effect of syngas composition on the growth and product formation of Butyribacteriummethylotrophicum.” Enzyme and Microbial Technology **41(3)**: 362-367.

Heo, J., Staples, C. R., and Ludden, P. W. (2001). “Redox-dependent CO_2 reduction activity of CO dehydrogenase from Rhodospirillumrubrum.” Biochemistry **40:** 7604-7611.

Hill, J., Nelson, E., Tilman, D., Polasky, S., and Tiffany, D. (2006) “Environmental, economic, and energetic costs and benefits of biodiesel and ethanol biofuels.” Proceedings of the national academy of sciences of the United States of America, **103(30)**: 11206 – 11210.

Ho, N.W.Y., Chen, Z., Brainard, A.P., and Sedlak, M. (2000). “Genetically engineered Saccharomyces yeasts for conversion of cellulosic biomass to environmentally friendly transportation fuel ethanol.” In ACS Symposium Series, ACS, p.143-159.

Hsieh, W. D., Chen, R. H., Wu, T. L., and Lin, T. H. (2002). “Engine performance and pollutant emission of an SI engine using ethanol-gasoline blended fuels.” Atmospheric Environment **36(3)**: 403-410.

Hurst, K. M. (2005). “Effects of carbon monoxide and yeast extract on growth, hydrogenase activity and product formation of *Clostridium carboxidivorans* P7T.”Chemical Engineering.Stillwater, Oklahoma, Oklahoma State University. Master Thesis of Science: 141.

Hurst, K. M., and Lewis, R. L. (2010). “Carbon monoxide partial pressure effects on the metabolic process of syngas fermentation.” Biochemical Engineering Journal, **48(2):**159-165.

Ingram, L.O., Lai, X., Moniruzzaman, M., Wood, B.E., and York, S.W. (1997). “Fuel ethanol production from lignocellulose using genetically engineered bacteria.” In American Chemical

Society Symposium Series 666, Washington, D.C., Saha, B. C.; Woodward, J. E.; American Chemical Society Press: Washington, D.C., p. 57-73.

Jarrell, K. F. and Sprott, G. D. (1981).“The transmembrance electrical potential and intracellular pH in methanogenic bacteria.” Canadian Journal of Microbiology. **27**(7): 720-728.

Jee, H. S., Nishio, N., and Nagai, S. (1987) “Influence of redox potential on bio-methanation of H_2 and CO_2 by Methanobacterium thermoautotrophicum in Eh-stat batch cultures.” The Journal of General and Applied Microbiology. **33(5)**: 401-408.

Joel, K., and Bourne, Jr. (2007). “Green Dreams.” National Geographic Magazine, **10.** http://ngm.nationalgeographic.com/2007/10/biofuels/biofuels-interactive

Jones, G. A., and Pickard, M. D. (1980). “Effect of Titanium (III) Citrate as reducing agent on growth of rumen bacteria.” Applied and Environmental Microbiology. **39(6)**: 1144-1147.

Jormakka, M., Byrne, B., and Iwata, S. (2003) “Formate dehydrogenase – a versatile enzyme in changing environments.” Current Opinion in Structural Biology, **13**(4): 418-423.

Kadar, Z., Szengyel, Z., and Reczey, K. (2004). “Simultaneous saccharification and fermentation (SSF) of industrial wastes for the production of ethanol.” Industrial Crops and Products **20 (1)**, 103-110.

Kaden, J., and Galushko, A. S. (2002). “Cysteine-mediated electron transfer in syntrophic acetate oxidation by cocultures of Geobactersulfurreducens and Wolinellasuccinogenes.” Archives of Microbiology **178(1)**: 53-58.

Kim, J., and Bajapai, R. (1988). “Redox potential in acetone-butanol fermentations.” Applied Biochemistry and Biotechnology **18**: 175-186.

Kim, S., and Dale, B. E. (2005). “Life cycle assessment of various cropping systems utilized for producing biofuels: Bioethanol and biodiesel.” Biomass & Bioenergy **29(6)**: 426-439.

Klasson, K. T., Ackerson, M. D., Clausen, E. C., and Gaddy, J. L. (1992). “Bioconversion of synthesis gas into liquid or gaseous fuels.” Enzyme Microb. Technol., **14(8)**, 602-608.

Kundiyana, D. K., Huhnke, R. L., Maddipati, P., Atiyeh, H. K., and Wilkins, M. R. (2010) “Feasibility of incorporating cotton seed extract in Clostridium strain P11 fermentation medium during synthesis gas fermentation” Bioresource Technology, **101(24)**: 9673-9680.

Kwong, S. C. W., and Randers, L. (1992). “On-line assessment of metabolic activities based on culture redox potential and dissolved oxygen profiles during aerobic fermentation. “Biotechnology progress **8(6)**: 576-579.

Lee, S. K., H. Chou, et al. (2008). "Metabolic engineering of microorganisms for biofuels production: from bugs to synthetic biology to fuels." Current Opinion in Biotechnology **19(6)**: 556-563.

Lewis R S., Tree D., Hu, P., and Frankman A. "Syngas fermentation to ethanol: challenges and opportunities." in: Khanal (Eds.), Biofuel and Bioenergy from Biowastes and Residues. American Society of Civil Engineers. 2010.

Lide, D. R. and H. P. R. Frederikse, editors. (1995). "CRC Handbook of Chemistry and Physics, 76th Edition." CRC Press, Inc., Boca Raton, FL.

Liou, J. S.C., Balkwill, D. L., Drake, G. R., and Tanner, R. S. (2005). "Clostridium carboxidivorans sp. nov., a solvent-producing clostridium isolated from an agricultural settling lagoon, and reclassification of the acetogen Clostridium scatologenes strain SL1 as Clostridium drakei sp. nov." International Journal of Systematic and Evolutionary Microbiology, **55(5)**: 2085-2091.

Ljungdahl, L. G. (1986). "The autotrophic pathway of acetate synthesis in acetogenic bacteria." Annual Review of Microbiology **40**: 415-450.

Long, S., Jones, D. T., and Woods, D. R. (1984) "Initiation of solvent production, Clostridial stage and endospore formation in Clostridium-Acetobutylicum P262." Applied microbiology and biotechnology. **20(4)**: 256 – 261.

Lynd, L. R. (1996). "Overview and evaluation of fuel ethanol from cellulosic biomass: Technology, economics, the environment, and policy." Annual Review of Energy and the Environment **21**: 403-465.

Malazzo, G., Caroli, S., and Sharma, V. K. (1978) "Tables of standard electrode potentials." John Wiley & Sons, New York.

McKendry, P. (2002). "Energy production from biomass (part 1): overview of biomass." Bioresource Technology **83(1)**: 55-63.

Menon,S. and Ragsdale, S.W. (1996). "Unleashing hydrogenase activity in carbon monoxide dehydrogenase/aceytl-CoA synthase and pyruvate: ferredoxin oxidoreductase." Biochemistry, **35(49)**, 15814-15821.

Meyer, C. L., Roos, J. W. and Papoutsakis, E. T. (1986). "Carbon-monoxide gassing leads to alcohol production and butyrate uptake without acetone formation in continuous cultures of *Clostridium acetobutylicum*." Applied Microbiology and Biotechnology **24(2)**: 159-167.

Munasinghe, P. C., and Khanal, S. K. (2010) "Biomass-derived syngas fermentation into biofuels: opportunities and challenges." Bioresource Technology. **101(13)**: 5013 – 5022.

Novozymes. (2004). “Novozymes cuts biomass ethanol enzyme cost.” Industrial Bioprocess **26 (3)**: 4.

Patzek, T. W., and Pimentel, D. (2005) “Thermodynamics of energy production from biomass.” Critical Reviews in plant sciences.” **24(5-6)**: 327 -364.

Payot, S. (1998). “Metabolism of cellobiose by Clostridium cellulolyticum growing in continuous culture: evidence for decreased NADH reoxidation as a factor limiting growth.” Microbiology. **144**: 375-384.

Pepper, C. B. and Monbouquette, H. G. (1993) “Issues in the culture of the extremely thermophilic methanogen, Methanothermusfervidus.” Biotechnology and Bioengineering. **41**: 970-978.

Picataggio, S.K., Zhang, M., Eddy, C., Deanda, K.A., and Finkelstein, M. (1997). “Recombinant zymomonas for pentose fermentation.” United States of America Patent #5,514,583.

Ragauskas, A. J., Williams, C. K., Davison, B. H., Britovsek, G., Cairney, J., and Eckert, C. A. (2006). “The path forward for biofuels and biomaterials.” Science **311(5760)**: 484-489.

Ragsdale, S. W. and Pierce, E. (2008) “Acetogenesis and the Wood-Ljungdahl pathway of CO2 fixation.” Biochemica ET biophysica-proteins and proteomics. **1784(12)**: 1873 – 1898.

Rajagopalan, S., Datar, R. P., and Lewis, R. S. (2002) “Formation of ethanol from carbon monoxide via a new microbial catalyst.” Biomass Bioenergy. **23**: 487-493.

Rao, G., and Mutharasan, R. (1987) “Altered electron flow in continuous cultures of Clostridium acetobutylicum induced by viologen dyes.” Applied Environmental Microbiology. **53**: 1232-1235.

RFA. (2010). “Changing the climate: ethanol industry outlook 2010.” Renewable fuel association. http://www.ethanolrfa.org/objects/pdf/outlook/RFA_Outlook_2010.pdf

Pimentel, D. (2001) “Ethanol fuels: energy, economics and environmental impact.” International Sugar Journal. **103(1235)**: 491.

RFA. (2010). Geoff Cooper. “Ethanol and gasoline prices.” http://www.ethanolrfa.org/exchange/entry/ethanol-and-gasoline-prices/

Rohde, M., Mayer, F., Jacobitz, S., and Meyer, O. (2002) “Attachment of CO dehydrogenase to the cytoplasmic membrane is limiting the respiratory rate of Pseudomonas carboxydovorans.” FEMS Microbiology Letters**28**(2): 141-144.

Sim, J. H., and Kamaruddin, A. H. (2008) “Optimization of acetic acid production from synthesis gas by chemolithotrophic bacterium - Clostridium aceticum using statistical approach.” Bioresource Technology. **99**: 2724-2735.

Shah, M. M., Akanbi, F., and Cheryan, M. (1997). “Potassium acetate by fermentation with Clostridium thermoaceticum.” Applied Biochemistry Biotechnology. **63**: 423-433.

Skidmore, B (2010), “Syngas fermentation: quantification of assay techniques, reaction kinetics, and pressure dependencies of Clostridial P11 hydrogenase.” in Master dissertation of Department of Chemical Engineering, Brigham Young University, Provo, UT.

Sridhar, J., and Eiteman, M. A. (2001). “Metabolic flux analysis of Clostridium thermosuccinogenes - Effects of pH and culture redox potential.” Applied Biochemistry Biotechnology. **94**: 51-69.

Shleser, R. (1994). “Ethanol production in Hawaii: processes, feedstocks and current economic feasibility of fuel grade ethanol production in Hawaii.” HD9502.5.B54.S4, Hawaii State Department of Business, Economic Development & Tourism: Honolulu, HI.

Srinivasan, S. (2009). “The food v. fuel debate: a nuanced view of incentive structures.” Renewable Energy **34(4)**: 950-954.

Subramani, V., and Gangwal, S. K. (2008). “A review of recent literature to search for an efficient catalytic process for the conversion of syngas to ethanol.” Energy and Fuels **22(2)**: 814-839.

Valli, M., and Sauer, M. (2005). "Intracellular pH distribution in *Saccharomyces cerevisiae* cell populations, analyzed by flow cytometry." Applied and Environmental Microbiology **71(3)**: 1515-1521.

Valli, M., Sauer, M. (2005). “Intracellular pH distribution in Saccharomyces cerevisiae cell populations, analyzed by flow cytometry.”Applied and Environmental Microbiology**71**(3): 1515-1521.

Van Dijk, C., and Veeger, C. (1981) “The effects of pH and redox potential on the hydrogen production activity of the hydrogenase from Megasphaeraelsdenii.” European Journal of Biochemistry. **114**: 209-19.

Vega, J. L., Prieto, S., Elmore, B. B., Clausen, E. C., and Gaddy, J. L. (1989) “The biological production of ethanol from synthesis gas.” Applied Biochemistry and Biotechnology **20(1)**: 781-797.

Vega, J. L., Clausen, E. C., and Gaddy, J. L. (1990). “Design of bioreactors for coal synthesis gas fermentations.” Resources, Conservation and Recycling **3(2-3)**: 149-160.

Wang, D. I. C., Cooney, C. L., Demain, A. L., Dunnill, P., Humphrey, A. E., and Lilly, M. D. (1979). “Fermentation and enzyme technology.” Stockholm, John Wiley & Sons.

Wang, M. (2005). “Energy and greenhouse gas emissions impacts of fuel ethanol.” NGCA Renewable Fuels Forum, The National Press Club.

Wang, M., and Hong, M. W. (2007). “Life-cycle energy and greenhouse gas emission impacts of different corn ethanol plant types.” Environmental Research Letters **2(2)**: 13.

Weil, J.R., Dien, B., Bothast, R., Hendrickson, R., Mosier, N.S., and Ladisch, M.R. (2002). “Removal of fermentation inhibitors formed during pretreatment of biomass by polymeric adsorbants.” Industrial & Engineering Chemistry Research **41 (24)**, 6132-6138.

Wood, H. G., and Ragsdale, S. W. (1986). “The Acetyl-CoA pathway of autotrophic growth.” Fems Microbiology Reviews **39(4)**: 345-362.

Wyman, C.E. (2003). “Potential synergies and challenges in refining cellulosic biomass to fuels, chemicals, and power.” Biotechnology Progress **19 (2)**, 254-262.

Yang, Q., and Chen, B. (2009). “Exergetic evaluation of corn-ethanol production in China.” Communications in Nonlinear Science and Numerical Simulation **14(5)**: 2450-2461.

Younesi,H., Najafpour,G., and Mohamed, A.R. (2005). “Ethanol and acetate production from synthesis gas via fermentation processes using anaerobic bacterium, Clostridium ljungdahlii.” Biochemical Engineering Journal **27(2)**, 110-119.